

July the 25th, 2024, Alan Turing Institute, London UK

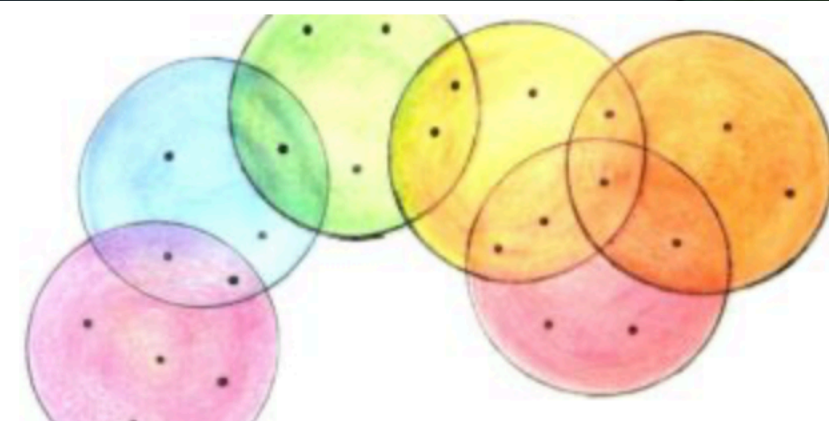
Theory and applications of hypergraphs

HTAW01

22 July 2024 to 26 July 2024

Alan Turing Institute

Isaac Newton Institute
for Mathematical Sciences



Timoteo Carletti

Turing patterns:
from network to higher-order structures



Acknowledgements

Master Students

Gwendoline Planchon

Marine Jamoulle

Alice Bellière

PhD Students

* Martin Moriamé

* Jean-François De Kemmeter

* Cédric Simal

PostDocts

* **Marie Dorchain** **Riccardo Muolo**

Sara Nicoletti

Sarah De Nigris

Luca Gallo

Giulia Cencetti

Lorenzo Giambagli Nikos Kouvaris

* **Wilfried Segnou** Thierry-Sainclair Njouougou

* Maxime Lucas

* Marcelo Ramirez Avila

Collaborators

Malbor Asllani (Florida State University)

Federico Battiston (Central European Univ)

Duccio Fanelli (Università di Firenze)

Mattia Frasca (Università di Catania)

Valentina Gambuzza (Università di Catania)

Renaud Lambiotte (University of Oxford)

Vito Latora (Università di Catania & Queen Mary University)

Hiroya Nakao (Tokyo Institute of Technology)

Julien Petit (Ecole Royale Militaire)

Philip Maini (University of Oxford)

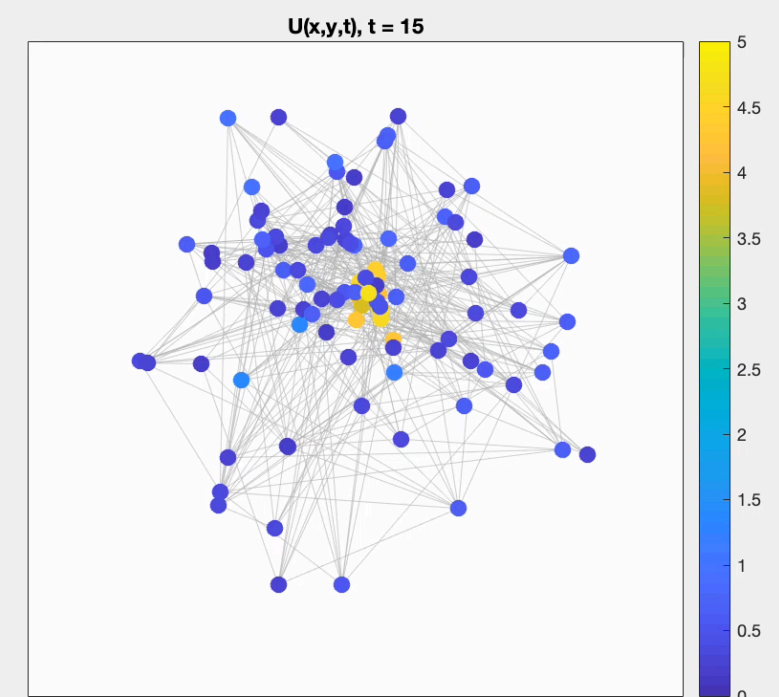
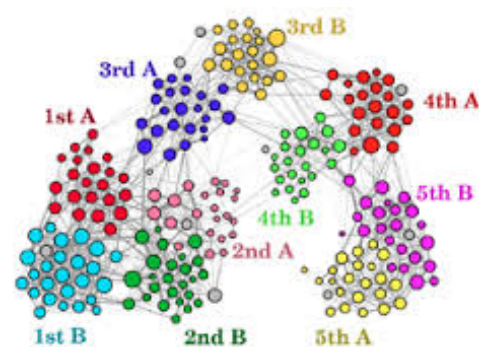
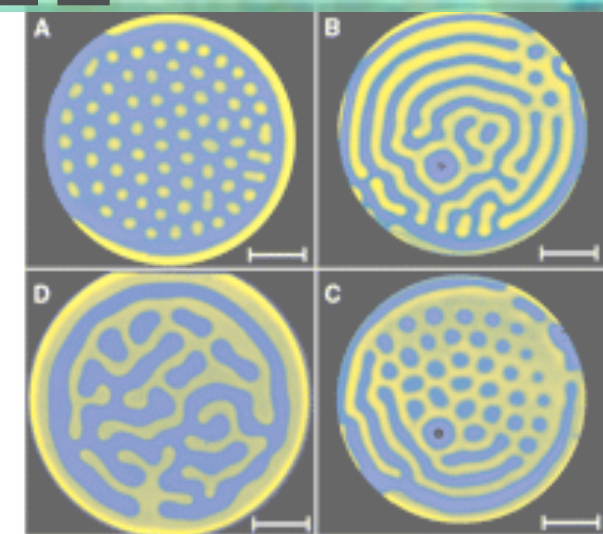
Ginestra Bianconi (Queen Mary University)

Dibakar Ghosh (ISI Kolkata)

Elio Tuci (UNamur)

Order from disorder is a leitmotif in

Nature



SocioPatterns

www.unamur.be

timoteo.carletti@unamur.be

How the Leopard Gets Its Spots

A single pattern-formation mechanism could underlie the wide variety of animal coat markings found in nature. Results from the mathematical model open lines of inquiry for the biologist

by James D. Murray

Mammals exhibit a remarkable variety of coat patterns; the variety has elicited a comparable variety of explanations—many of them at the level of cogency that prevails in Rudyard Kipling's delightful "How the Leopard Got Its Spots." Although genes control the processes involved in coat pattern formation, the actual mechanisms that create the patterns are still not known. It would be attractive from the viewpoint of both evolutionary and developmental biology if a single mechanism were found to produce the enormous assortment of coat patterns found in nature.

I should like to suggest that a single pattern-formation mechanism could in fact be responsible for most if not all of the observed coat markings. In this article I shall briefly describe a simple mathematical model for how these patterns may be generated in the course of embryonic development. An important feature of the model is that the patterns it generates bear a striking resemblance to the patterns found on a wide variety of animals such as the leopard, the cheetah, the jaguar, the zebra and the giraffe. The simple model is also consistent with the observation that although the distribution of spots on members of the cat family and of stripes on zebras varies widely and is unique to an individual, each kind of distribution adheres to a general theme. Moreover, the model also predicts that the patterns can take only certain forms, which in turn implies the existence of developmental constraints and begins to suggest how coat patterns may have evolved.

It is not clear as to precisely what happens during embryonic development to cause the patterns. There are now several possible mechanisms that are capable of generating such patterns. The appeal of the simple

model comes from its mathematical richness and its astonishing ability to create patterns that correspond to what is seen. I hope the model will stimulate experimenters to pose relevant questions that ultimately will help to unravel the nature of the biological mechanism itself.

Some facts, of course, are known about coat patterns. Physically, spots correspond to regions of differently colored hair. Hair color is determined by specialized pigment cells called melanocytes, which are found in the basal, or innermost, layer of the epidermis. The melanocytes generate a pigment called melanin that then passes into the hair. In mammals there are essentially only two kinds of melanin: eumelanin, from the Greek words *eu* (good) and *melas* (black), which results in black or brown hairs, and pheomelanin, from *phaeos* (dusty), which makes hairs yellow or reddish orange.

It is believed that whether or not melanocytes produce melanin depends on the presence or absence of chemical activators and inhibitors. Although it is not yet known what those chemicals are, each observed coat pattern is thought to reflect an underlying chemical prepattern. The prepattern, if it exists, should reside somewhere in or just under the epidermis. The melanocytes are thought to have the role of "reading out" the pattern. The model I shall describe could generate such a prepattern.

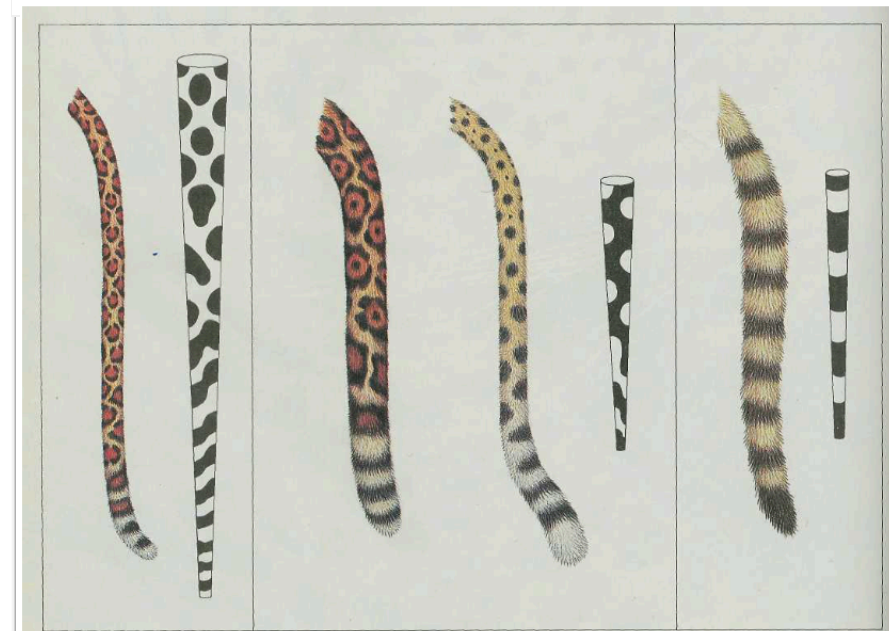
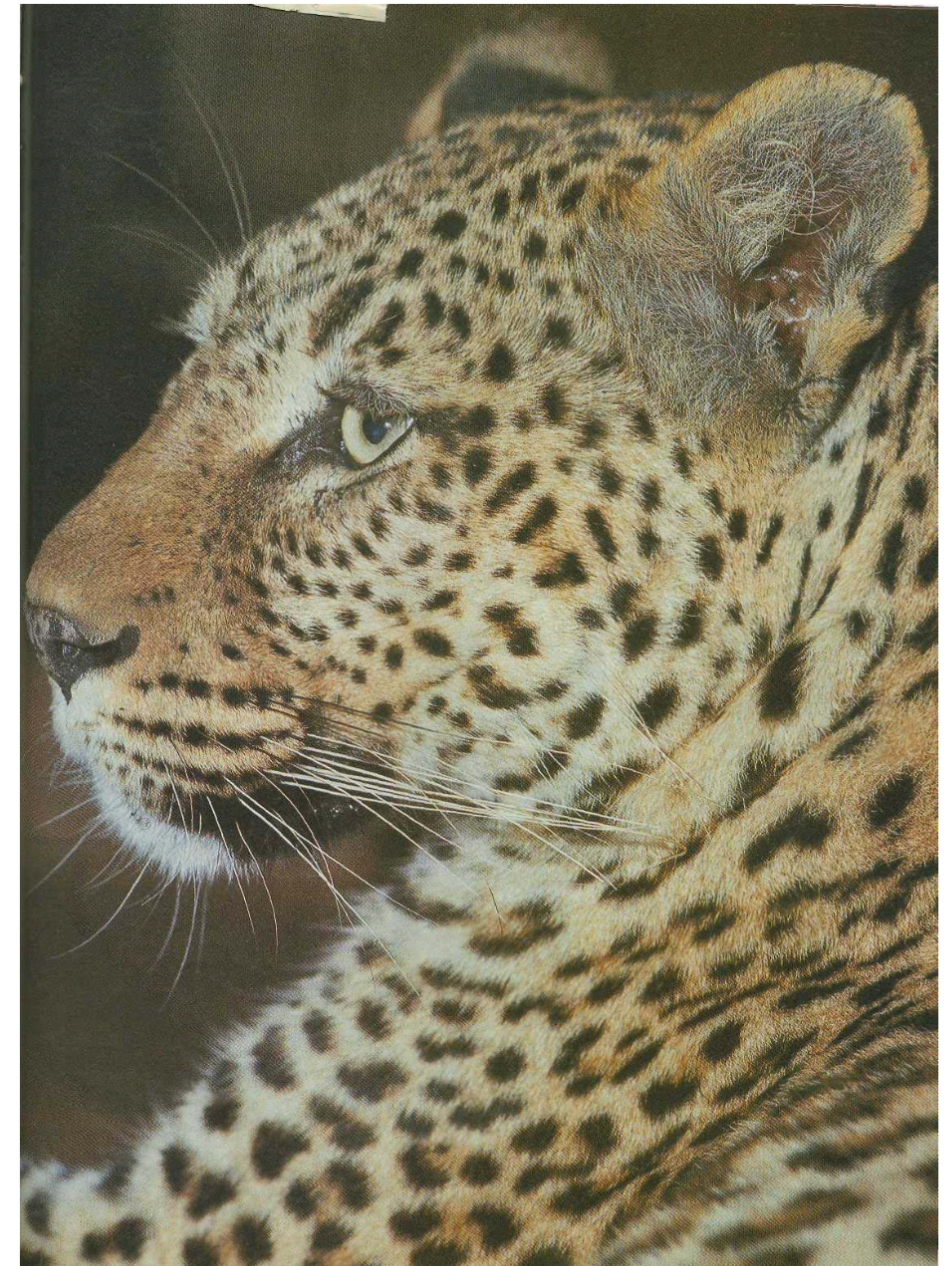
My work is based on a model developed by Alan M. Turing (the inventor of the Turing machine and the founder of modern computing science). In 1952, in one of the most important papers in theoretical biology, Turing postulated a chemical mechanism for generating coat patterns. He suggested that biological form fol-

lows a prepattern in the concentration of chemicals he called morpho-gens. The existence of morphogens is still largely speculative, except for circumstantial evidence, but Turing's model remains attractive because it appears to explain a large number of experimental results with one or two simple ideas.

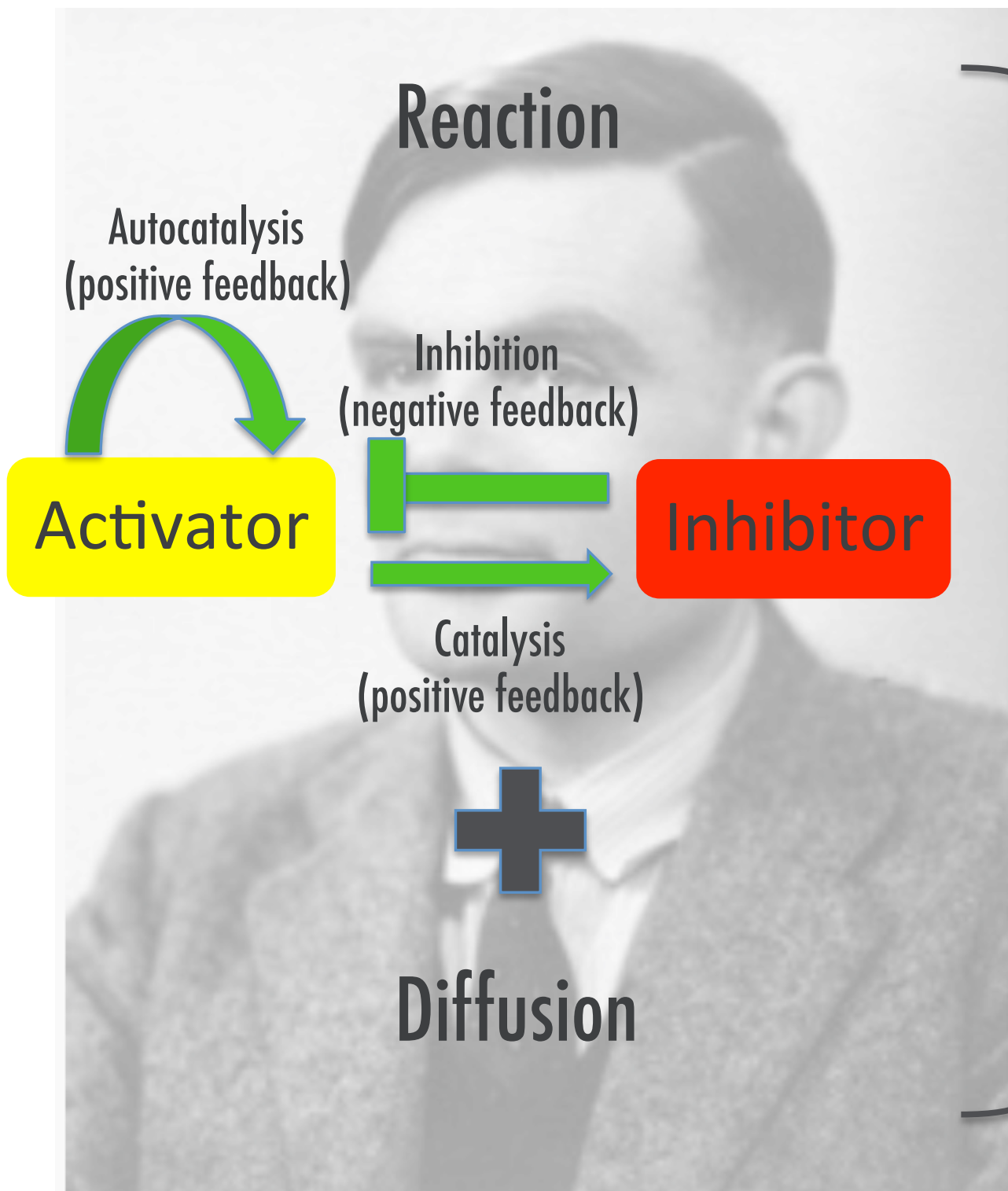
Turing began with the assumption that morphogens can react with one another and diffuse through cells. He then employed a mathematical model to show that if morphogens react and diffuse in an appropriate way, spatial patterns of morphogen concentrations can arise from an initial uniform distribution in an assemblage of cells. Turing's model has spawned an entire class of models that are now referred to as reaction-diffusion models. These models are applicable if the scale of the pattern is large compared with the diameter of an individual cell. The models are applicable to the leopard's coat, for instance, because the number of cells in a leopard spot at the time the pattern is laid down is probably on the order of 100.

Turing's initial work has been developed by a number of investigators, including me, into a more complete mathematical theory. In a typical reaction-diffusion model one starts with two morphogens that can react with each other and diffuse at varying rates. In the absence of diffusion—in a well-stirred reaction, for example—the two morphogens would react and reach a steady uniform state. If the morphogens are now allowed to diffuse at equal rates, any spatial variation from that steady state will be smoothed out. If, however, the diffusion rates are not equal,

LEOPARD reposes. Do mathematical as well as genetic rules produce its spots?



One possible mechanism: Turing instability



$u(x, y, t)$: Amount of activator at time t and position (x, y)

$v(x, y, t)$: Amount of inhibitor at time t and position (x, y)

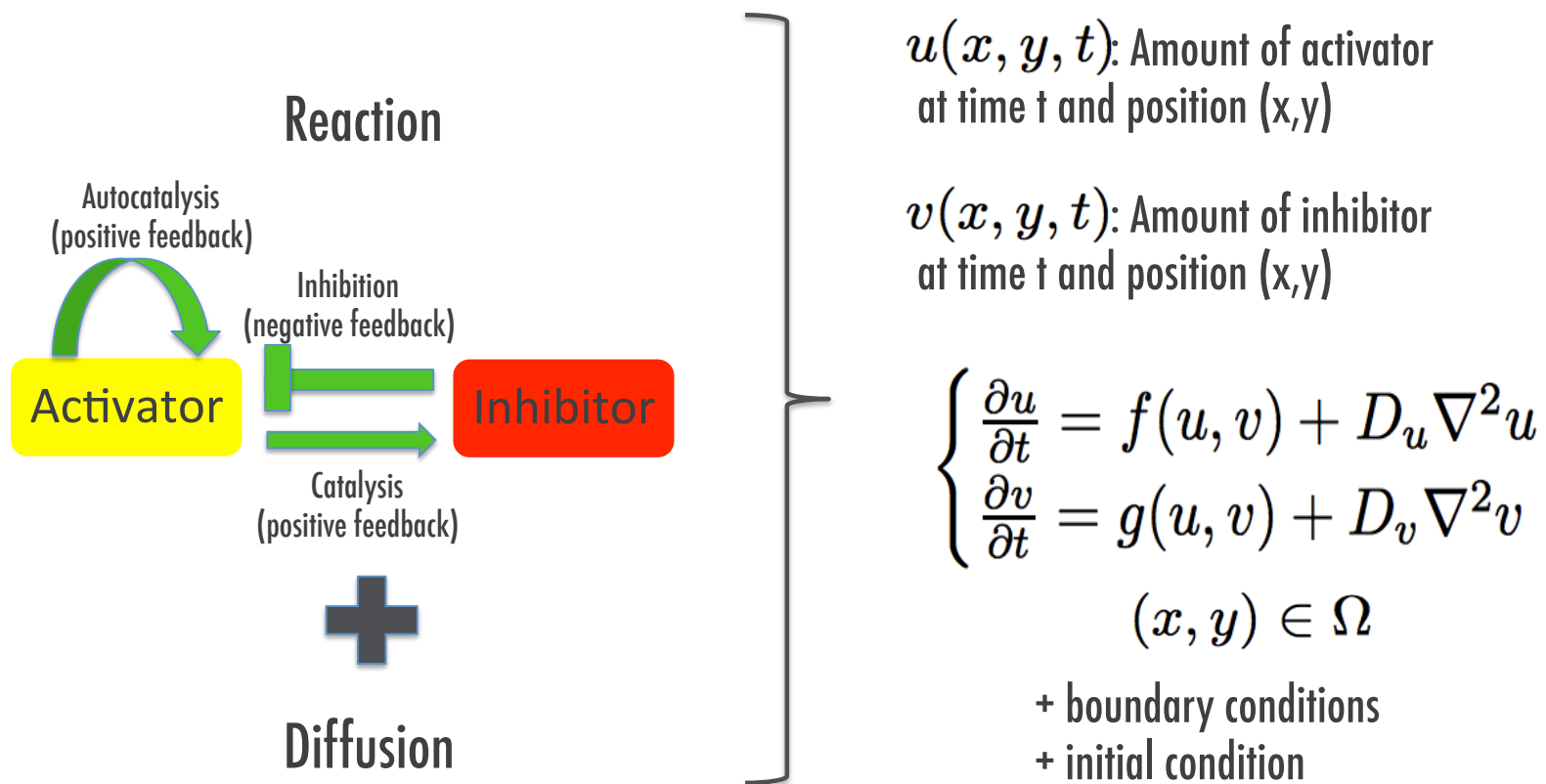
$$\begin{cases} \frac{\partial u}{\partial t} = f(u, v) + D_u \nabla^2 u \\ \frac{\partial v}{\partial t} = g(u, v) + D_v \nabla^2 v \end{cases}$$

$$(x, y) \in \Omega$$

+ boundary conditions
+ initial condition

A.M.Turing, *The chemical basis of morphogenesis*, Phil. Trans. R Soc London B, **237**, (1952), pp.37

One possible mechanism: Turing instability



$u(x, y, t)$: Amount of activator at time t and position (x, y)

$v(x, y, t)$: Amount of inhibitor at time t and position (x, y)

$$\begin{cases} \frac{\partial u}{\partial t} = f(u, v) + D_u \nabla^2 u \\ \frac{\partial v}{\partial t} = g(u, v) + D_v \nabla^2 v \end{cases}$$

$$(x, y) \in \Omega$$

+ boundary conditions

+ initial condition

Diffusion can drive an instability by perturbing a homogeneous stable (in absence of diffusion) fixed point.

Hence as the perturbation grows, non-linearities enter into the game yielding an asymptotic, spatially inhomogeneous, steady state (stationary pattern) or time varying one (wave like pattern).

A.M.Turing, *The chemical basis of morphogenesis*, Phil. Trans. R Soc London B, **237**, (1952), pp.37

Patterns of complexity

The Turing mechanism provides a paradigm for the spontaneous generation of patterns in reaction-diffusion systems. A framework that describes Turing-pattern formation in the context of complex networks should provide a new basis for studying the phenomenon.

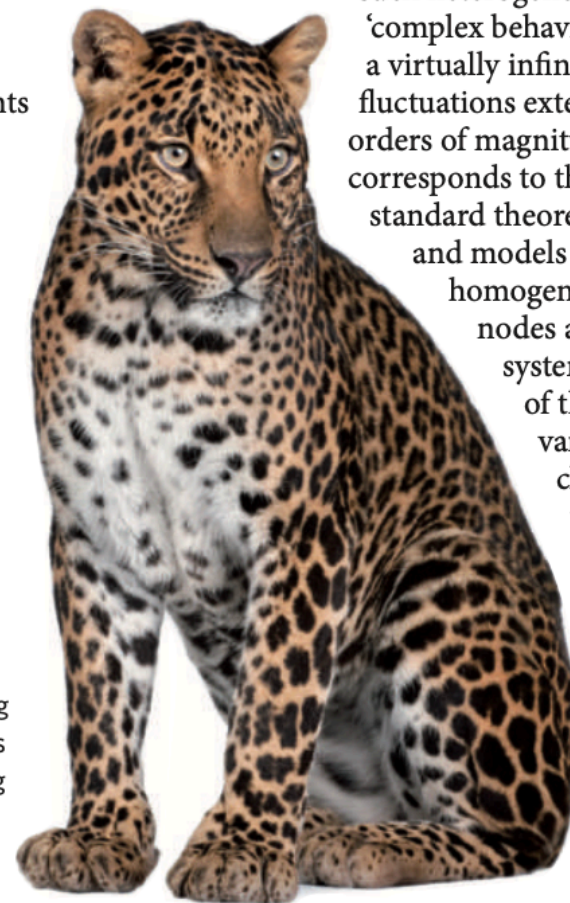
Romualdo Pastor-Satorras and Alessandro Vespignani

We live in the age of networks. The Internet and the cyberworld are networks that we navigate and explore on a daily basis. Social networks, in which nodes represent individuals and links potential interactions, serve to model human interaction. Mobility, ecological, and epidemiological models rely on networks that consist of entire populations interlinked by virtue of the exchange of individuals. Network science, therefore, is where we can expect answers to many pressing problems of our modern world, from controlling traffic flow and flu pandemics to constructing robust power grids and communication networks. But there is more than nodes and links. An important development of recent years has been the realization that the topology of a network critically influences the dynamical processes happening on it¹. Hiroya Nakao and Alexander Mikhailov have now tackled the problem of the effects of network structure on the emergence of so-called Turing patterns in nonlinear diffusive systems. With their study, reported in *Nature Physics*², they offer a new perspective on an area that has potential applications in ecology and developmental morphogenesis.

In the past decade the physics community has contributed greatly to the field of network science, by defining a fresh perspective to understand the complex interaction patterns of many natural and artificial complex systems. In particular, the application of nonlinear-dynamics and statistical-physics techniques,

boosted by the ever-increasing availability of large data sets and computer power for their storage and manipulation, has provided tools and concepts for tackling the problems of complexity and self-organization of a vast array of networked systems in the technological, social and biological realms³⁻⁶. Since the earliest works that unveiled the complex structural properties of networks, statistical-physics and nonlinear-dynamics approaches have been also exploited as a convenient strategy for characterizing emergent macroscopic phenomena in terms of the dynamical evolution of the basic elements of a given system. This has led to the development of mathematical methods that have helped to expose the potential implications of the structure of networks for the various physical and dynamical processes occurring on top of them.

A complex beast. The markings on leopards and other animals might be a manifestation of Turing-pattern formation during morphogenesis^{8,9}. A new framework for studying the Turing mechanism on complex networks should deepen our understanding of the process and its consequences. Image credit: © iStockphoto / Eric Isselée



It has come as a surprise then to discover that most of the standard results concerning dynamical processes obtained in the early studies of percolation and spreading processes in complex networks are radically altered once topological fluctuations and the complex features observed in most real-world networks are factored in¹. The resilience of networks, their vulnerability to attacks and their spreading-synchronization characteristics are all drastically affected by topological heterogeneities. By no means can

such heterogeneities be neglected: 'complex behaviour' often implies a virtually infinite amount of fluctuations extending over several orders of magnitude. This generally corresponds to the breakdown of standard theoretical frameworks and models that assume homogeneous distributions of nodes and links. Therefore systematic investigations of the impact of the various network characteristics on the basic features of equilibrium and non-equilibrium dynamical processes are called for.

The work of Nakao and Mikhailov², in which they study the Turing

A background graphic featuring a complex network of interconnected nodes and lines. The nodes are represented by circles in various shades of green and blue, some solid and some dashed. The lines connecting them are thin and light blue. The overall pattern is dense and abstract, suggesting a digital or biological network.

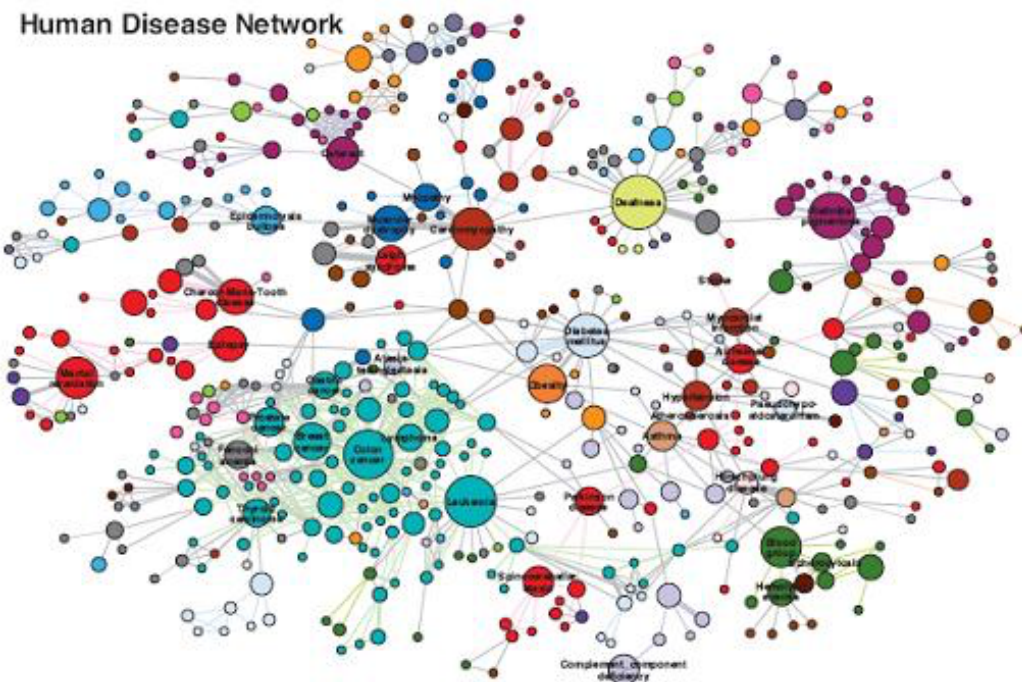
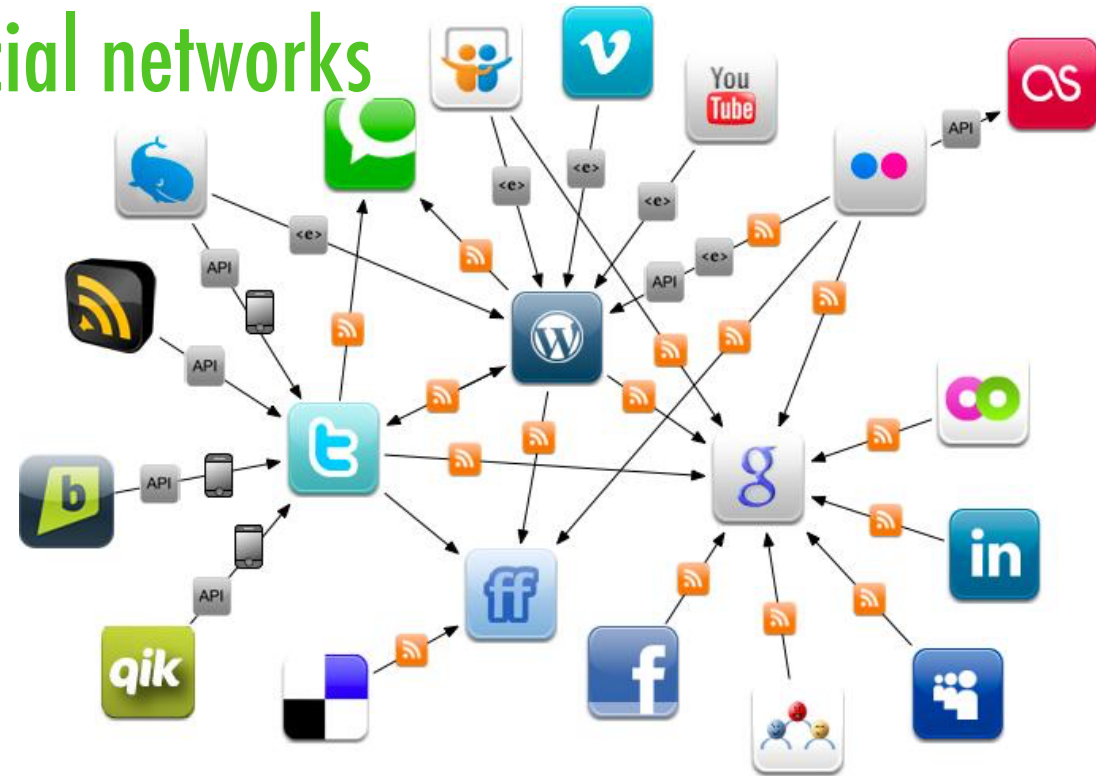
networks

Networks are everywhere

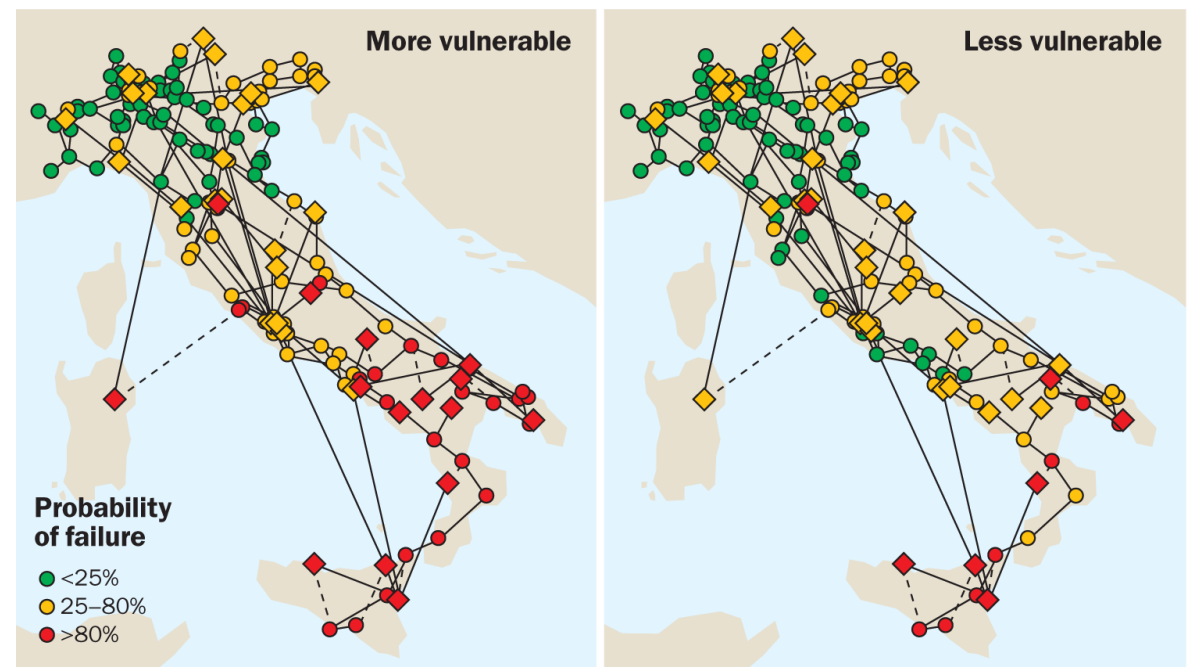


world flights map

social networks

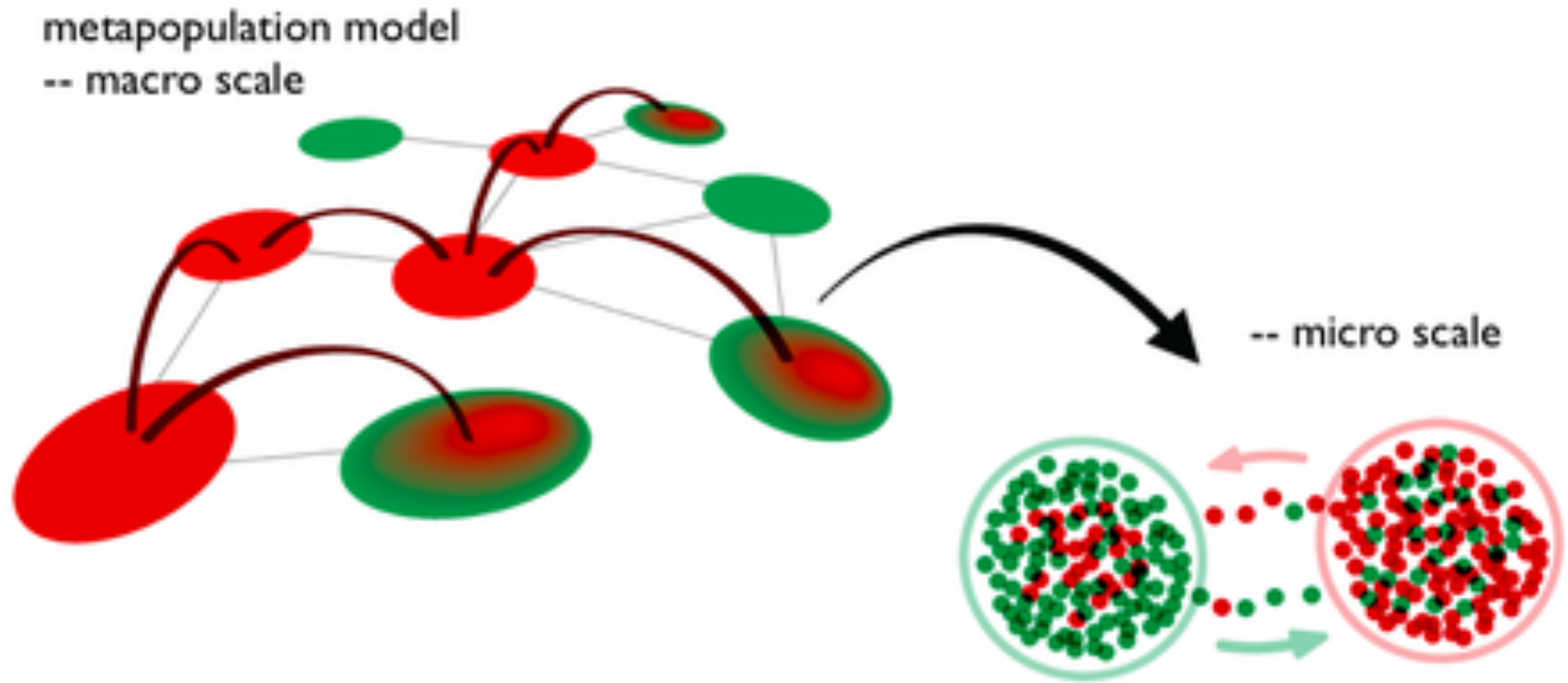


proteins networks



technological networks

Reactions occur at each node. Diffusion occurs across edges.



May R., Will a large complex system be stable? *Nature*, 238, pp. 413, (1972)

Reaction term :

$$\begin{cases} \dot{u}_i(t) &= f(u_i(t), v_i(t)) \\ \dot{v}_i(t) &= g(u_i(t), v_i(t)) \end{cases} \quad \forall i = 1, \dots, n \text{ and } t > 0.$$

At each node $i=1,\dots,n$, “species” u and v react through some non-linear functions f and g depending on the quantities available at node i -th (metapopulation assumption)

Nakao H. and Mikhailov A. S., Turing patterns in network-organized activator–inhibitor systems, Nature Physics, 6, pp. 544 (2010)

Diffusion term :

Incidence matrix

$$B_{ie} = \begin{cases} 1 & \text{if } e = \{i, j\} \text{ and } j > i \\ -1 & \text{if } e = \{i, j\} \text{ and } j < i \\ 0 & \text{otherwise} \end{cases}$$

System state vector $\vec{u}(t) = (u_1(t), \dots, u_n(t))^T$

Links current vector $\vec{\chi}(t) = (\chi_{e_1}(t), \dots, \chi_{e_m}(t))^T$

$$\chi_e(t) = -D_u [u_j(t) - u_i(t)] \equiv D_u [\mathbf{B}^T \vec{u}(t)]_e \quad \text{constitutive equation (Fick's first law)}$$

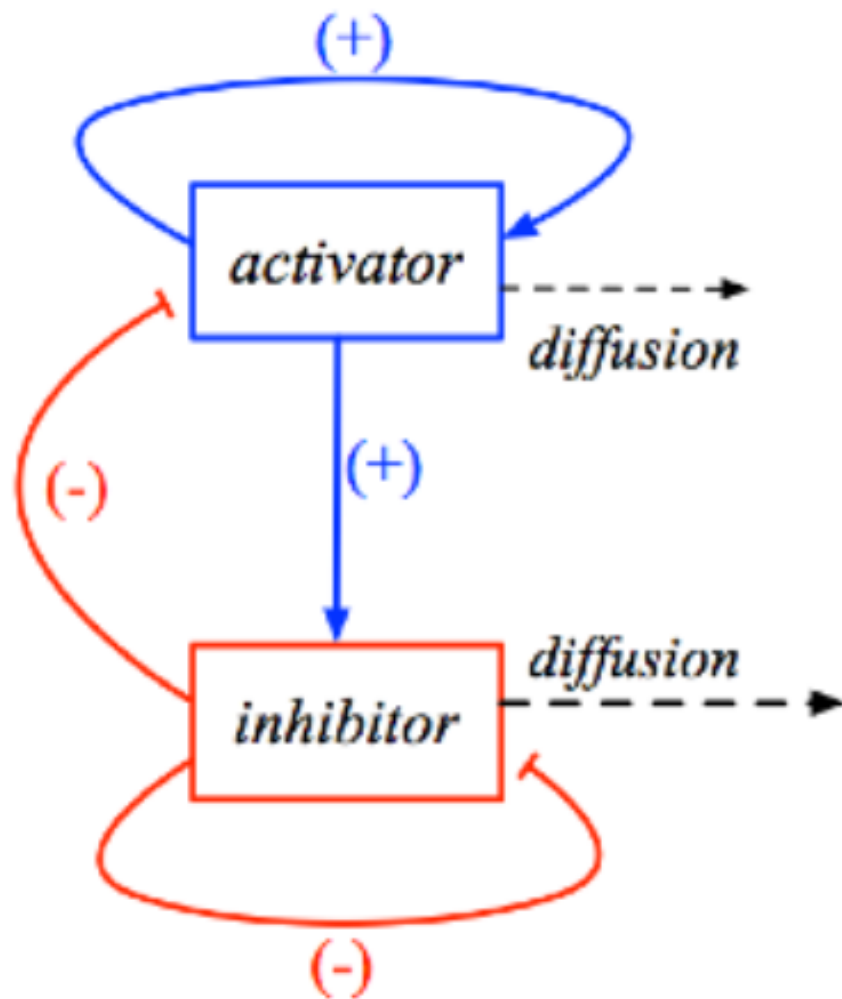
$$\dot{u}_i(t) = -[\mathbf{B} \vec{\chi}(t)]_i \quad \text{continuity equation}$$

$$\dot{\vec{u}}(t) = -\mathbf{B} \vec{\chi} = -D_u \mathbf{B} \mathbf{B}^T \vec{u} =: D_u \mathbf{L} \vec{u}, \quad \text{(Fick's second law)}$$

\mathbf{L} : Laplacian matrix of the network

Diffusive transport of species into a certain node i is given by the sum of incoming fluxes to node i from other connected nodes j , fluxes are proportional to the concentration difference between the nodes (Fick's law).

Turing mechanism: diffusion driven instability



$u_i(t)$ Amount of activator in node i at time t

$v_i(t)$ Amount of inhibitor in node i at time t

$$\begin{cases} \dot{u}_i &= f(u_i, v_i) + D_u \sum_j L_{ij} u_j \\ \dot{v}_i &= g(u_i, v_i) + D_v \sum_j L_{ij} v_j \end{cases}$$

Local reaction term

Diffusion term (Fick's law)

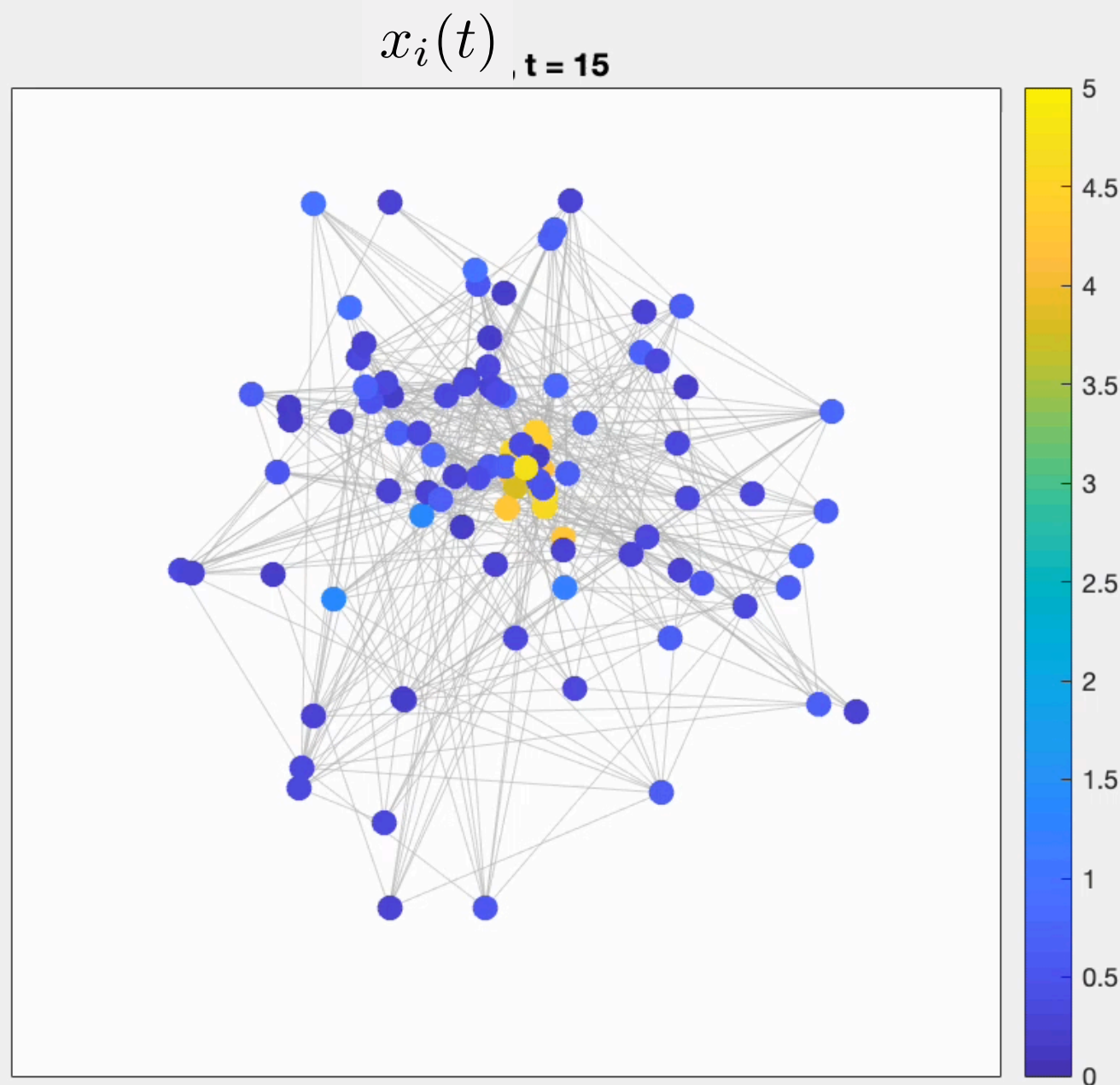
$L_{ij} = A_{ij} - k_i \delta_{ij}$ Symmetric Laplace matrix

A_{ij} Symmetric Adjacency matrix

Nakao H. and Mikhailov A. S., Turing patterns in network-organized activator-inhibitor systems, Nature Physics, 6, pp. 544 (2010)

Turing patterns on networks

Patterns:
Sets of nodes whose
asymptotic state is far from
the homogeneous equilibrium.



The Brusselator

$$\begin{cases} f_x(x_i, y_i) = 1 - (b + 1)x_i + cx_i^2y_i \\ f_y(x_i, y_i) = bx_i - cx_i^2y_i, \end{cases}$$

Turing mechanism: diffusion driven instability

1) Assume there exists a spatially homogeneous stable solution:

$$u_i = \hat{u} \text{ and } v_i = \hat{v} \quad \forall i$$

2) Linearise around this solution: $u_i = \delta u_i + \hat{u}$ and $v_i = \hat{v} + \delta v_i$

$$\begin{pmatrix} \dot{\delta u} \\ \dot{\delta v} \end{pmatrix} = \tilde{\mathcal{J}} \begin{pmatrix} \delta u \\ \delta v \end{pmatrix} \quad \tilde{\mathcal{J}} = \begin{pmatrix} f_u + D_u \mathbf{L} & f_v \\ g_u & g_v + D_v \mathbf{L} \end{pmatrix}$$

3) Prove that the spatially homogeneous solution:

$$u_i = \hat{u} \text{ and } v_i = \hat{v} \quad \forall i$$

turns out to be unstable once the diffusion is in action

$$D_u > 0 \text{ and } D_v > 0$$

3) Prove that the spatially homogeneous solution:

$$u_i = \hat{u} \text{ and } v_i = \hat{v} \quad \forall i$$

turns out to be unstable once the diffusion is in action

$$D_u > 0 \text{ and } D_v > 0$$

Sketch of the proof

i) Let $L\vec{\phi}^\alpha = \Lambda^\alpha \vec{\phi}^\alpha$, $\alpha = 1, \dots, n$ $\vec{\phi}^\alpha = (\phi_1^\alpha, \dots, \phi_n^\alpha)^\top$

$$\sum_i \phi_i^\alpha \phi_i^\beta = \delta_{\alpha\beta} \quad \Lambda^\alpha \leq 0$$

ii) decompose the solution on the eigenbasis and use the ansatz

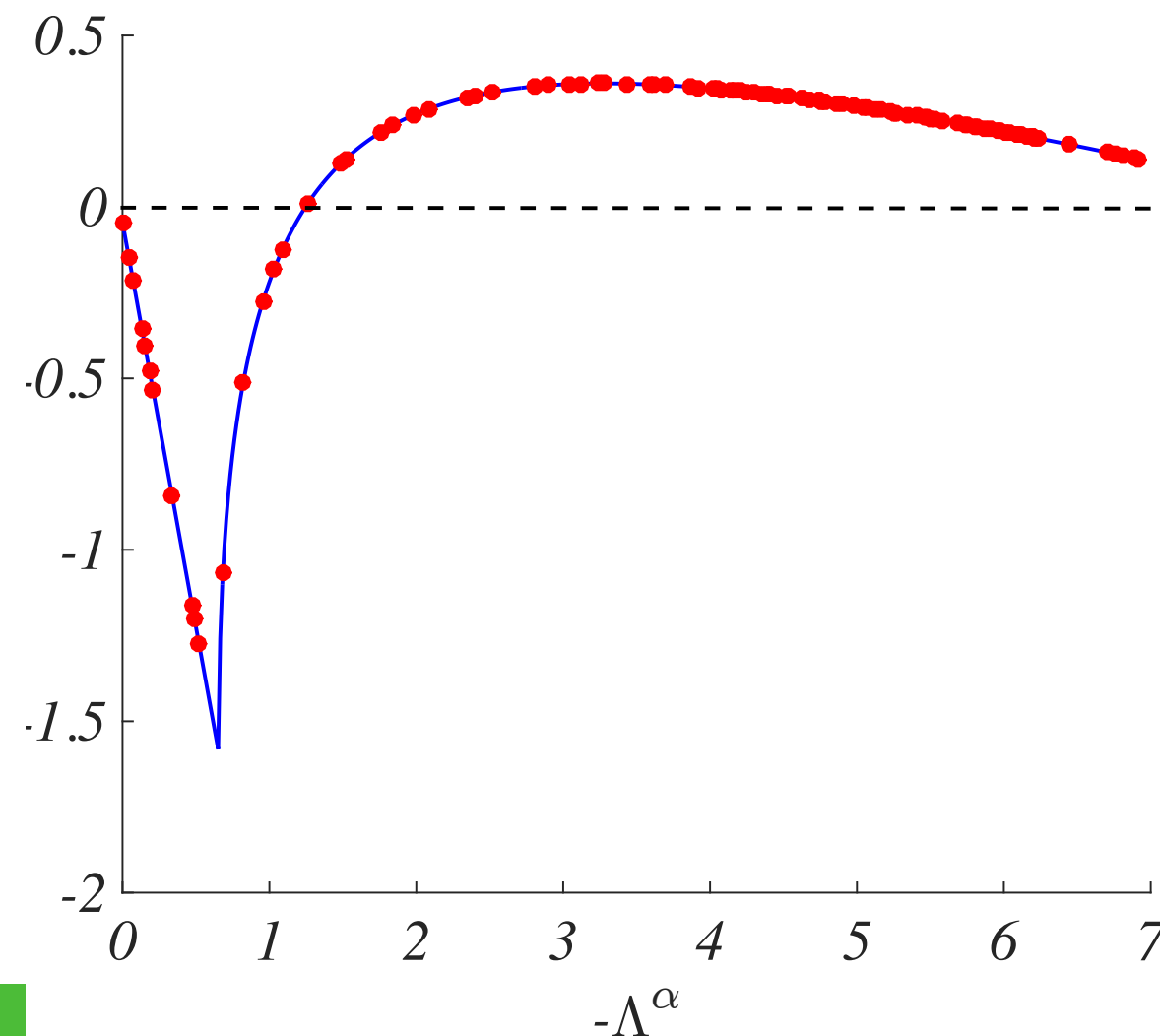
$$\delta u_i(t) = \sum_{\alpha=1}^n c_\alpha \phi_i^\alpha e^{\lambda_\alpha t}$$

General strategy for the network case

iii) λ_α (called dispersion relation) is solution of

$$\det \left[\lambda_\alpha - \begin{pmatrix} f_u + D_u \Lambda^\alpha & f_v \\ g_u & g_v + D_v \Lambda^\alpha \end{pmatrix} \right] = 0$$

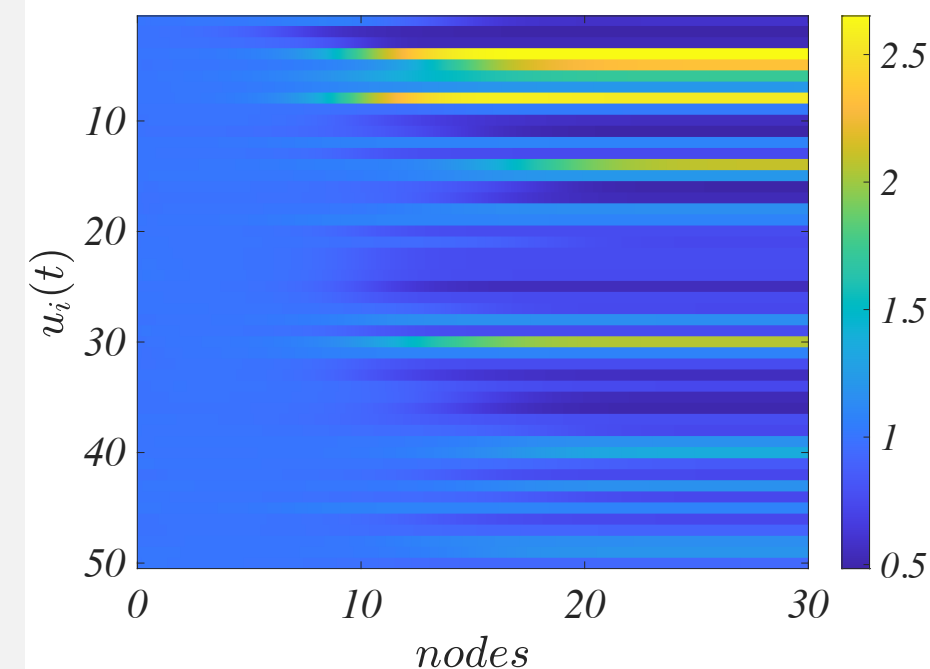
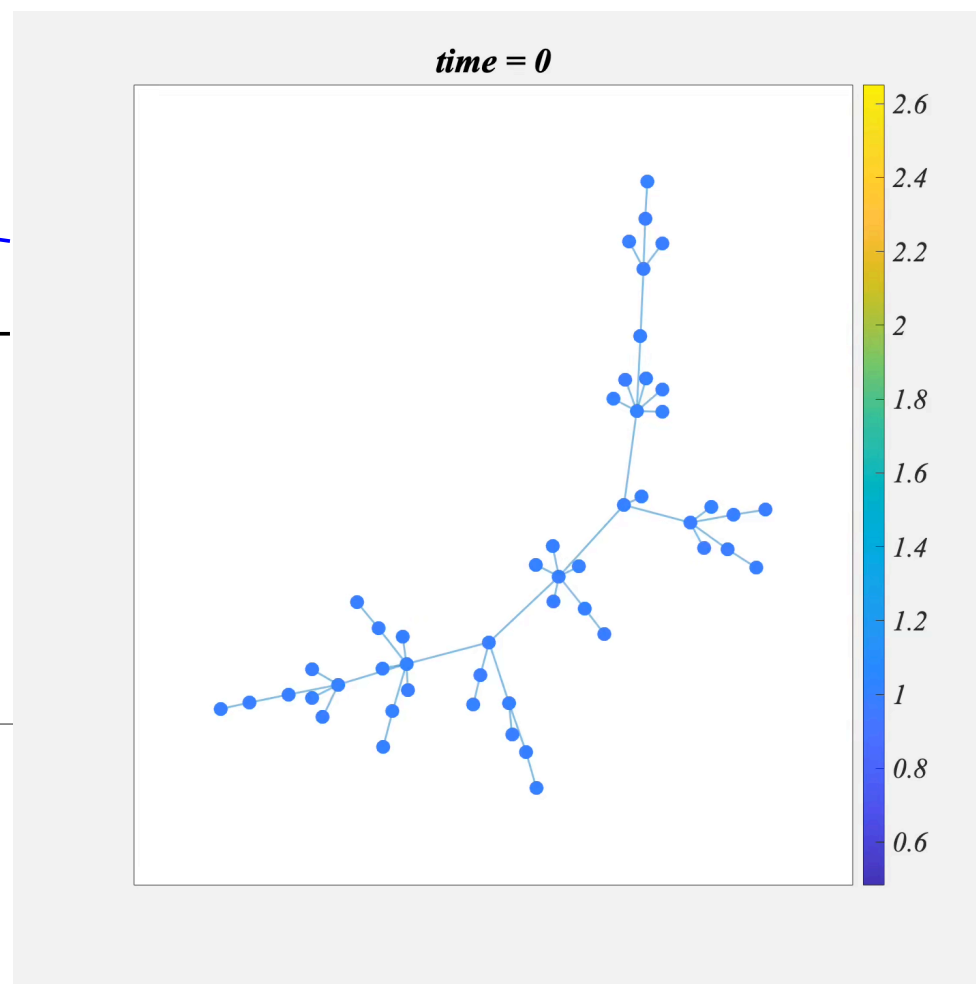
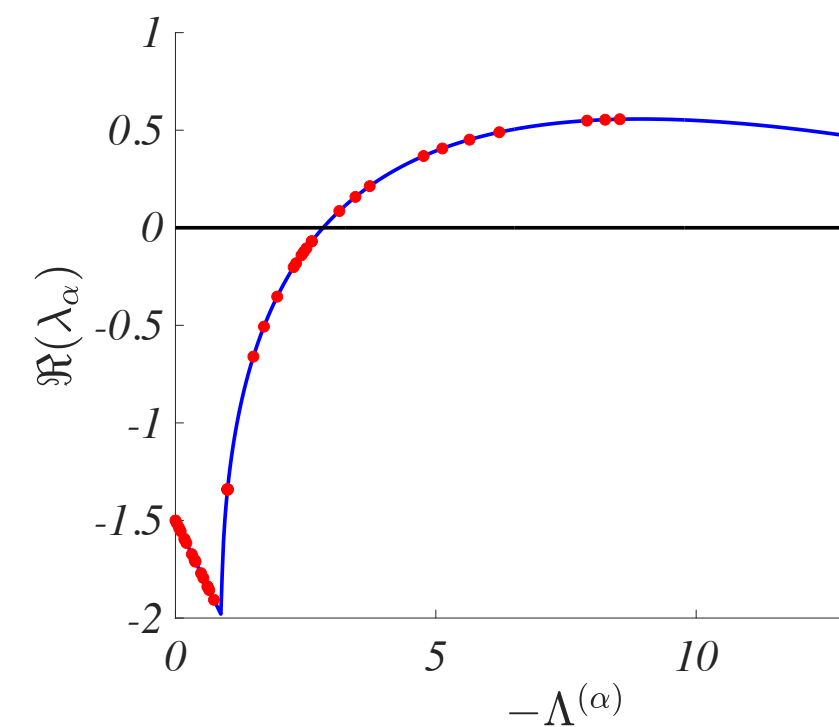
iv) if there exists Λ^{α_c} such that $\Re \lambda_{\alpha_c} > 0$ then Turing patterns do emerge.



The Brusselator

$$\begin{cases} \dot{u}_i &= 1 - (b + 1)u_i + cu_i^2v_i + D_u \sum_j L_{ij}u_j \\ \dot{v}_i &= bu_i - cu_i^2v_i + D_v \sum_j L_{ij}v_j \end{cases}$$

$(u^*, v^*) = (1, b/c)$ equilibrium isolated system (no diffusion)



The theory of pattern formation on directed networks

Malbor Asllani^{1,2}, Joseph D. Challenger², Francesco Saverio Pavone^{2,3,4}, Leonardo Sacconi^{3,4} & Duccio Fanelli²

$$\begin{cases} \dot{u}_i &= f(u_i, v_i) + D_u \sum_j L_{ij} u_j \\ \dot{v}_i &= g(u_i, v_i) + D_v \sum_j L_{ij} v_j \end{cases}$$

A_{ij} **Asymmetric Adjacency matrix** $A_{ij} = 1$ if $j \rightarrow i$

$L_{ij} = A_{ij} - k_i^{(in)} \delta_{ij}$ **Asymmetric Laplace matrix**

$$k_i^{(in)} = \sum_j A_{ij}$$

Complex spectrum

$$\Lambda^{(\alpha)} \in \mathbb{C}$$

Turing patterns on directed networks

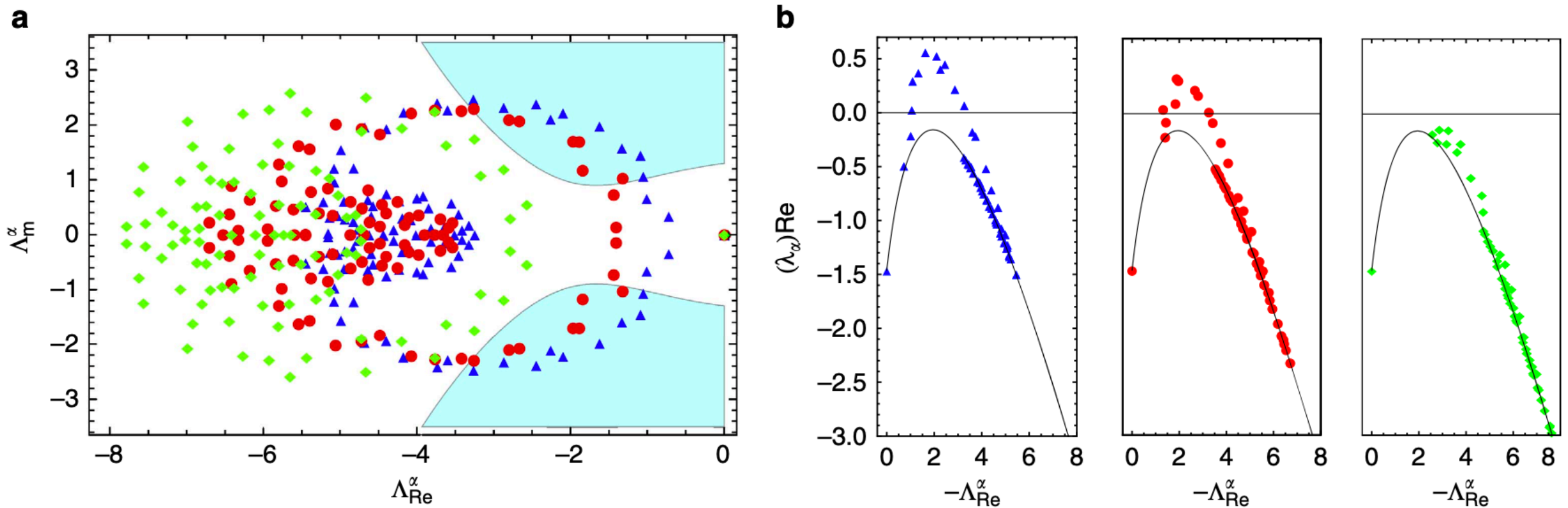


Figure 1 | Instabilities on NW networks. (a) Spectral plot of three Laplacians generated from the NW algorithm for $p = 0.27$, $p = 0.5$ and $p = 0.95$ (blue triangles, red circles and green diamonds, respectively) and network size $\Omega = 100$. The shaded area indicates the instability region for the case of the Brusselator model, where the parameters are $b = 9$, $c = 30$, $D_\phi = 1$ and $D_\psi = 7$. (b) The real part of the dispersion relation for the same three choices of NW networks as in (a). The black line originates from the continuous theory.

$$\left[\Im \Lambda^{(s)} \right]^2 S_2 \left(\Re \Lambda^{(s)} \right) < -S_1 \left(\Re \Lambda^{(s)} \right)$$

Region of (in)stability

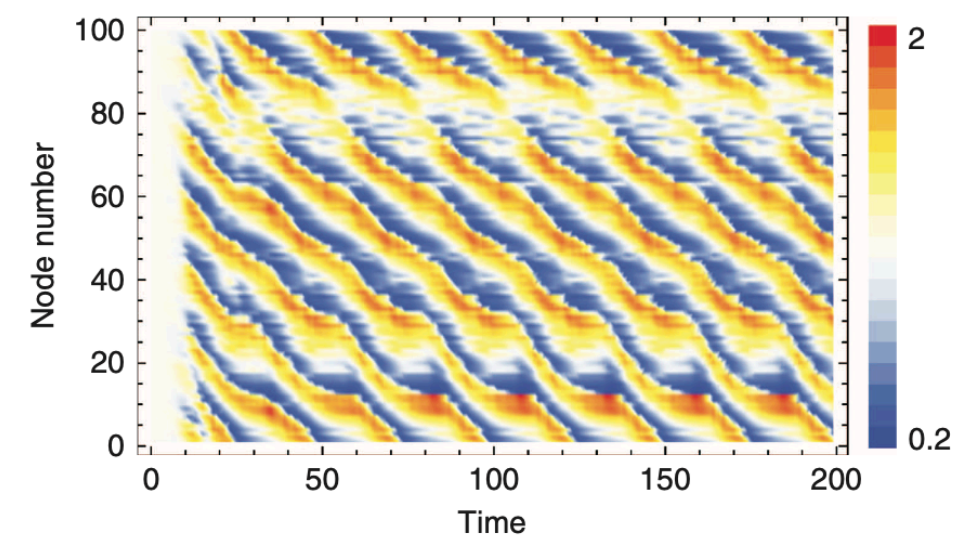


Figure 2 | Waves on an NW network. Time series for the case of the Brusselator model on an NW network, generated with $p = 0.27$. The nodes are ordered as per the original lattice. Details of the network's spectra and the system's instability are displayed by the blue, triangular symbols in Fig. 1. The reaction parameters are $b = 9$, $c = 30$, $D_\phi = 1$ and $D_\psi = 7$.

Pattern reconstruction through generalized eigenvectors on defective networks

MARIE DORCHAIN, RICCARDO MUOLO and TIMOTEO CARLETTI^(a) 

No need for eigenvectors !

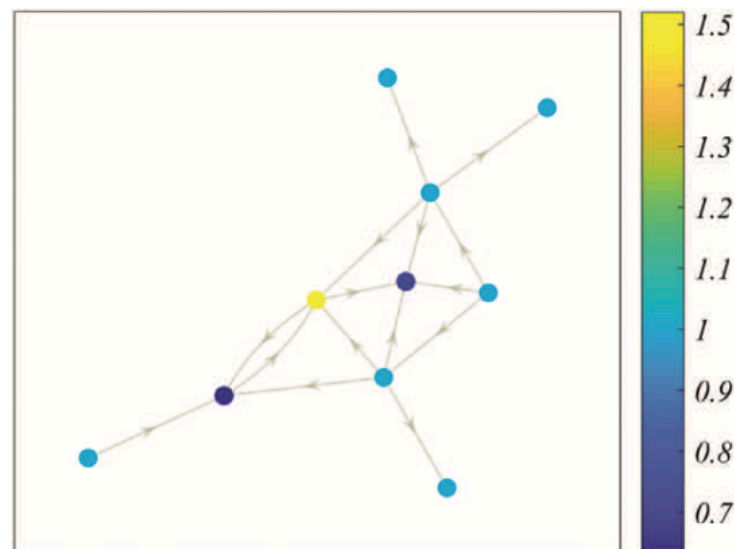
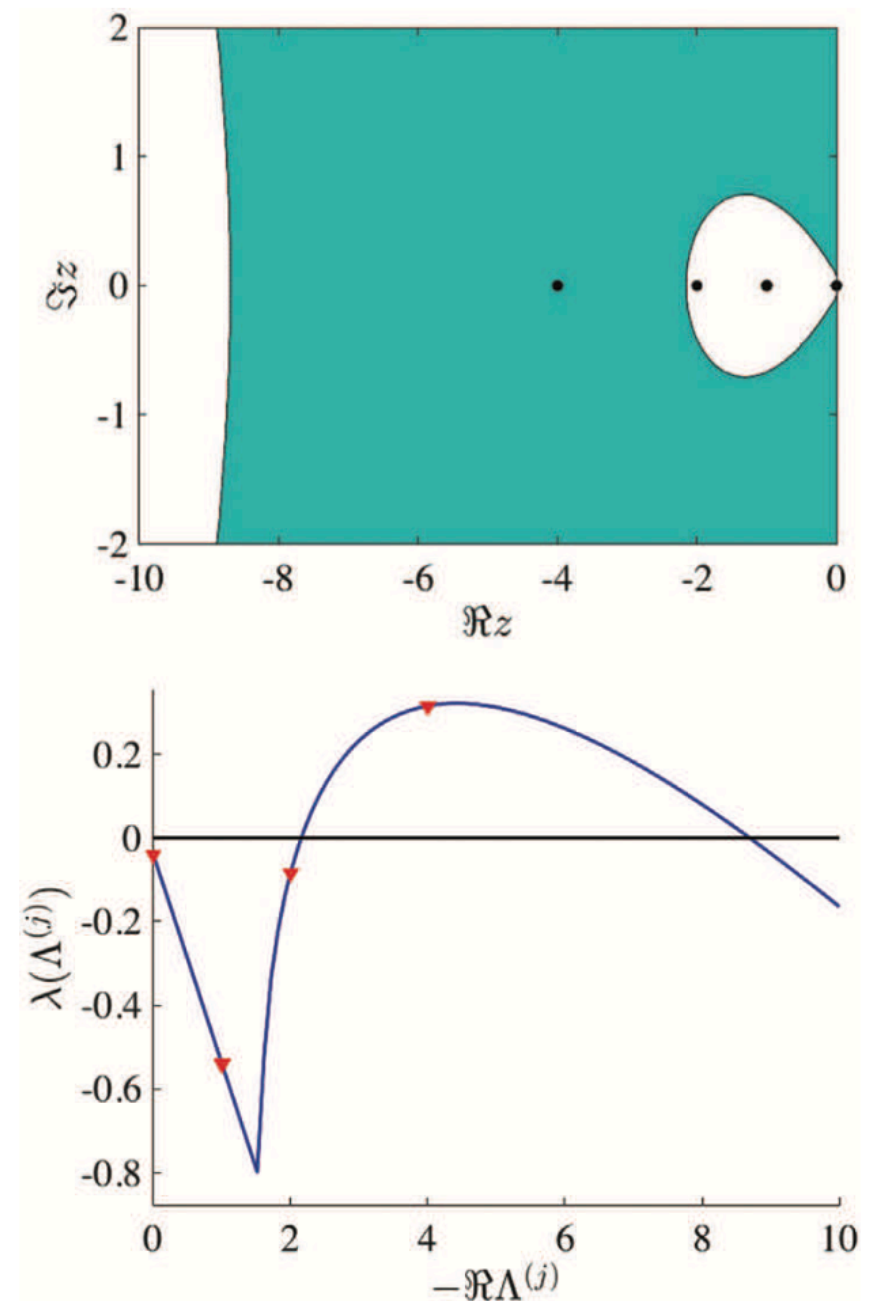


Fig. 2: Random non-normal defective network composed by $n = 10$ nodes, built by using a directed Erdős-Rényi algorithm where the probability to create a bidirectional link is 0.2 and the probability to transform it into a directed one is 0.6. Nodes have been colored according to the value of species u at time $\hat{t} = 200$ (see colorbar).



Turing mechanism: diffusion driven instability

Elegant and simple, but unable to describe patterns onset in some real scenarios.

▶ At least two diffusing species are needed;

▶ Activator and inhibitor are both necessary :

$$f_u g_v < 0$$

▶ The inhibitor must diffuse much faster than the activator;

$$D_v \gg D_u$$

▶ Based on parabolic PDE (heat equation), hence infinite propagation of signals.

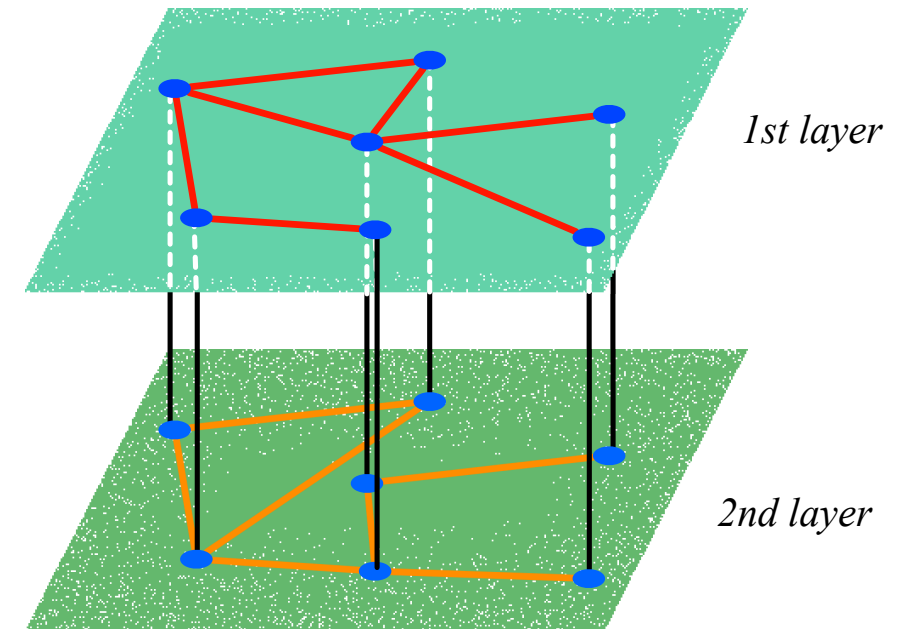
Turing instability on multiplex networks

adjacency matrix of
layer K

degree of i-th node
in layer K

$$L_{ij}^K = A_{ij}^K - \delta_{ij} k_i^K$$

Laplacian matrix of
layer K



The same Ω nodes are present in each layer

$D_{u,v}^K$ **inter-layer** diffusion coefficient

$D_{u,v}^{12}$ **intra-layer** diffusion coefficient

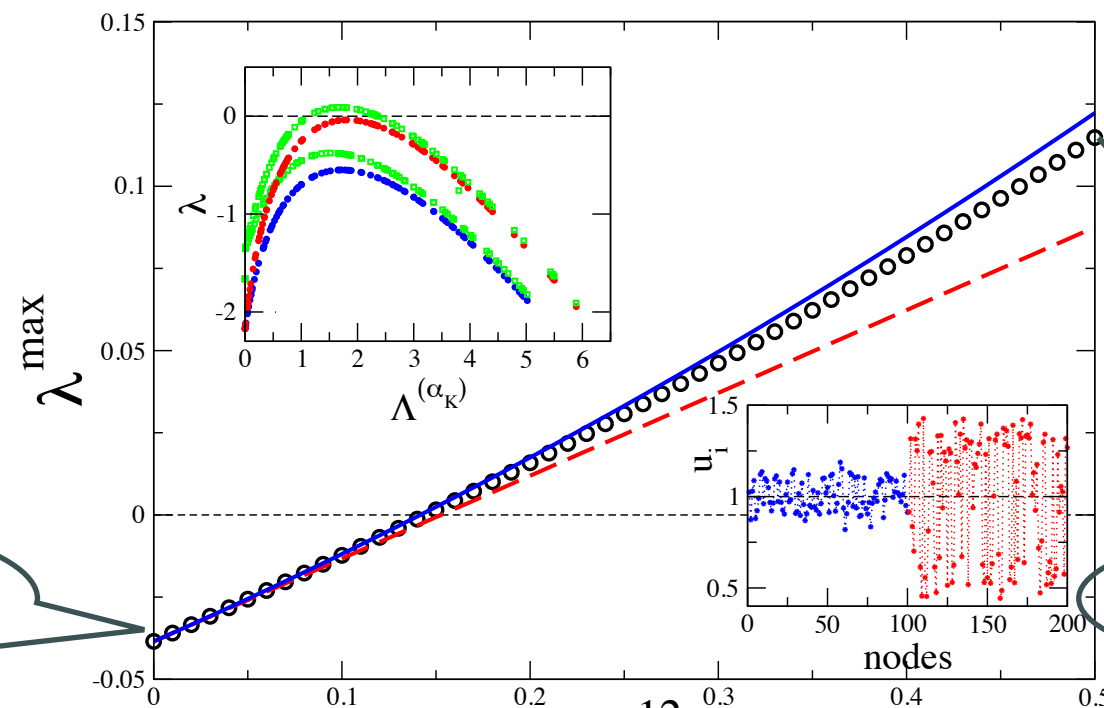
$$\begin{cases} \dot{u}_i^K &= f(u_i^K, v_i^K) + D_u^K \sum_{j=1}^{\Omega} L_{ij}^K u_j^K + D_u^{12} (u_i^{K+1} - u_i^K) \\ \dot{v}_i^K &= g(u_i^K, v_i^K) + D_v^K \sum_{j=1}^{\Omega} L_{ij}^K v_j^K + D_v^{12} (v_i^{K+1} - v_i^K) \end{cases}$$

Onset of patterns

PHYSICAL REVIEW E **90**, 042814 (2014)

Turing patterns in multiplex networks

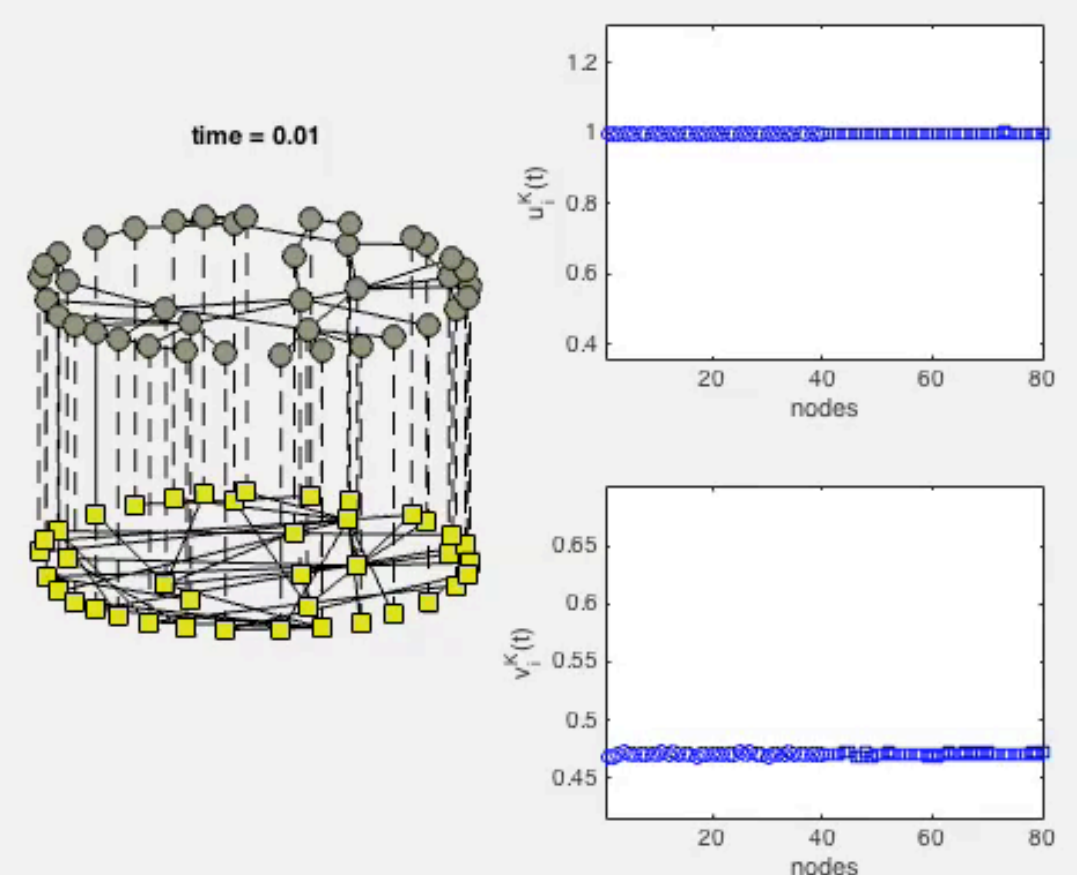
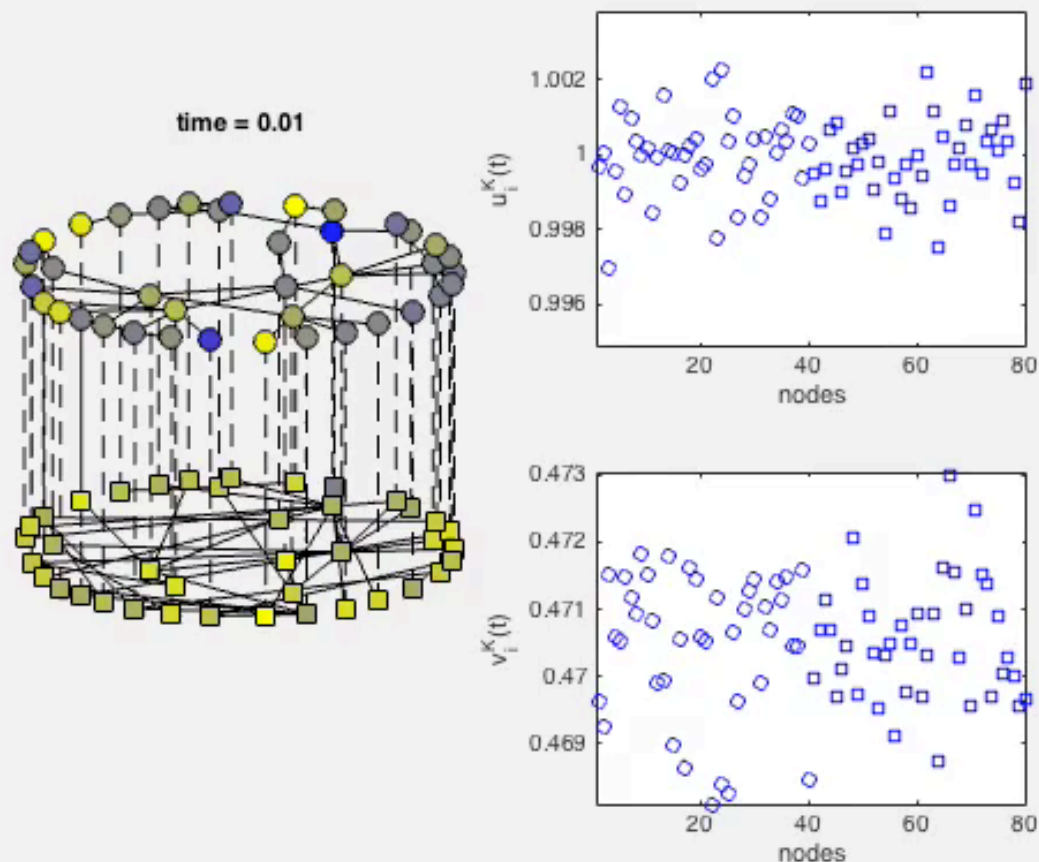
Malbor Asllani,^{1,2} Daniel M. Busiello,² Timoteo Carletti,³ Duccio Fanelli,² and Gwendoline Planchon^{2,3}



$$D_v^{12} = D_u^{12} = 0$$

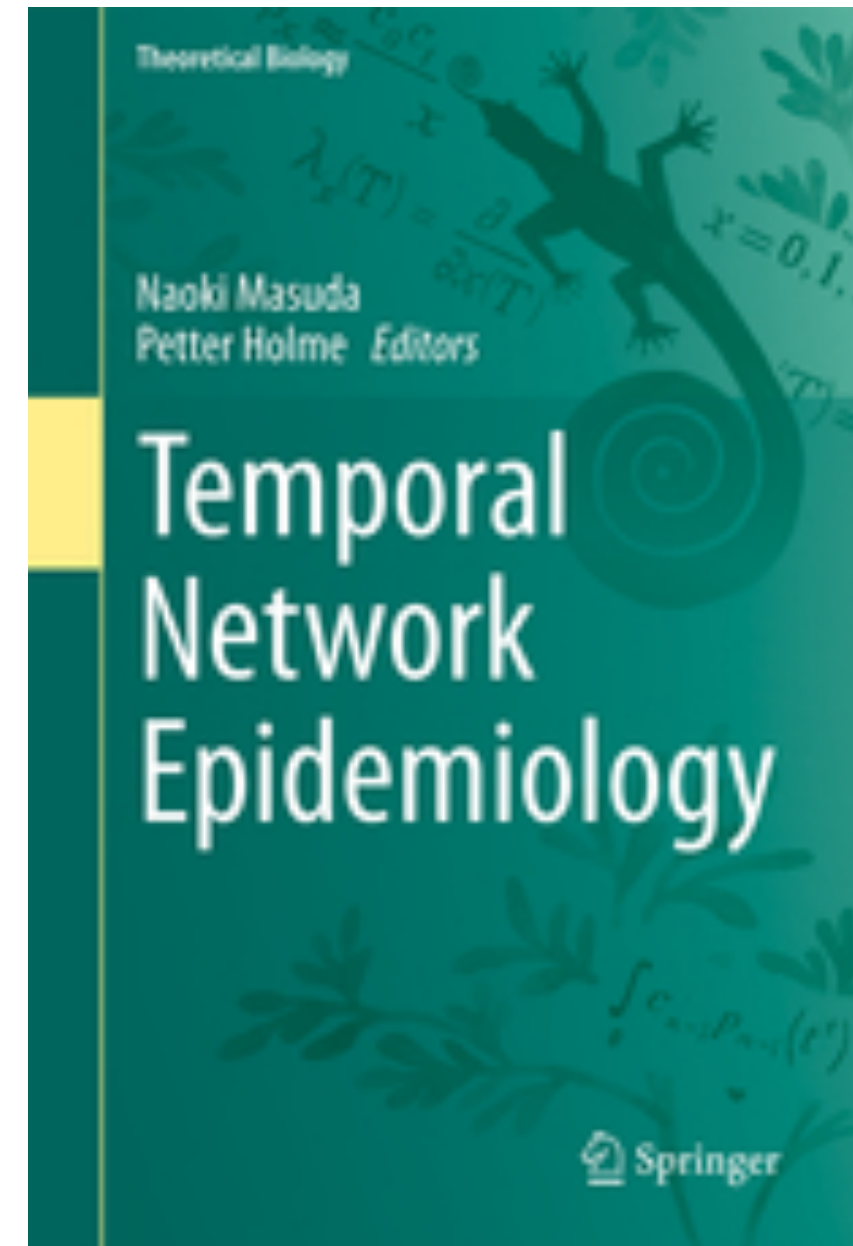
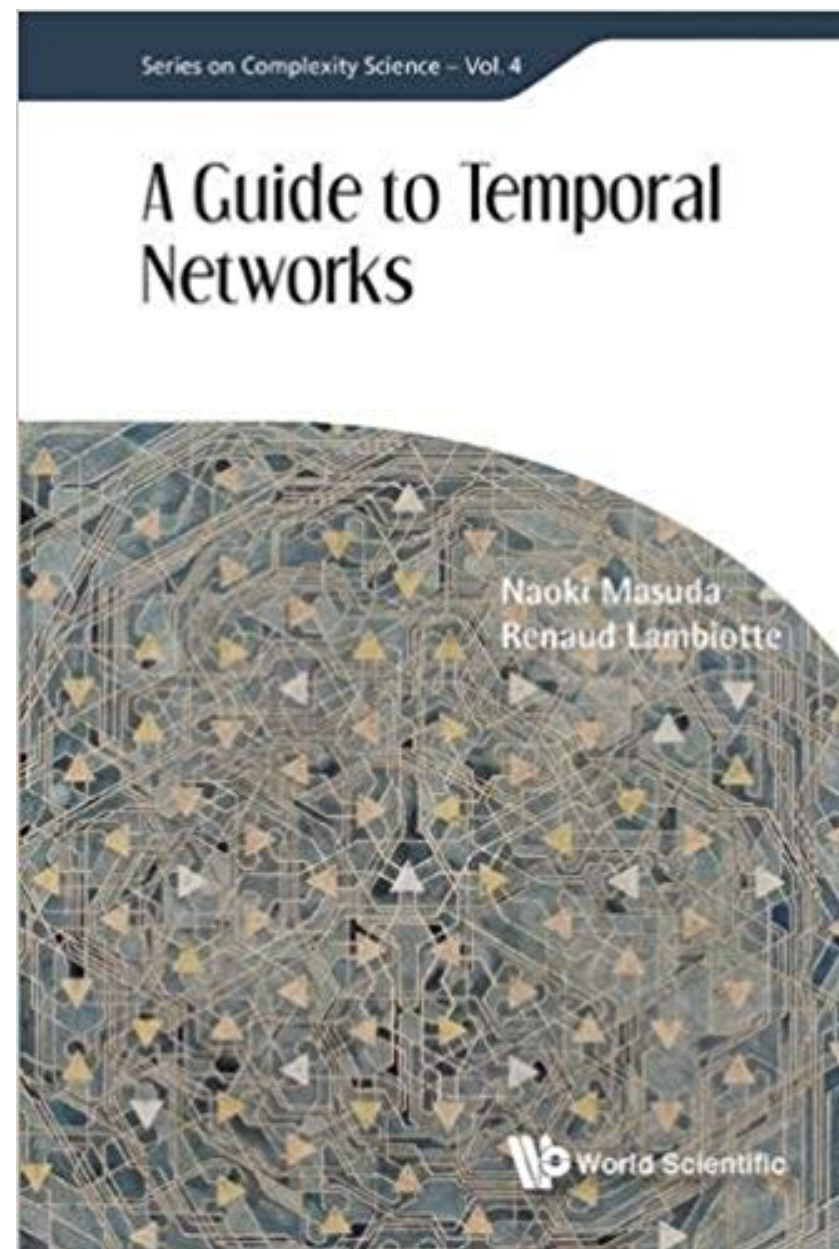
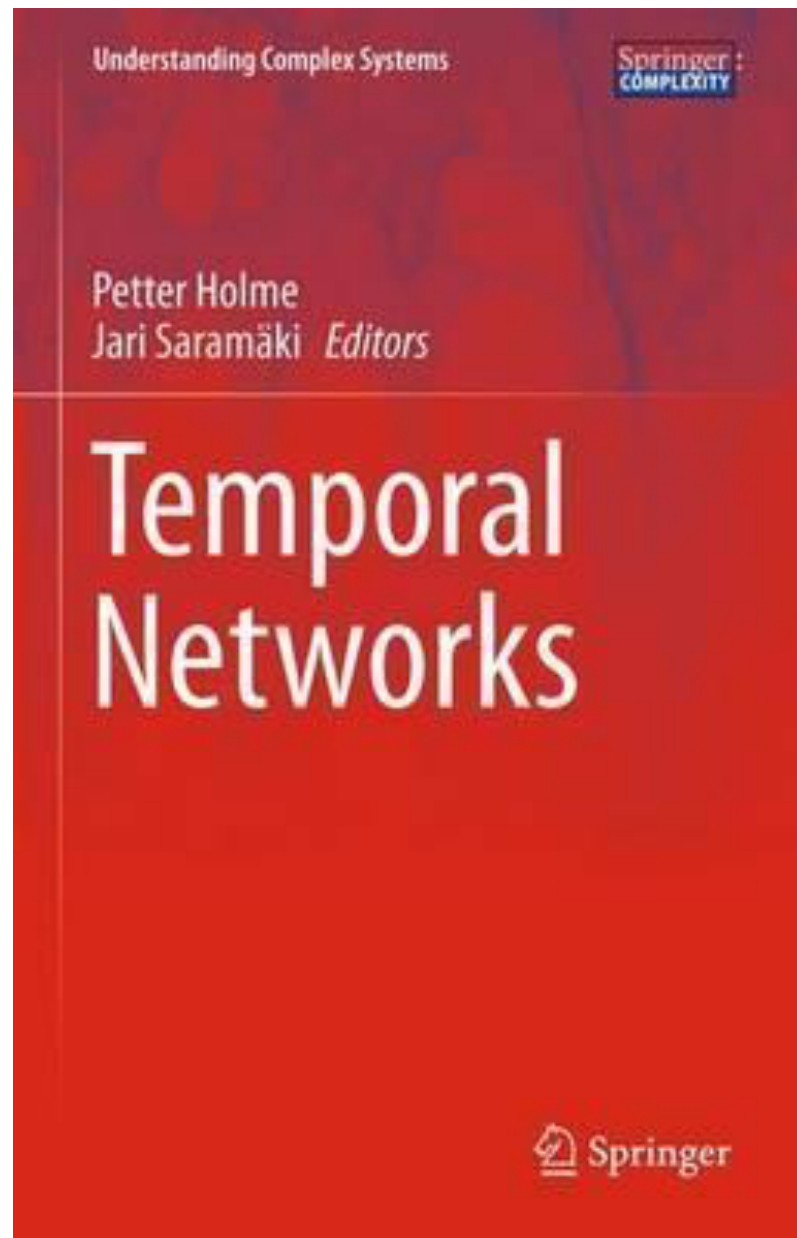
$$D_u^{12} = 0 \quad D_v^{12} = 0.5$$

D_v^{12}



etti@u

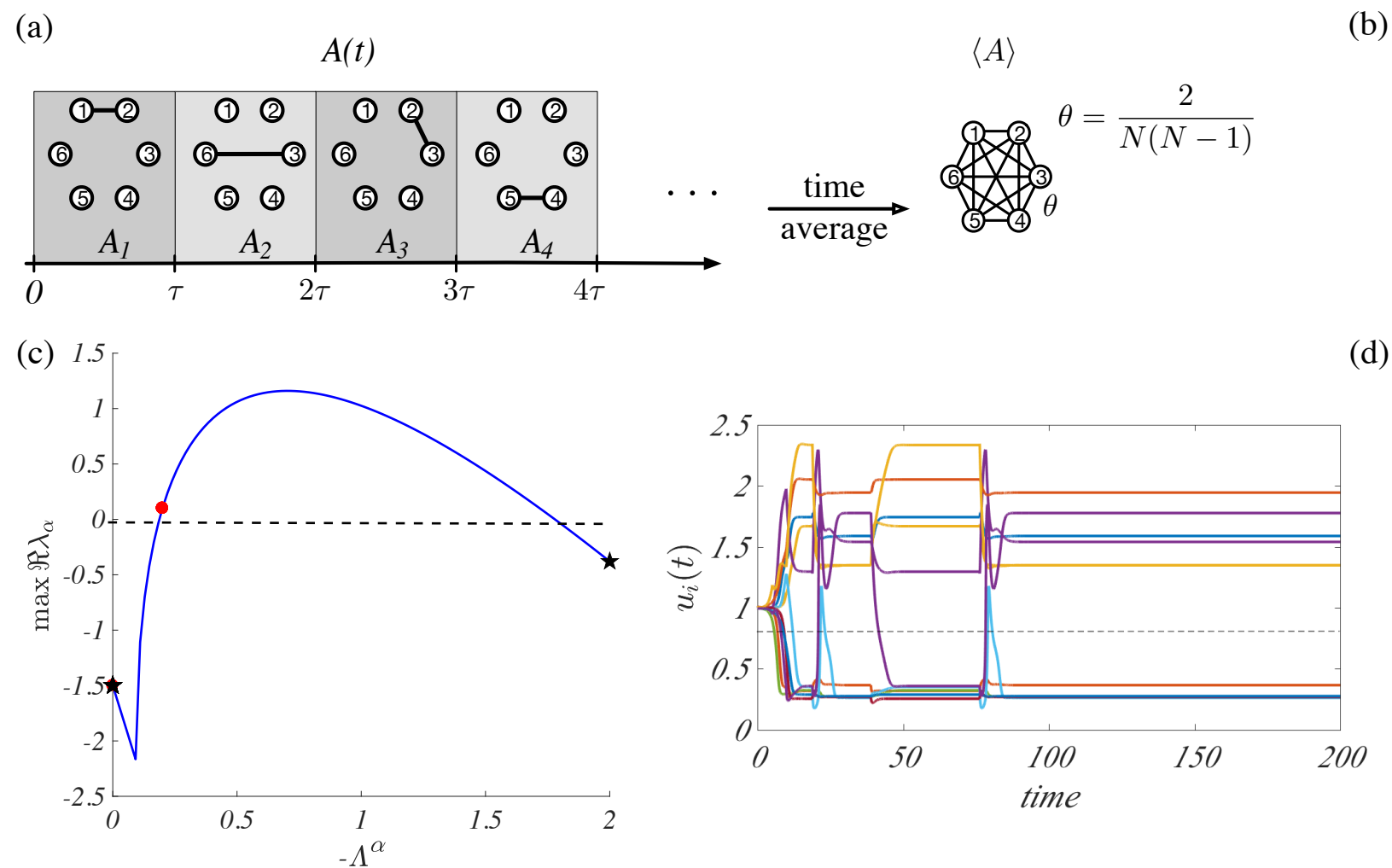
Temporal networks



Temporal networks: fast switch

$$\dot{u}_i(t) = f(u_i, v_i) + D_u \sum_{j=1}^N L_{ij}(t/\epsilon) u_j(t)$$

$$\dot{v}_i(t) = g(u_i, v_i) + D_v \sum_{j=1}^N L_{ij}(t/\epsilon) v_j(t)$$



PRL **119**, 148301 (2017)

PHYSICAL REVIEW LETTERS

week ending
6 OCTOBER 2017

Theory of Turing Patterns on Time Varying Networks

Julien Petit,^{1,2} Ben Lauwens,² Duccio Fanelli,^{3,4} and Timoteo Carletti^{1,*}

Temporal networks: generic case

$$\frac{d\mathbf{x}_i}{dt} = \mathbf{F}(\mathbf{x}_i) + \varepsilon \sum_j L_{ij}(t) \mathbf{H}(\mathbf{x}_j), \quad \mathbf{L}(t) \vec{\phi}^{(\alpha)}(t) = \Lambda^{(\alpha)}(t) \vec{\phi}^{(\alpha)}(t) \quad \forall \alpha = 1, \dots, n \text{ and } \forall t$$

$$\left(\vec{\phi}^{(\alpha)}(t) \right)^T \cdot \vec{\phi}^{(\beta)}(t) = \delta_{\alpha\beta}$$

$$\frac{d\vec{\phi}^{(\alpha)}}{dt}(t) = \sum_{\beta} c_{\alpha\beta}(t) \vec{\phi}^{(\beta)}(t) \quad \forall \alpha = 1, \dots, n. \quad c_{\alpha\beta} + c_{\beta\alpha} = 0 \text{ and } c_{1\alpha} = 0.$$

$$\frac{d\delta\hat{\mathbf{x}}_{\beta}}{dt} = \sum_{\alpha} c_{\beta\alpha}(t) \delta\hat{\mathbf{x}}_{\alpha} + \left[\mathbf{J}_{\mathbf{F}}(\mathbf{s}(t)) + \varepsilon \Lambda^{(\beta)}(t) \mathbf{J}_{\mathbf{H}}(\mathbf{s}(t)) \right] \delta\hat{\mathbf{x}}_{\beta}.$$

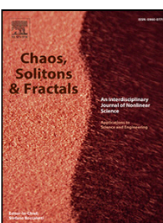


Contents lists available at [ScienceDirect](https://www.sciencedirect.com)

Chaos, Solitons and Fractals

Nonlinear Science, and Nonequilibrium and Complex Phenomena

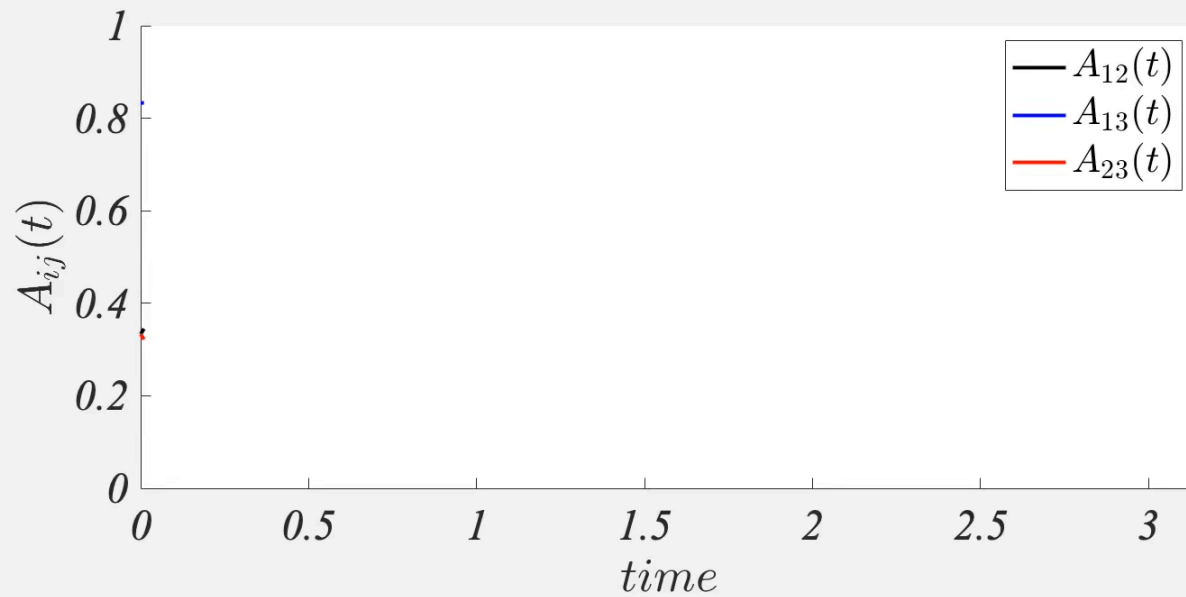
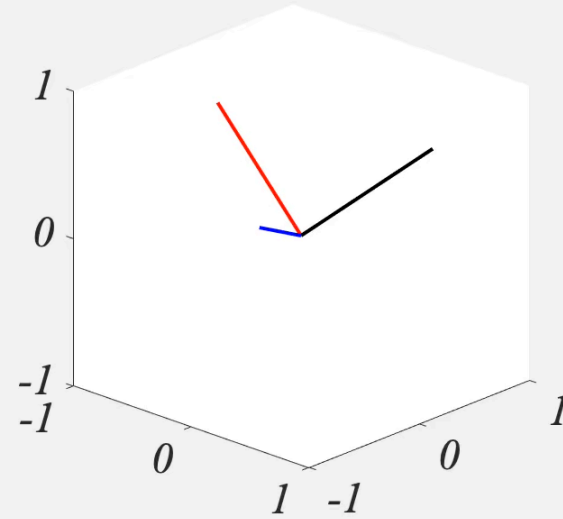
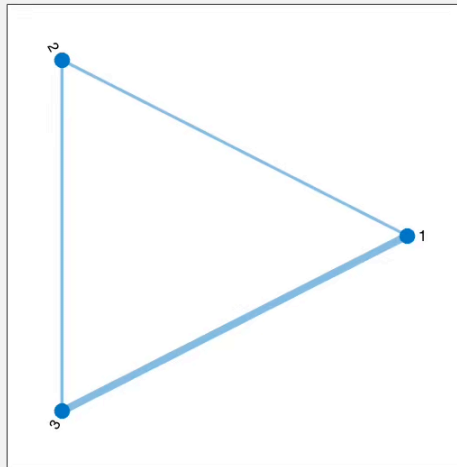
journal homepage: www.elsevier.com/locate/chaos



Theory of synchronisation and pattern formation on time varying networks

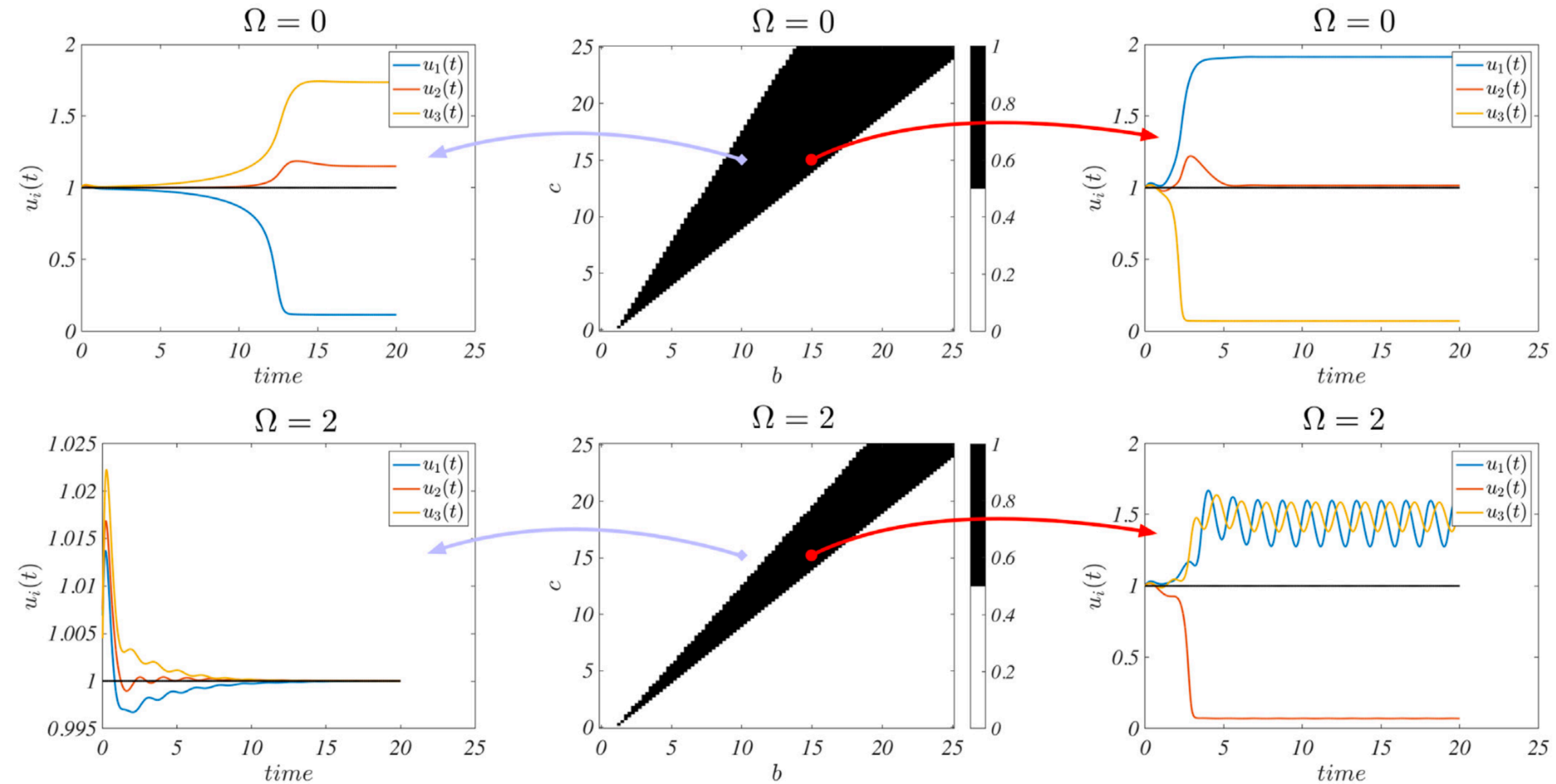


Temporal networks: generic case



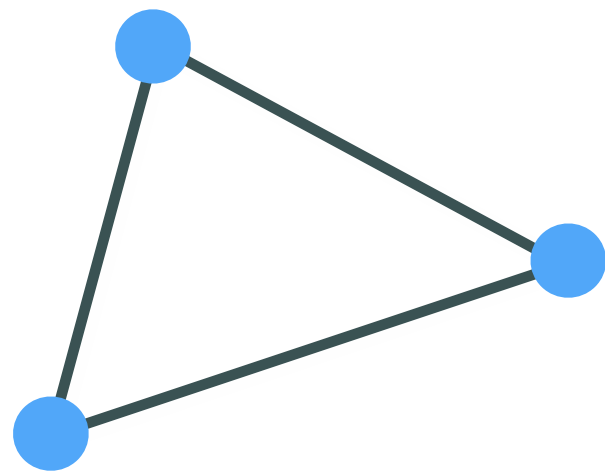
$$A_{ij}(t) = \begin{pmatrix} 0 & \frac{1}{2} - \frac{\cos\left(\frac{\pi}{3} + 2\Omega t\right)}{3} & \frac{\cos(2\Omega t)}{3} + \frac{1}{2} \\ \frac{1}{2} - \frac{\cos\left(\frac{\pi}{3} + 2\Omega t\right)}{3} & 0 & \frac{1}{2} - \frac{\cos\left(\frac{\pi}{3} - 2\Omega t\right)}{3} \\ \frac{\cos(2\Omega t)}{3} + \frac{1}{2} & \frac{1}{2} - \frac{\cos\left(\frac{\pi}{3} - 2\Omega t\right)}{3} & 0 \end{pmatrix}$$

Turing patterns on temporal networks: generic case

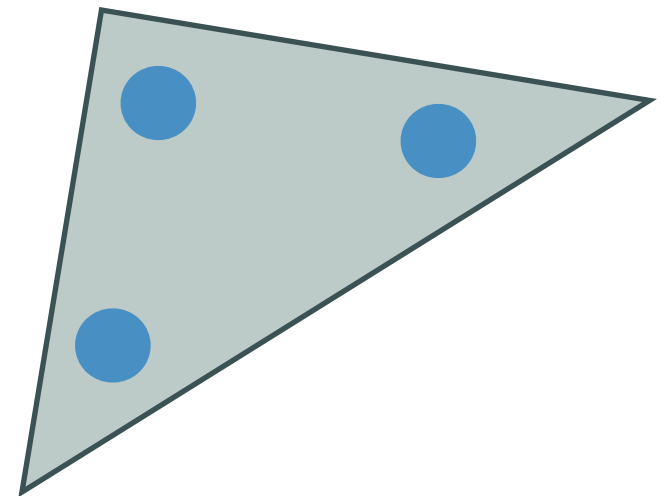


networks

limitation

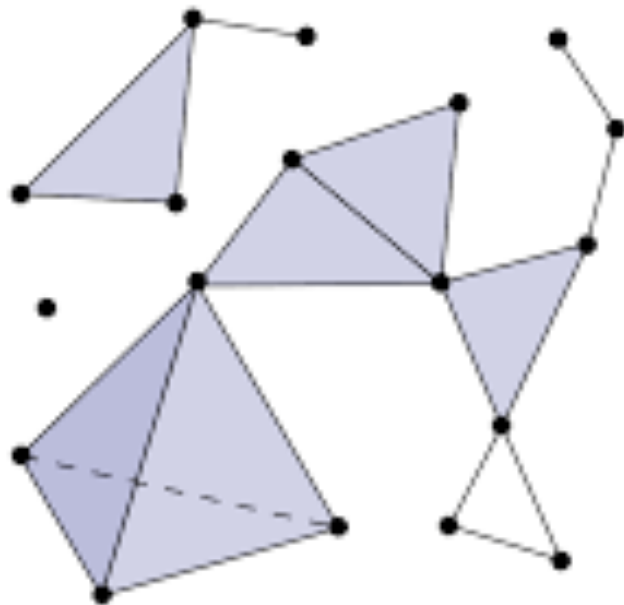


\neq



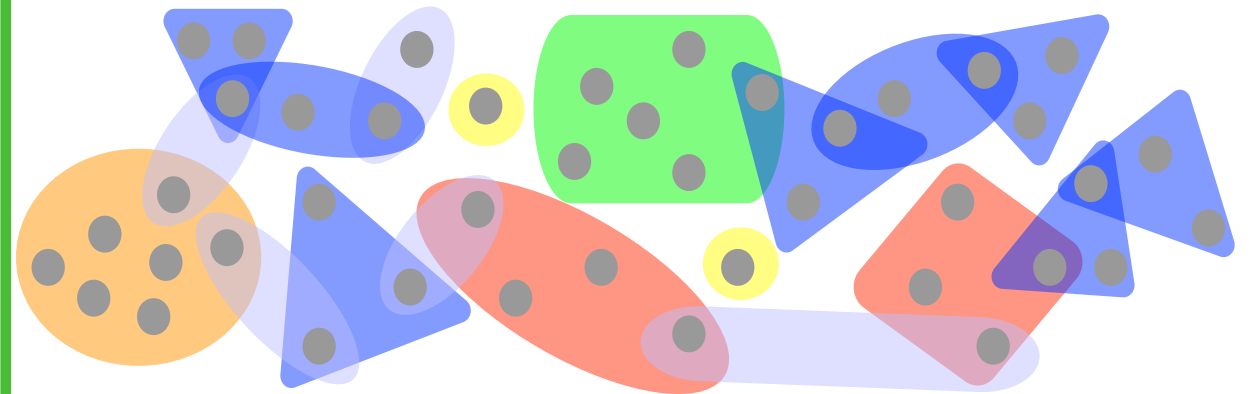
Simplicial complexes and Hypergraphs

Simplicial complexes



d-simplex = $d+1$ nodes
(all linked together)
0-simplex = node
1-simplex = link
2-simplex = triangle
3-simplex = tetrahedron

Hypergraphs

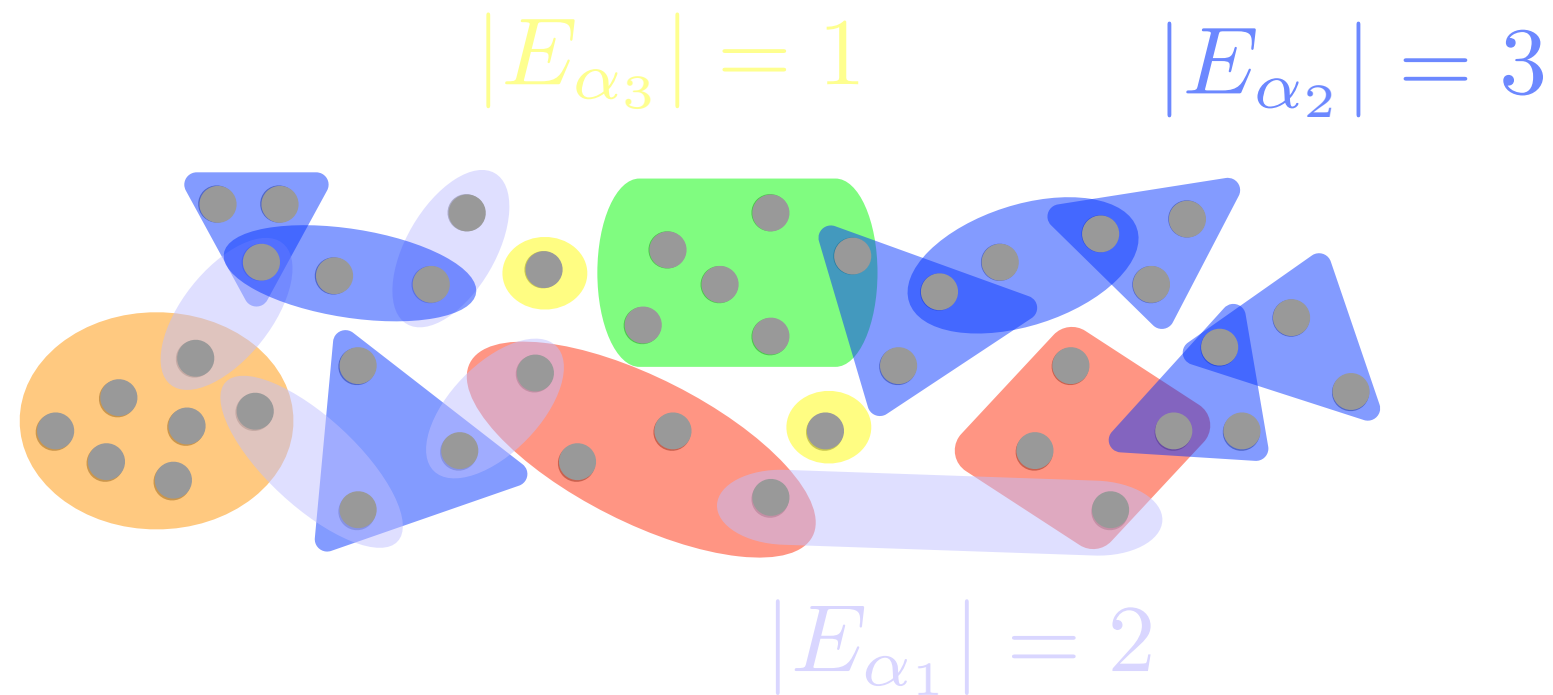


hyperedge = set of nodes

The background of the slide features a light blue gradient. Overlaid on this are several semi-transparent, overlapping shapes in various colors: blue, green, orange, yellow, and purple. These shapes include circles, triangles, and irregular polygons. Scattered throughout these shapes are numerous small, solid grey dots, some of which are positioned directly on the letters of the main title.

Hypergraphs

Hypergraphs. Some definitions.



ensemble of nodes
=
hyperedges

Incidence matrix

$$e_{i\alpha} = 1 \quad \text{iff } i \in E_{\alpha}$$

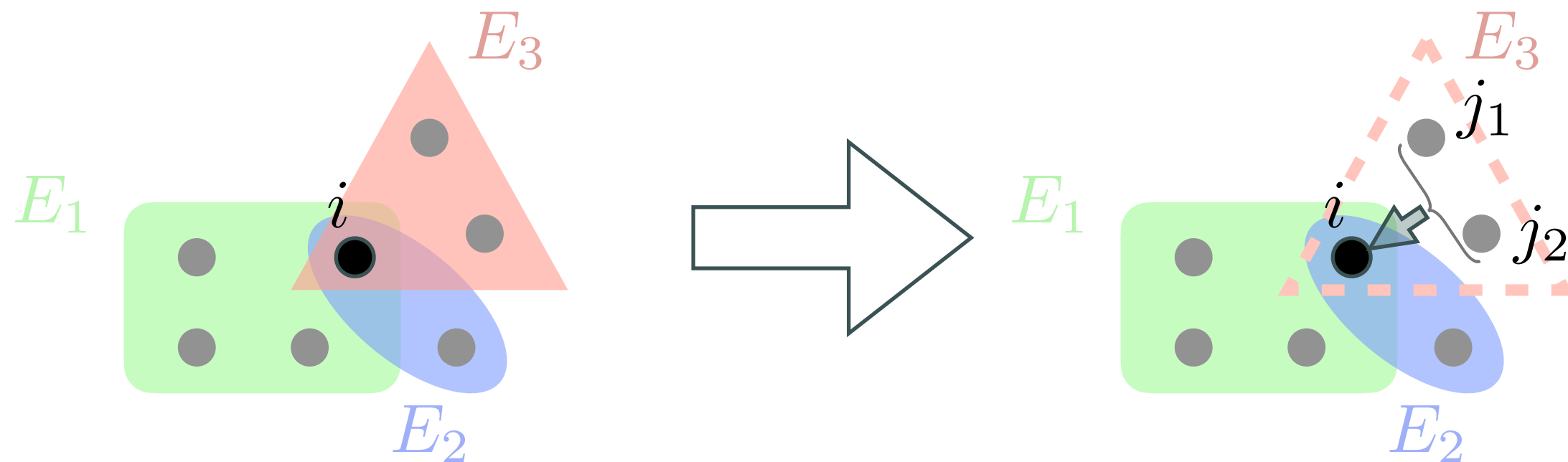
Hyperadjacency matrix

$$\mathbf{A} = \mathbf{e}\mathbf{e}^{\top}$$

Hyperedge matrix

$$\mathbf{C} = \mathbf{e}^{\top}\mathbf{e}$$

Hyperedge Mean Field



non-linearity

$$k_{ij}^H = \sum_{\alpha} (C_{\alpha\alpha} - 1)^{\tau} e_{i\alpha} e_{j\alpha}$$

hyperedge size

incidence matrices

Turing patterns on hypergraphs

$$\tau = 1$$

$$\begin{aligned} \frac{d\mathbf{x}_i}{dt} &= \mathbf{F}(\mathbf{x}_i) - \varepsilon \sum_{\alpha, j} e_{i\alpha} e_{j\alpha} (C_{\alpha\alpha} - 1) (\mathbf{G}(\mathbf{x}_i) - \mathbf{G}(\mathbf{x}_j)) \\ &= \mathbf{F}(\mathbf{x}_i) - \varepsilon \sum_j k_{ij}^H (\mathbf{G}(\mathbf{x}_i) - \mathbf{G}(\mathbf{x}_j)) = \mathbf{F}(\mathbf{x}_i) - \varepsilon \sum_j (\delta_{ij} k_i^H - k_{ij}^H) \mathbf{G}(\mathbf{x}_j) \\ &= \mathbf{F}(\mathbf{x}_i) - \varepsilon \sum_j L_{ij}^H \mathbf{G}(\mathbf{x}_j), \end{aligned}$$

L_{ij}^H Higher-order Laplace matrix

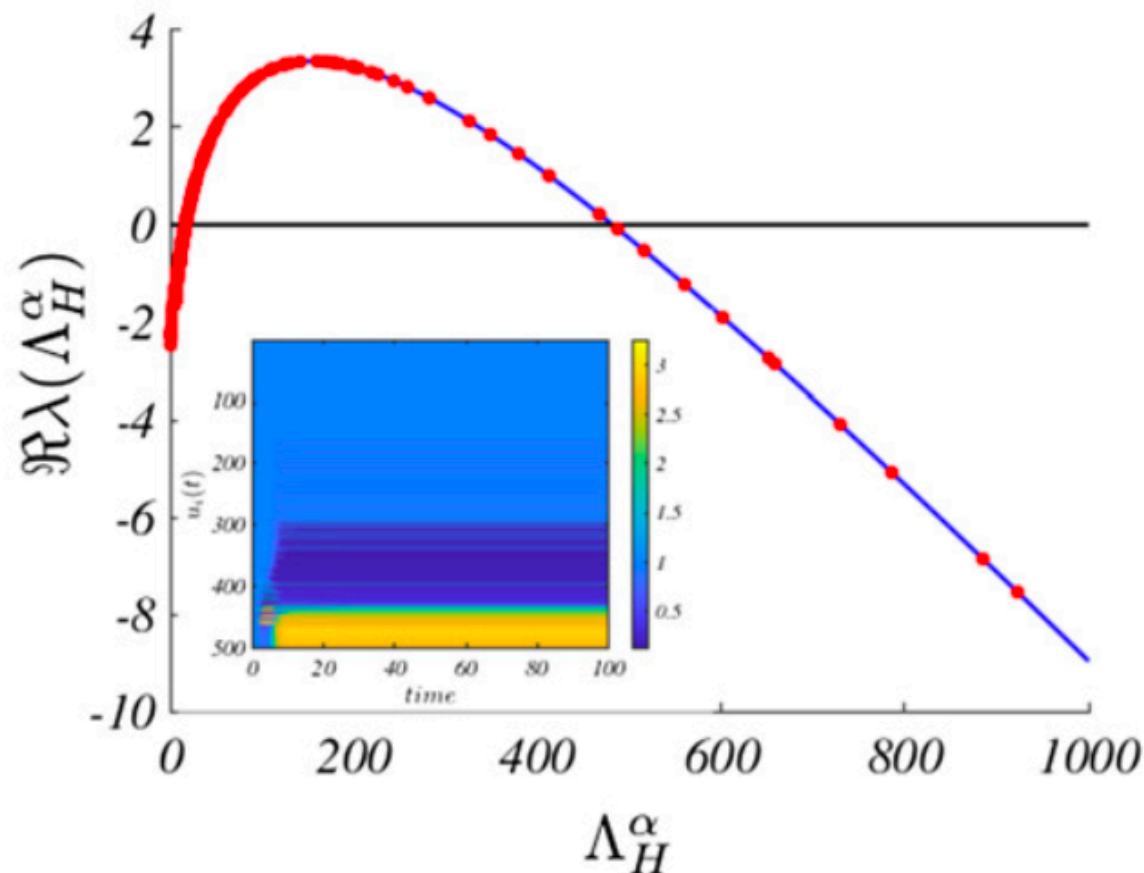
J.Phys.Complex. 1 (2020) 035006 (16pp)

Journal of Physics: Complexity

PAPER

Dynamical systems on hypergraphs

Timoteo Carletti^{1,4} , Duccio Fanelli²  and Sara Nicoletti^{2,3}

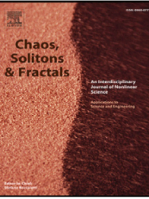


Higher-order (many-body) interactions



Contents lists available at ScienceDirect

Chaos, Solitons and Fractals

journal homepage: www.elsevier.com/locate/chaos

Turing patterns in systems with high-order interactions

Riccardo Muolo ^{a,b,c,*}, Luca Gallo ^{a,d,1}, Vito Latora ^{d,e,f}, Mattia Frasca ^{g,h}, Timoteo Carletti ^{a,b}

$$\begin{cases} \frac{du_i}{dt} = f_1(u_i, v_i) + \sum_{d=1}^P \sigma_d \sum_{j_1=1}^N \cdots \sum_{j_d=1}^N A_{i,j_1,\dots,j_d}^{(d)} \left[\begin{aligned} &h_1^{(d)}(u_{j_1}, \dots, u_{j_d}, v_{j_1}, \dots, v_{j_d}) \\ &-h_1^{(d)}(u_i, \dots, u_i, v_i, \dots, v_i) \end{aligned} \right] \\ \frac{dv_i}{dt} = f_2(u_i, v_i) + \sum_{d=1}^P \sigma_d \sum_{j_1=1}^N \cdots \sum_{j_d=1}^N A_{i,j_1,\dots,j_d}^{(d)} \left[\begin{aligned} &h_2^{(d)}(u_{j_1}, \dots, u_{j_d}, v_{j_1}, \dots, v_{j_d}) \\ &-h_2^{(d)}(u_i, \dots, u_i, v_i, \dots, v_i) \end{aligned} \right] \end{cases}$$

Equilibrium

$$f_1(u^*, v^*) = f_2(u^*, v^*) = 0$$

$$A_{ij_1,\dots,j_d}^{(d)} = A_{\pi(ij_1,\dots,j_d)}^{(d)}$$

symmetric tensor

Linearize

$$\delta u_i = u_i - u^*, \quad \delta v_i = v_i - v^*$$

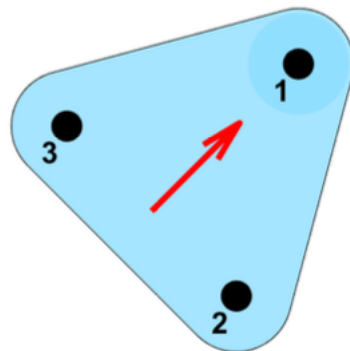
P = 2

$$\frac{d\vec{\xi}}{dt} = \left(\mathbb{I}_N \otimes \mathbf{J}_0 + \sigma_1 \mathbf{L}^{(1)} \otimes \mathbf{J}_{H(1)} + \sigma_2 \mathbf{L}^{(2)} \otimes \mathbf{J}_{H(2)} \right) \vec{\xi}$$

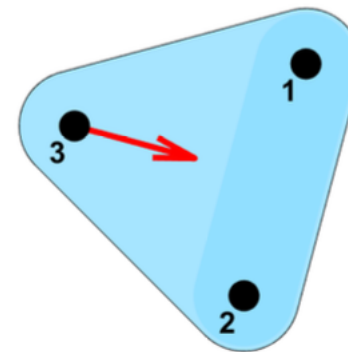
Note: need for assumptions on L or H

Turing patterns on hypergraphs : m-directed

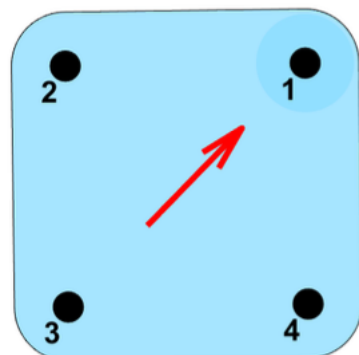
1-directed 2-hyperedge



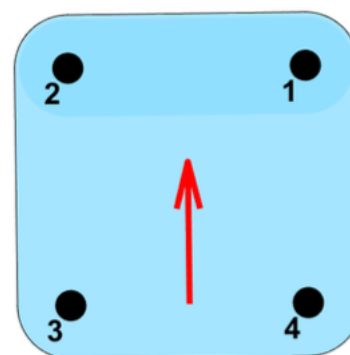
2-directed 2-hyperedge



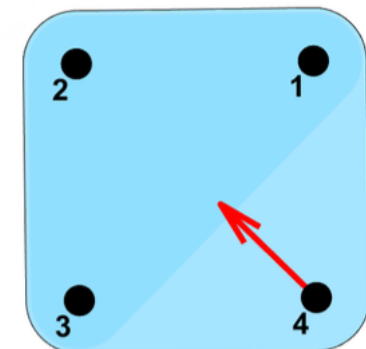
1-directed 3-hyperedge



2-directed 3-hyperedge

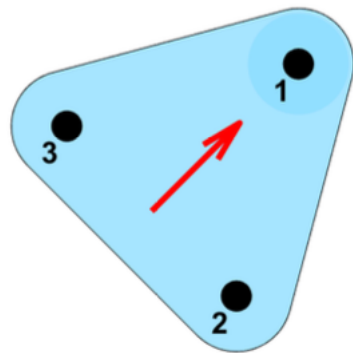


3-directed 3-hyperedge



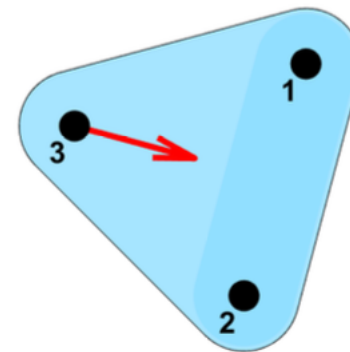
Turing patterns on hypergraphs : m-directed

1-directed 2-hyperedge



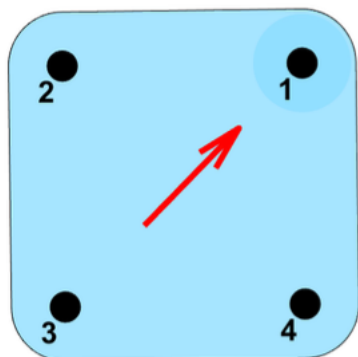
$$A_{1\pi(2,3)}^{(2,1)} = 1$$

2-directed 2-hyperedge



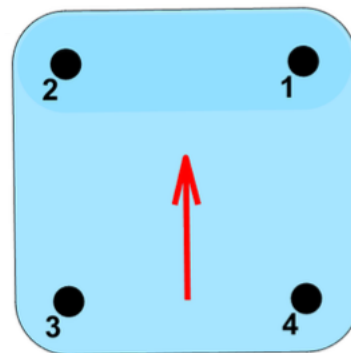
$$A_{\pi(1,2)3}^{(2,2)} = 1$$

1-directed 3-hyperedge



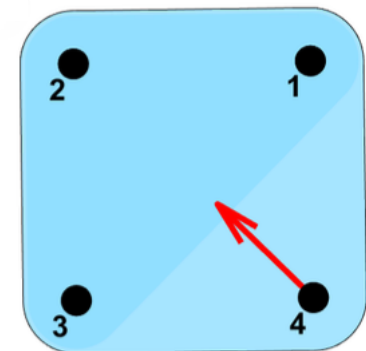
$$A_{1\pi(2,3,4)}^{(3,1)} = 1$$

2-directed 3-hyperedge



$$A_{\pi_1(1,1)\pi_2(3,4)}^{(3,2)} = 1$$

3-directed 3-hyperedge



$$A_{\pi(1,2,3)4}^{(3,3)} = 1$$

Turing patterns on hypergraphs : m-directed

m-directed d-hyperedge

$$A_{\pi_1(i_1, \dots, i_m) \pi_2(j_1, \dots, j_q)}^{(d, m)} = 1 \quad m + q = d + 1$$

$$\frac{d\vec{x}_i}{dt} = \vec{g}^{(0)}(\vec{x}_i) + \sum_{d=1}^D \sigma_d \sum_{m=1}^d \sum_{i_1, \dots, i_{m-1}} \sum_{j_1, \dots, j_q} \vec{g}^{(d, m)}(\vec{x}_i, \vec{x}_{i_1}, \dots, \vec{x}_{i_{m-1}} \vec{x}_{j_1}, \dots, \vec{x}_{j_q}) A_{(ii_1 \dots i_{m-1})(j_1 \dots j_q)}^{(d, m)}$$

Diffusive-like

$$\vec{g}^{(d, m)}(\vec{x}_i, \vec{x}_{i_1}, \dots, \vec{x}_{i_{m-1}} \vec{x}_{j_1}, \dots, \vec{x}_{j_q}) = \vec{h}^{(d, m)}(\vec{x}_{i_1}, \dots, \vec{x}_{i_{m-1}} \vec{x}_{j_1}, \dots, \vec{x}_{j_q}) - \vec{h}^{(d, m)}(\vec{x}_i, \dots, \vec{x}_i)$$

Turing patterns on hypergraphs : m-directed

$$\hat{k}_{i,s}^{(d,m)} = \frac{1}{q!(m-2)!} \sum_{\substack{i_2, \dots, i_{m-1} \\ j_1, \dots, j_q}} A_{(i,s,i_2, \dots, i_{m-1})(j_1, \dots, j_q)}^{(d,m)}$$

$$\check{k}_{i,s}^{(d,m)} = \frac{1}{(q-1)!(m-1)!} \sum_{\substack{i_1, \dots, i_{m-1} \\ j_2, \dots, j_q}} A_{(i,i_1, \dots, i_{m-1})(s,j_2, \dots, j_q)}^{(d,m)}$$

$$k_i^{(d,m)} = \frac{1}{q!(m-1)!} \sum_{\substack{i_1, \dots, i_{m-1} \\ j_1, \dots, j_q}} A_{(ii_1 \dots i_{m-1})(j_1 \dots j_q)}^{(d,m)}$$

Symmetric Laplacian

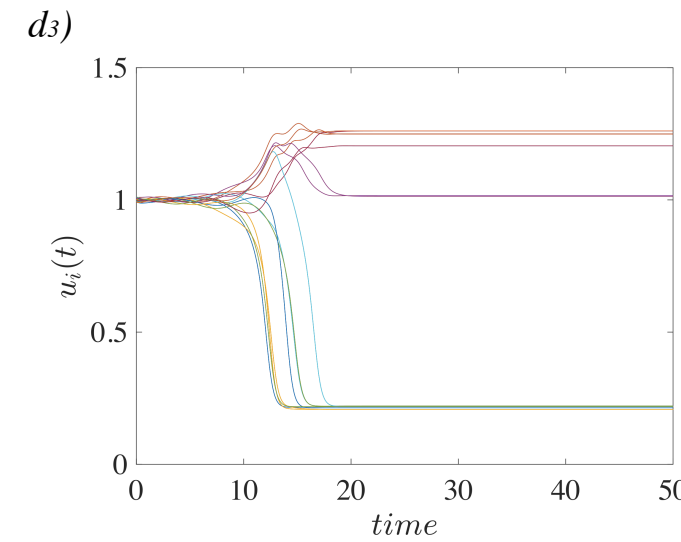
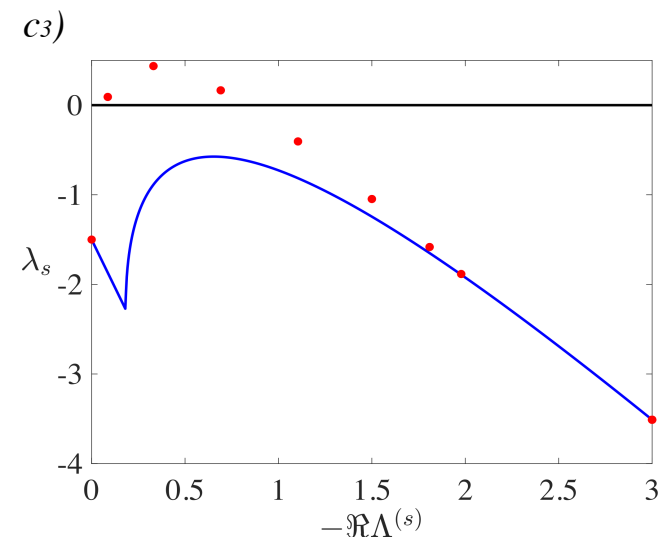
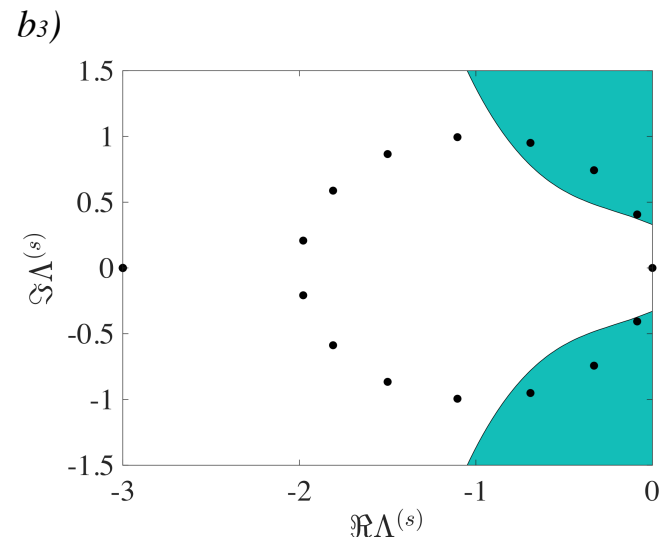
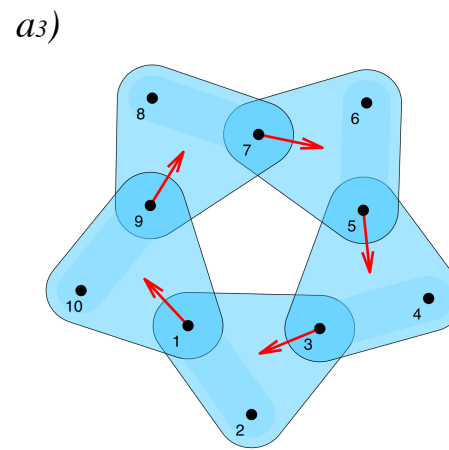
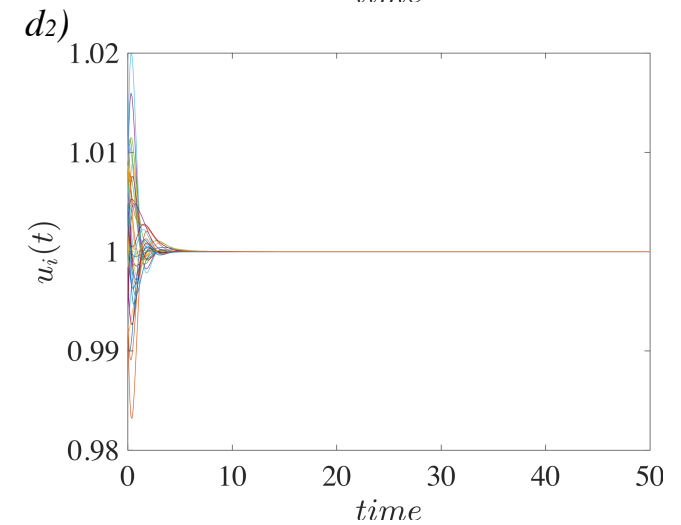
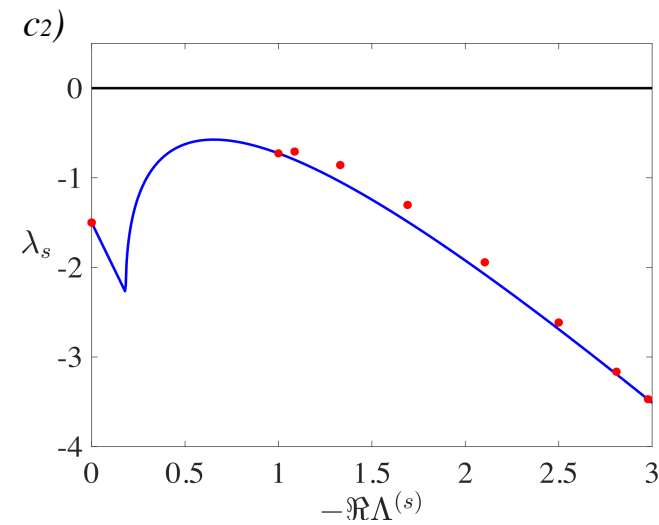
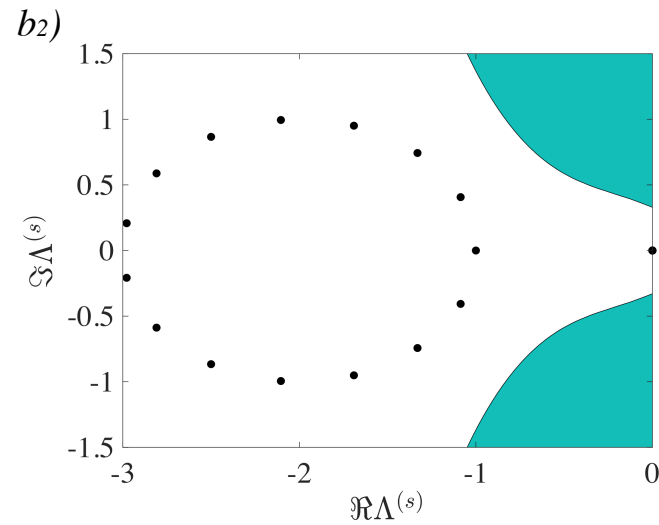
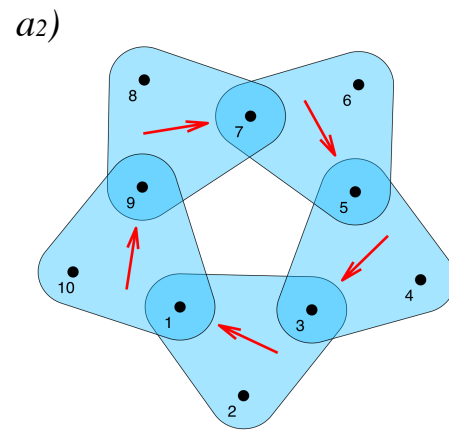
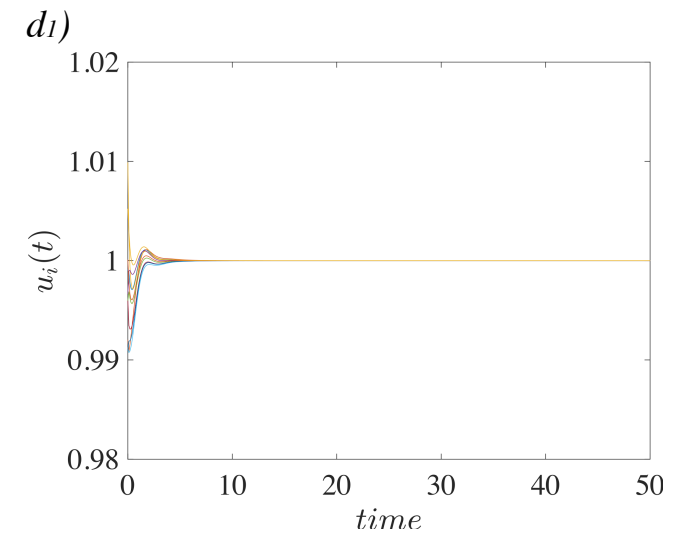
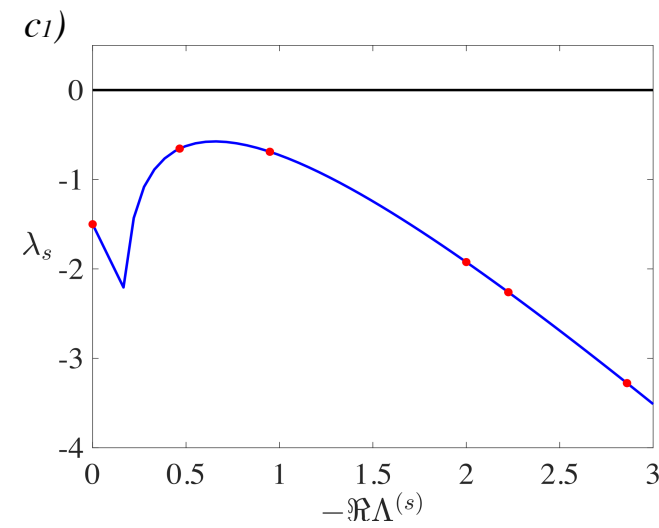
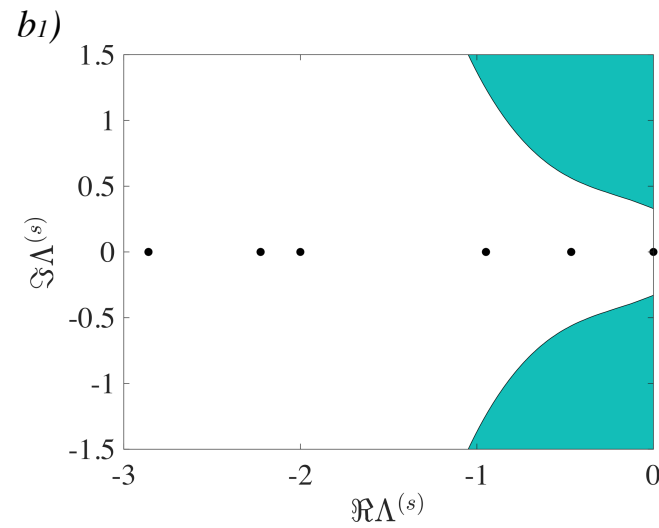
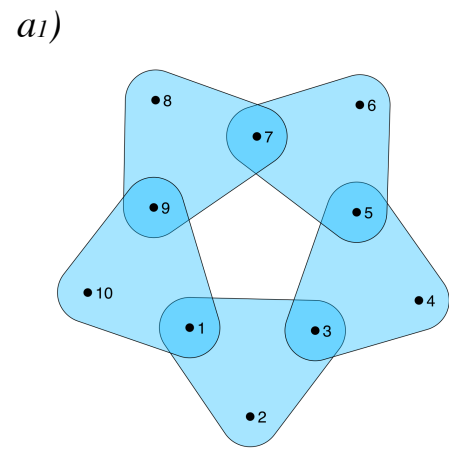
$$\hat{L}_{is}^{(d,m)} = \begin{cases} q!(m-2)! \hat{k}_{i,s}^{(d,m)} & i \neq s \\ -q!(m-1)! k_i^{(d,m)} & i = s \\ 0 & i \notin h \text{ or } s \notin h \end{cases}$$

Asymmetric Laplacian

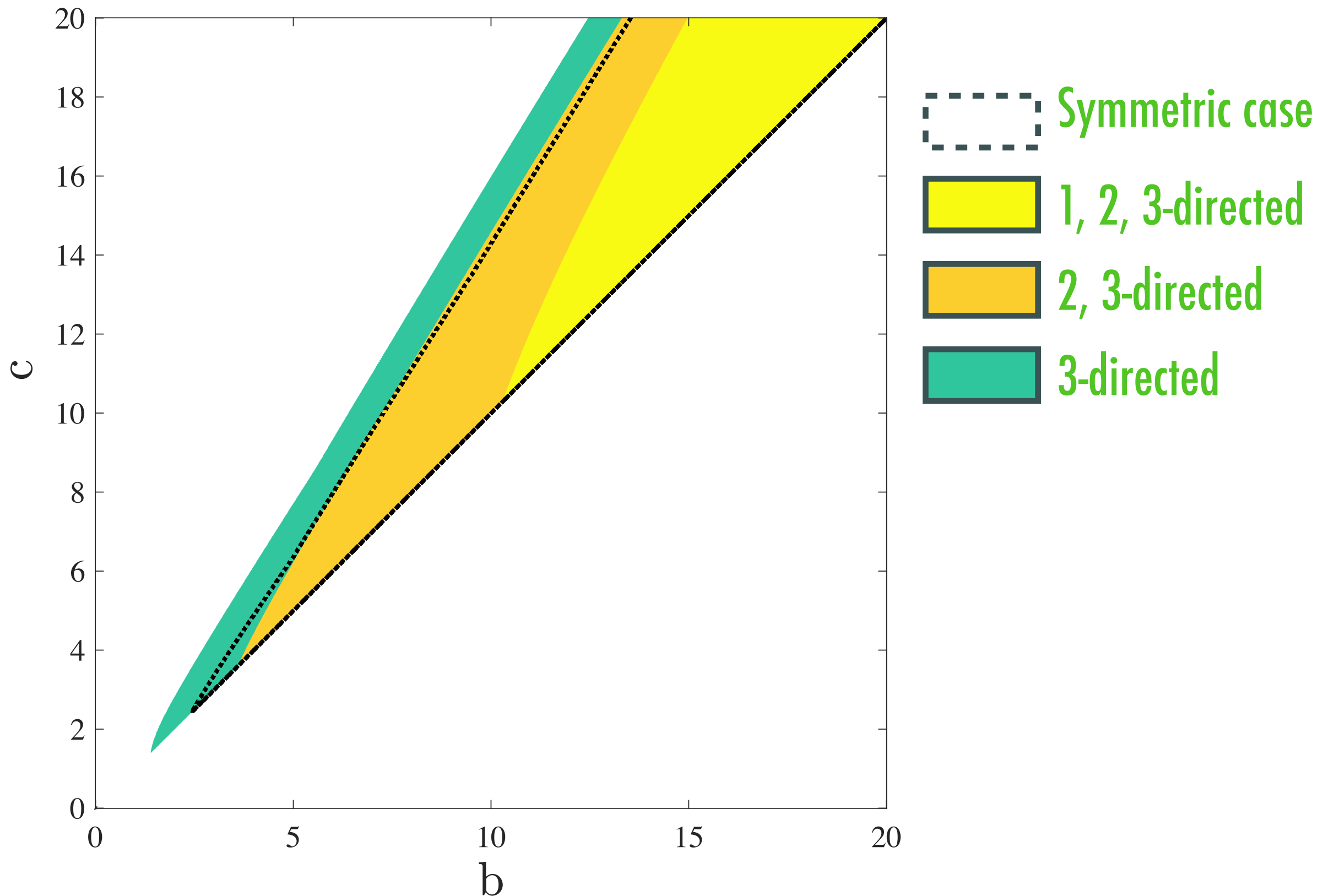
$$\check{L}_{is}^{(d,m)} = \begin{cases} (q-1)!(m-1)! \check{k}_{i,s}^{(d,m)} & i \neq s \\ -q!(m-1)! k_i^{(d,m)} & i = s \\ 0 & i \notin h \text{ or } s \notin t \end{cases}$$

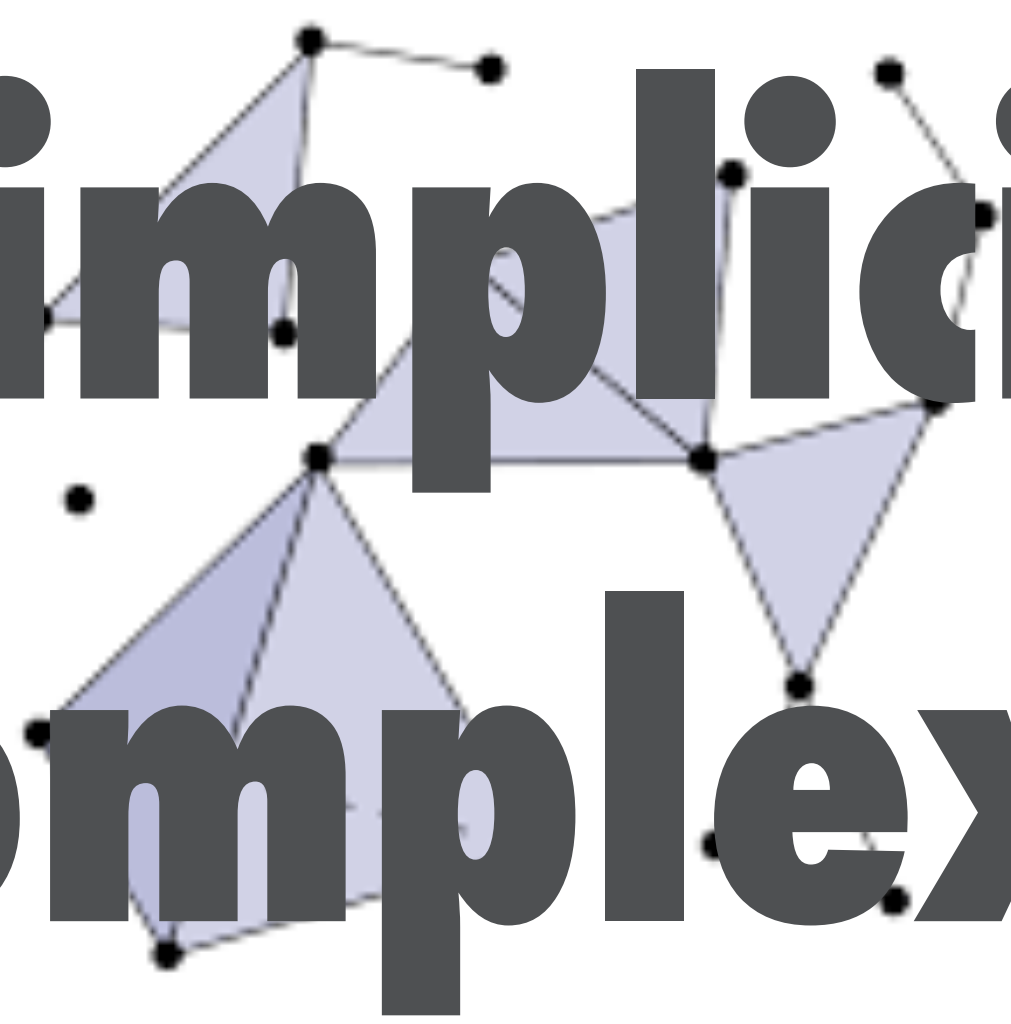
Turing patterns on hypergraphs : m-directed

increasing m



Turing patterns on hypergraphs : m-directed





Simplicial complexes

PHYSICAL REVIEW E **107**, 014216 (2023)

Turing patterns in simplicial complexes

Shupeng Gao,^{1,2} Lili Chang,^{3,4,*} Matjaž Perc,^{5,6,7,8,9} and Zhen Wang^{1,2,†}

¹*School of Mechanical Engineering, Northwestern Polytechnical University, Xi'an 710072, China*

²*School of Artificial Intelligence, Optics, and Electronics (iOPEN), Northwestern Polytechnical University, Xi'an 710072, China*

³*Complex Systems Research Center, Shanxi University, Taiyuan 030006, China*

⁴*Shanxi Key Laboratory of Mathematical Techniques and Big Data Analysis for Disease Control and Prevention, Taiyuan 030006, China*

⁵*Faculty of Natural Sciences and Mathematics, University of Maribor, Koroška cesta 160, 2000 Maribor, Slovenia*

⁶*Department of Medical Research, China Medical University Hospital, China Medical University, Taichung 404332, Taiwan*

⁷*Alma Mater Europaea, Slovenska ulica 17, 2000 Maribor, Slovenia*

⁸*Complexity Science Hub Vienna, Josefstädterstraße 39, 1080 Vienna, Austria*

⁹*Department of Physics, Kyung Hee University, 26 Kyungheedaero, Dongdaemun-gu, Seoul, Republic of Korea*

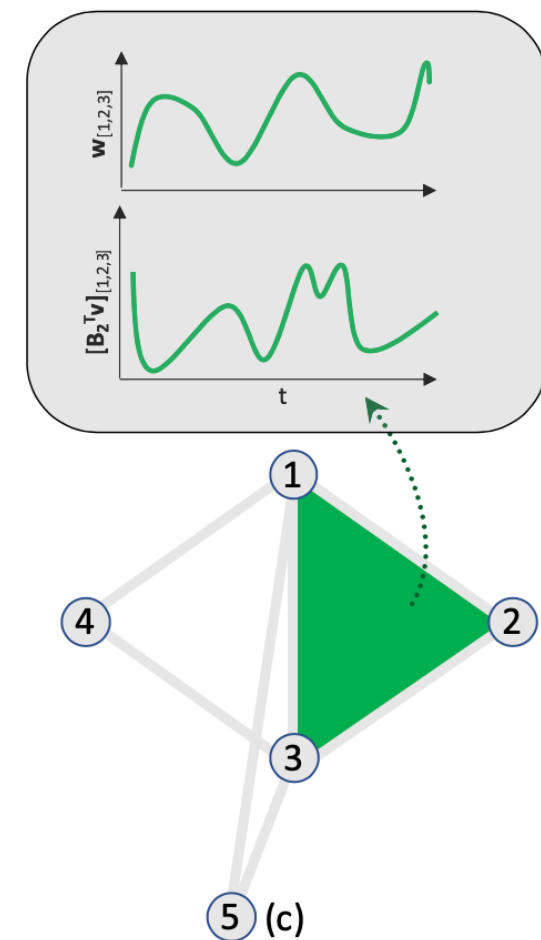
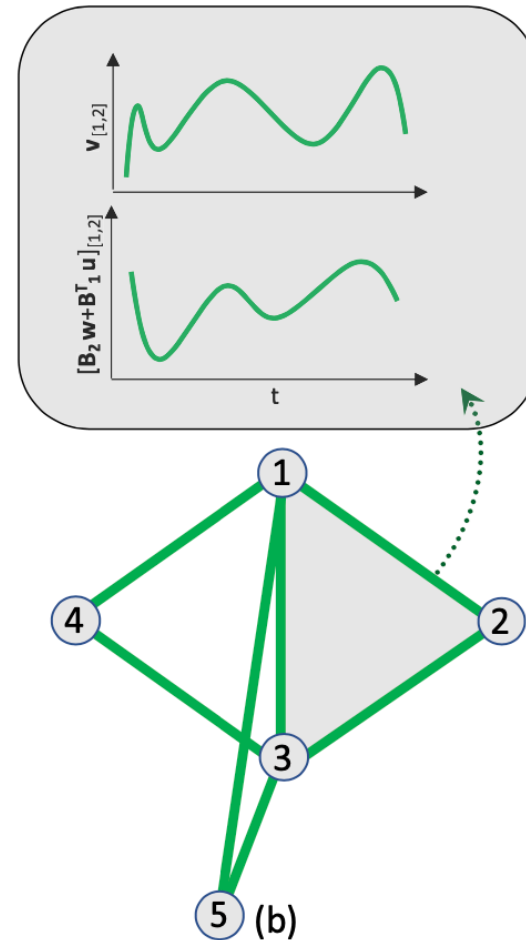
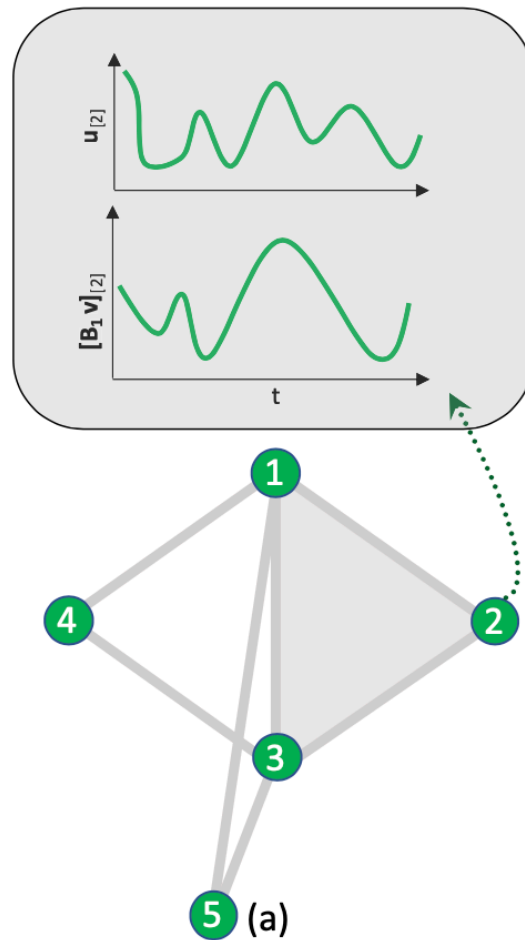


(Received 18 June 2022; revised 3 November 2022; accepted 6 December 2022; published 27 January 2023)

- Node-centric

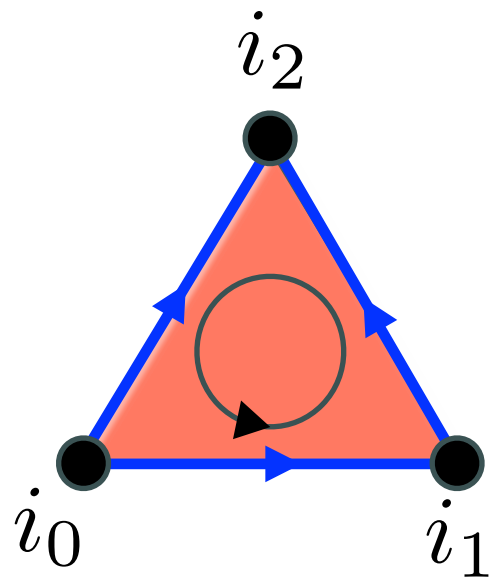
- Use a single incidence matrix => network projection

Topological signals



Simplicial complex: an example

$k = 2$ Three nodes, hence a triangle



Incidence matrices

$$\mathbf{B}_1 \in M^{N_0 \times N_1}$$

$$\mathbf{B}_2 \in M^{N_1 \times N_2}$$

$$\sigma_1^{(1)} = [i_0, i_1] \quad \sigma_2^{(1)} = [i_1, i_2] \quad \sigma_3^{(1)} = [i_0, i_2]$$

$$\mathbf{B}_1(\sigma_i^{(0)}, \sigma_j^{(1)}) = \begin{matrix} & [i_0, i_1] & [i_1, i_2] & [i_0, i_2] \\ \begin{matrix} i_0 \\ i_1 \\ i_2 \end{matrix} & \begin{pmatrix} -1 & 0 & -1 \\ 1 & -1 & 0 \\ 0 & 1 & 1 \end{pmatrix} \end{matrix}$$

$$\mathbf{B}_2(\sigma_i^{(1)}, \sigma_j^{(2)}) = \begin{matrix} & [i_0, i_1, i_2] \\ \begin{matrix} [i_0, i_1] \\ [i_1, i_2] \\ [i_0, i_2] \end{matrix} & \begin{pmatrix} 1 \\ 1 \\ -1 \end{pmatrix} \end{matrix}$$

Simplicial complex

$$\sigma_i^{(k)} = [i_0, \dots, i_k]$$

$$B_k(\sigma_i^{(k-1)}, \sigma_j^{(k)}) = 1 \text{ if } \sigma_i^{(k-1)} \sim \sigma_j^{(k)}$$

$$\mathbf{B}_k \in M^{N_{k-1} \times N_k}$$

$$B_k(\sigma_i^{(k-1)}, \sigma_j^{(k)}) = -1 \text{ if } \sigma_i^{(k-1)} \not\sim \sigma_j^{(k)}$$

Incidence matrix

$$B_k(\sigma_i^{(k-1)}, \sigma_j^{(k)}) = 0 \text{ otherwise}$$

$$\mathbf{L}_k = \mathbf{B}_k^\top \mathbf{B}_k + \mathbf{B}_{k+1} \mathbf{B}_{k+1}^\top$$

Hodge Laplace matrix

Turing patterns on simplicial complex

$$\frac{du}{dt} = f(u, \mathbf{B}_1 v) - D_0 \mathbf{L}_0 u, \quad u \text{ nodes species (1 dim)}$$

$$\frac{dv}{dt} = g(v, \mathbf{B}_1^\top u) - D_1 \mathbf{L}_1 v, \quad v \text{ links species (1 dim)}$$

Existence of an homogeneous stable solution

$$f(\mathbf{u}^*, \mathbf{B}_1 \mathbf{v}^*) = 0 \quad g(\mathbf{v}^*, \mathbf{B}_1^\top \mathbf{u}^*) = 0 \quad \begin{aligned} \mathbf{u}^* &= u^*(1, \dots, 1)^\top \\ \mathbf{v}^* &= v^*(1, \dots, 1)^\top \end{aligned}$$

We need extra conditions for the homogenous solutions to be a solution for the whole system :

PHYSICAL REVIEW LETTERS **130**, 187401 (2023)

Editors' Suggestion

$$\begin{aligned} \mathbf{L}_0 \mathbf{u}^* &= 0 \\ \mathbf{L}_1 \mathbf{v}^* &= 0 \end{aligned} \quad \Leftrightarrow \quad \begin{aligned} \mathbf{B}_1^\top \mathbf{u}^* &= 0 \\ \mathbf{B}_1 \mathbf{v}^* &= 0 \end{aligned}$$

Global Topological Synchronization on Simplicial and Cell Complexes

Timoteo Carletti¹, Lorenzo Giambagli^{1,2} and Ginestra Bianconi^{3,4}

¹Department of Mathematics and naXys, Namur Institute for Complex Systems, University of Namur, Rue Grafé 2, B5000 Namur, Belgium

²Department of Physics and Astronomy, University of Florence, INFN and CSDC, 50019 Sesto Fiorentino, Italy





³School of Mathematical Sciences, Queen Mary University of London, London, E1 4NS, United Kingdom

⁴The Alan Turing Institute, 96 Euston Road, London, NW1 2DB, United Kingdom



(Received 31 August 2022; revised 17 February 2023; accepted 11 April 2023; published 3 May 2023)

Diffusion-driven instability of topological signals coupled by the Dirac operator

Lorenzo Giambagli ^{1,2,*} Lucille Calmon,^{3,†} Riccardo Muolo ^{2,4,†} Timoteo Carletti ² and Ginestra Bianconi ^{3,5,‡}

Dirac operator

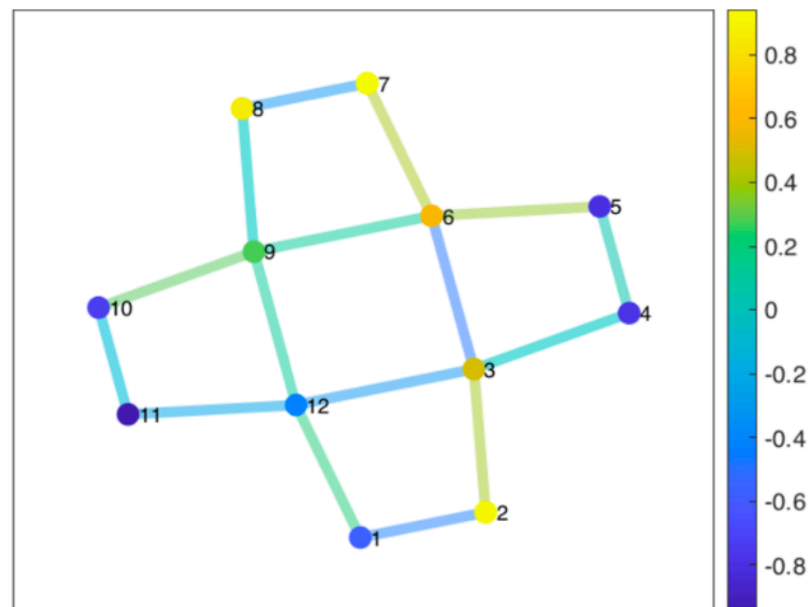
$$\mathcal{D} = \begin{pmatrix} 0 & \mathbf{B}_1 \\ \mathbf{B}_1^\top & 0 \end{pmatrix}$$

Laplace - Dirac coupling

$$\begin{aligned} \frac{du}{dt} &= f(u, \mathbf{B}_1 v) - D_{01} \mathbf{B}_1 v - D_0 \mathbf{L}_0 u, \\ \frac{dv}{dt} &= g(v, \mathbf{B}_1^\top u) - D_{10} \mathbf{B}_1^\top u - D_1 \mathbf{L}_1 v. \end{aligned}$$

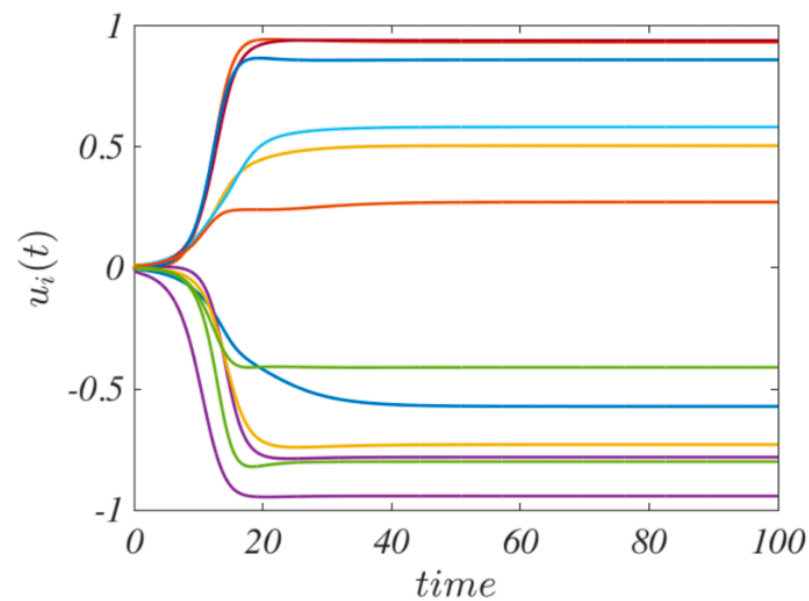
One can have patterns even if $D_0 = D_1 = 0$

Turing patterns on simplicial complex

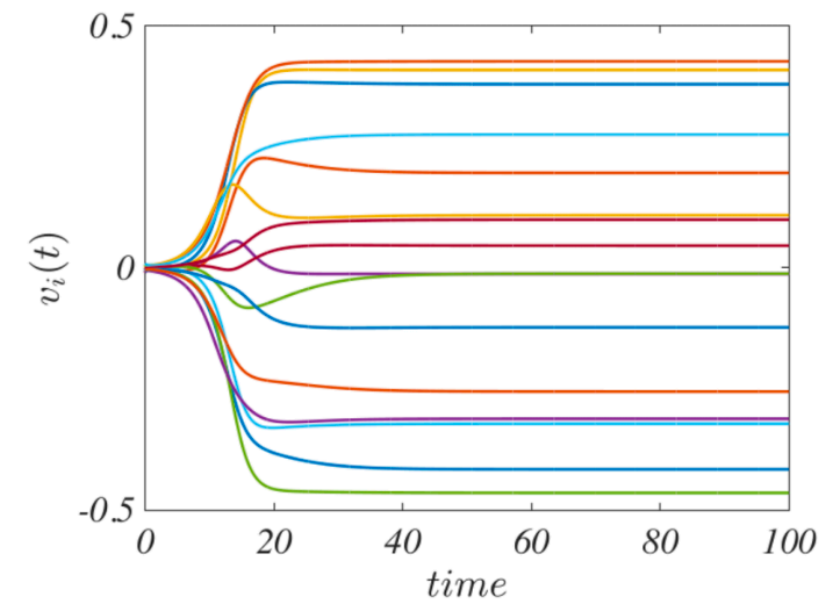


(a)

Inhibitor-inhibitor



(b)



(c)

Turing patterns on simplicial complexes with Dirac coupling

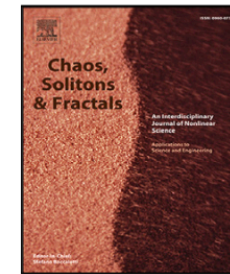
Chaos, Solitons and Fractals 178 (2024) 114312



Contents lists available at ScienceDirect

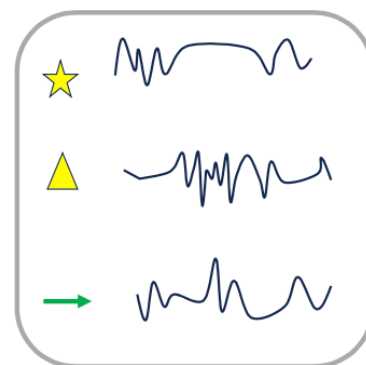
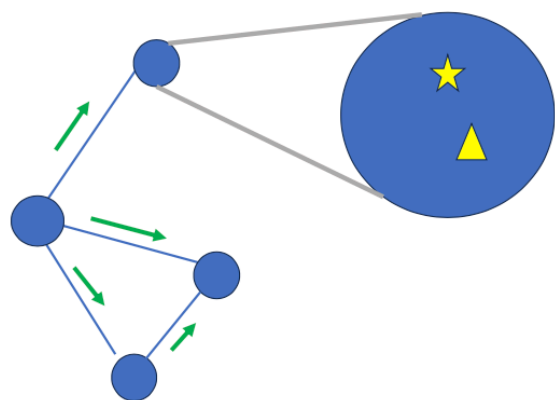
Chaos, Solitons and Fractals

journal homepage: www.elsevier.com/locate/chaos



The three way Dirac operator and dynamical Turing and Dirac induced patterns on nodes and links

Riccardo Muolo ^{a,b}, Timoteo Carletti ^b, Ginestra Bianconi ^{c,d,*}



$$\chi = \begin{pmatrix} u \\ v \end{pmatrix}$$

nodes species (2dim)

$$\psi = w$$

links species (1dim)

$$\partial = \begin{pmatrix} 0 & 0 & \mathbf{B} \\ \mathbf{B}^\top & 0 & 0 \\ 0 & \mathbf{B}^\top & 0 \end{pmatrix}$$

$$\gamma = \begin{pmatrix} \alpha_u \mathbf{I}_{N_0} & 0 & 0 \\ \alpha_v \mathbf{I}_{N_0} & 0 & 0 \\ 0 & \beta_u \mathbf{I}_{N_1} & \beta_v \mathbf{I}_{N_1} \end{pmatrix}$$

$$\mathcal{D} = \gamma \partial = \begin{pmatrix} 0 & 0 & \alpha_u \mathbf{B} \\ 0 & 0 & \alpha_v \mathbf{B} \\ \beta_u \mathbf{B}^\top & \beta_v \mathbf{B}^\top & 0 \end{pmatrix}$$

3 ways Hodge-Dirac

γ matrix

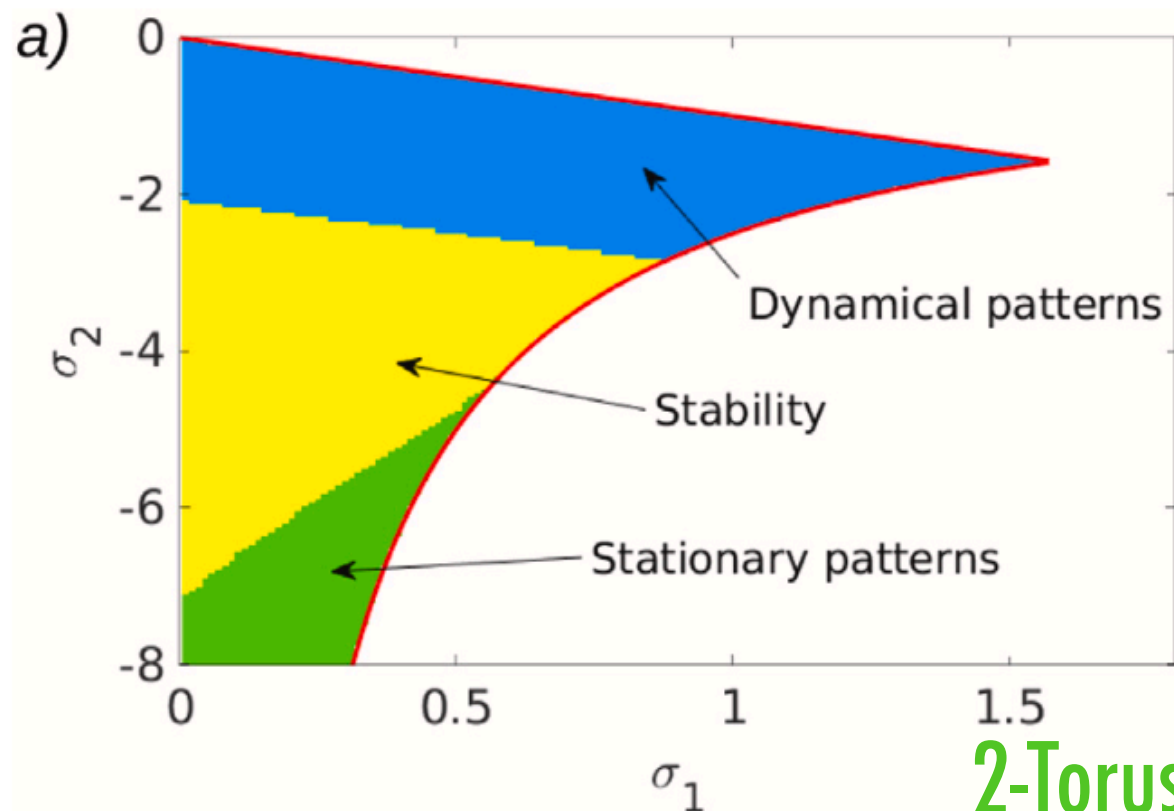
3 ways Dirac

Turing patterns on simplicial complexes with Dirac coupling

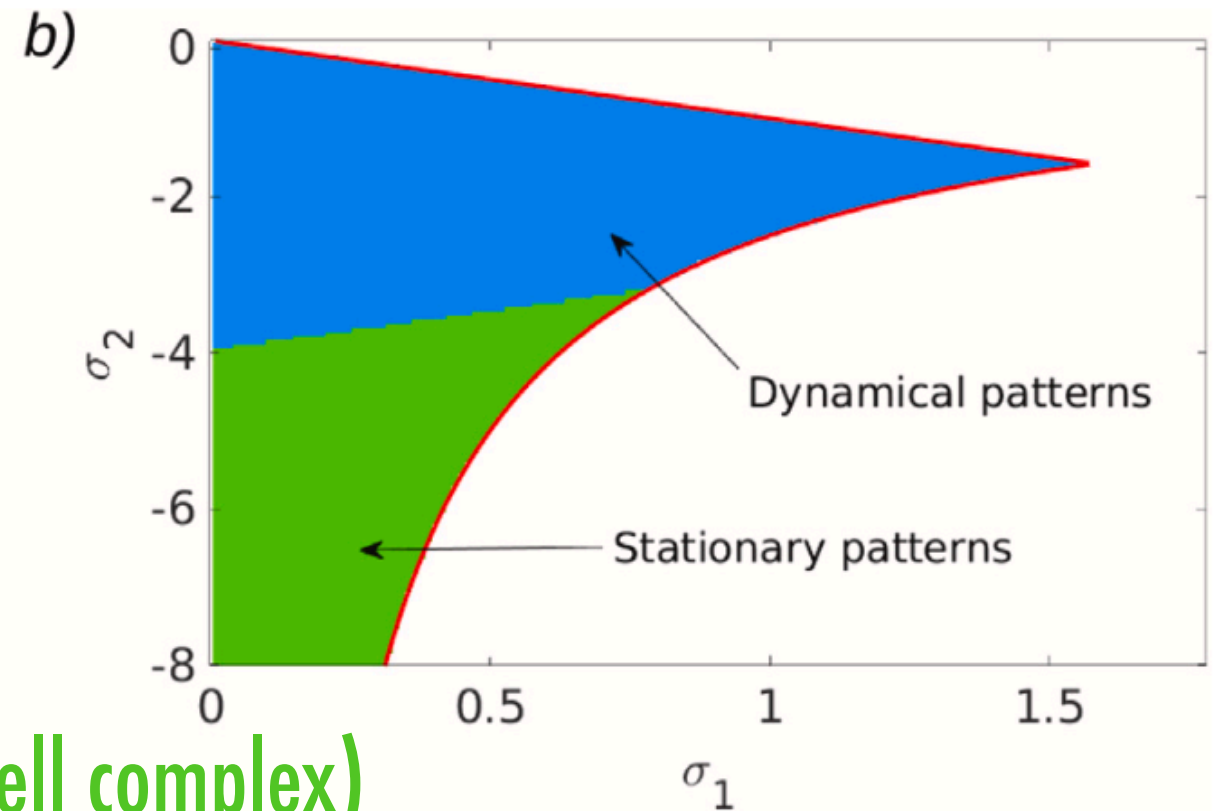
$$\Phi = \begin{pmatrix} u \\ v \\ w \end{pmatrix} \quad \dot{\Phi} = \mathbf{F}(\Phi, \partial\Phi) - c_1 \mathcal{D}\Phi - c_2 \mathcal{L}\Phi \quad \mathcal{D} = \gamma \partial = \begin{pmatrix} 0 & 0 & \alpha_u \mathbf{B} \\ 0 & 0 & \alpha_v \mathbf{B} \\ \beta_u \mathbf{B}^\top & \beta_v \mathbf{B}^\top & 0 \end{pmatrix}$$

$$\begin{cases} \dot{u} = \sigma_1 u - \eta_1 u^3 + \xi_1 v + \zeta_1 \mathbf{B}w - c_2 \mathbf{L}_{[0]}(D_{uu}u + D_{uv}v) - c_1 \alpha_u \mathbf{B}w \\ \dot{v} = \sigma_2 v + \xi_2 u + \zeta_2 \mathbf{B}w - c_2 \mathbf{L}_{[0]}(D_{vu}u + D_{vv}v) - c_1 \alpha_v \mathbf{B}w \\ \dot{w} = \sigma_3 w + \zeta_3 \mathbf{B}^\top u + \zeta_4 \mathbf{B}^\top v - c_2 D_{ww} \mathbf{L}_{[1]} - c_1 \mathbf{B}^\top (\beta_u u + \beta_v v), \end{cases}$$

$c_2 \neq 0$ Dirac & Laplace



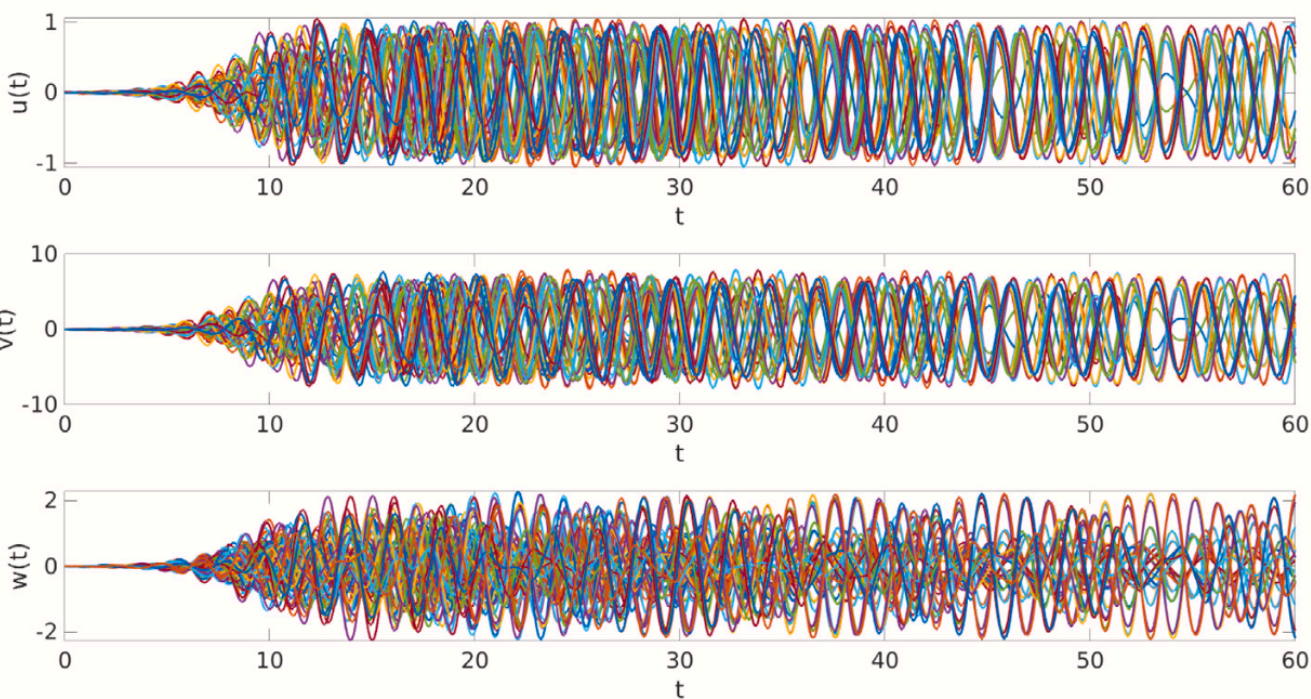
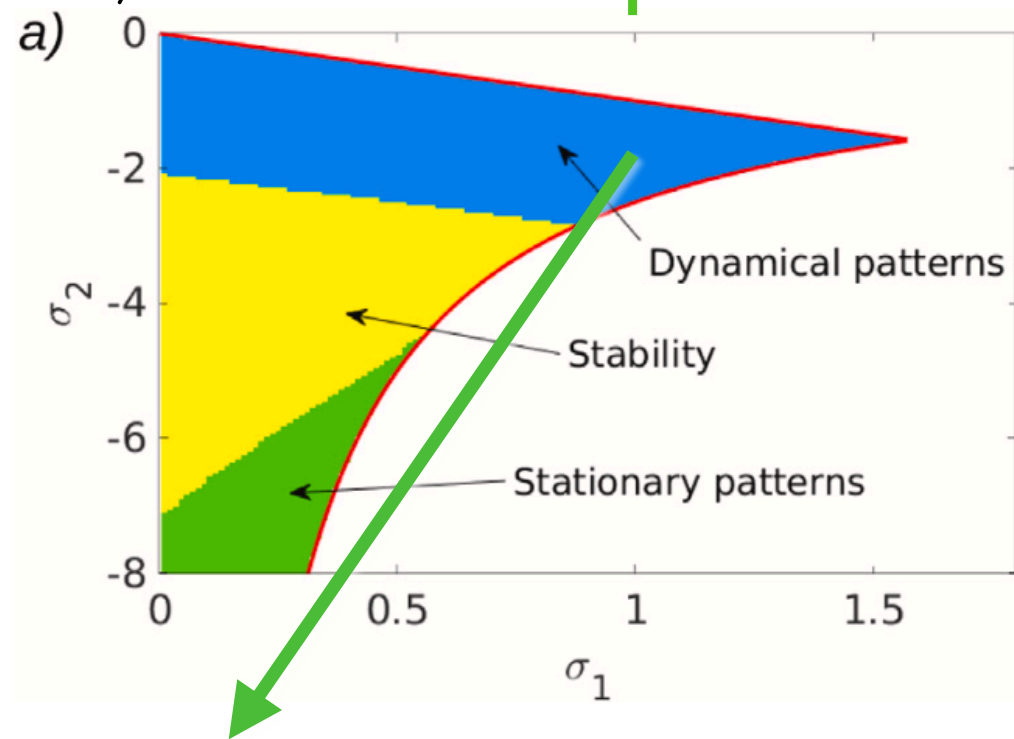
$c_2 = 0$ Dirac



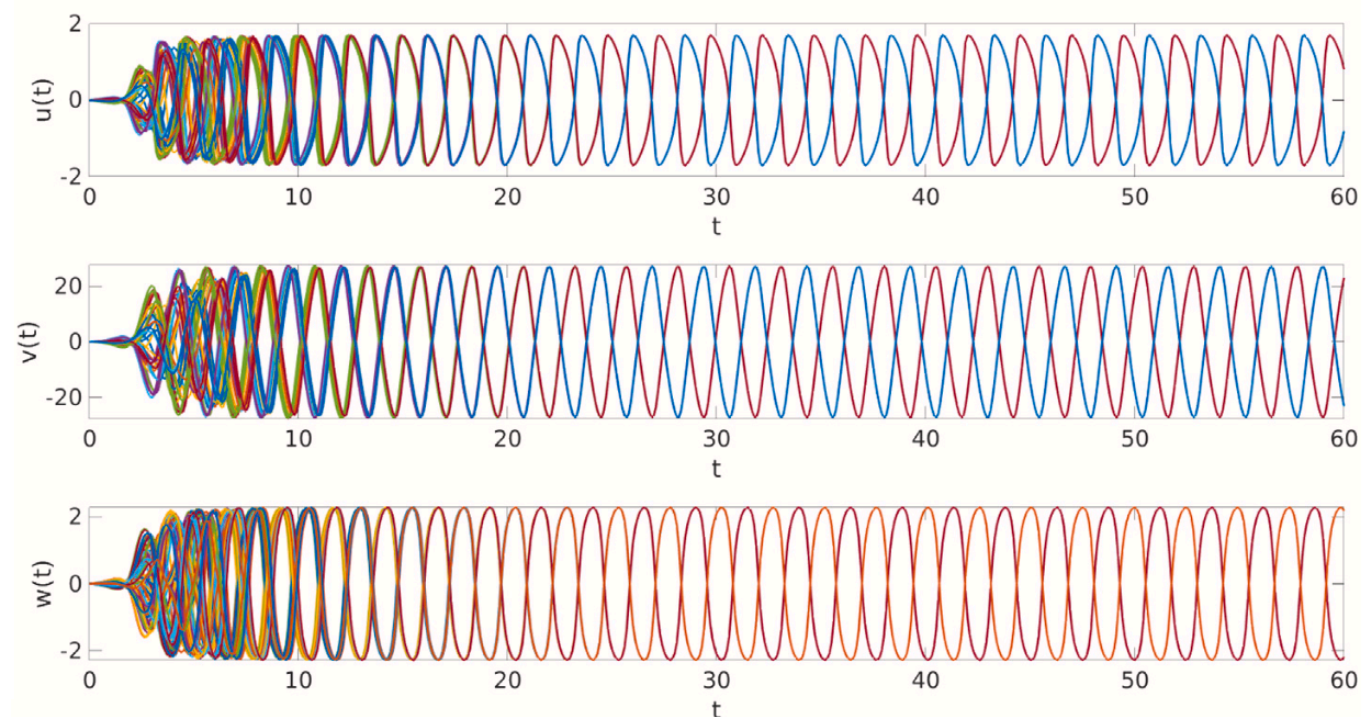
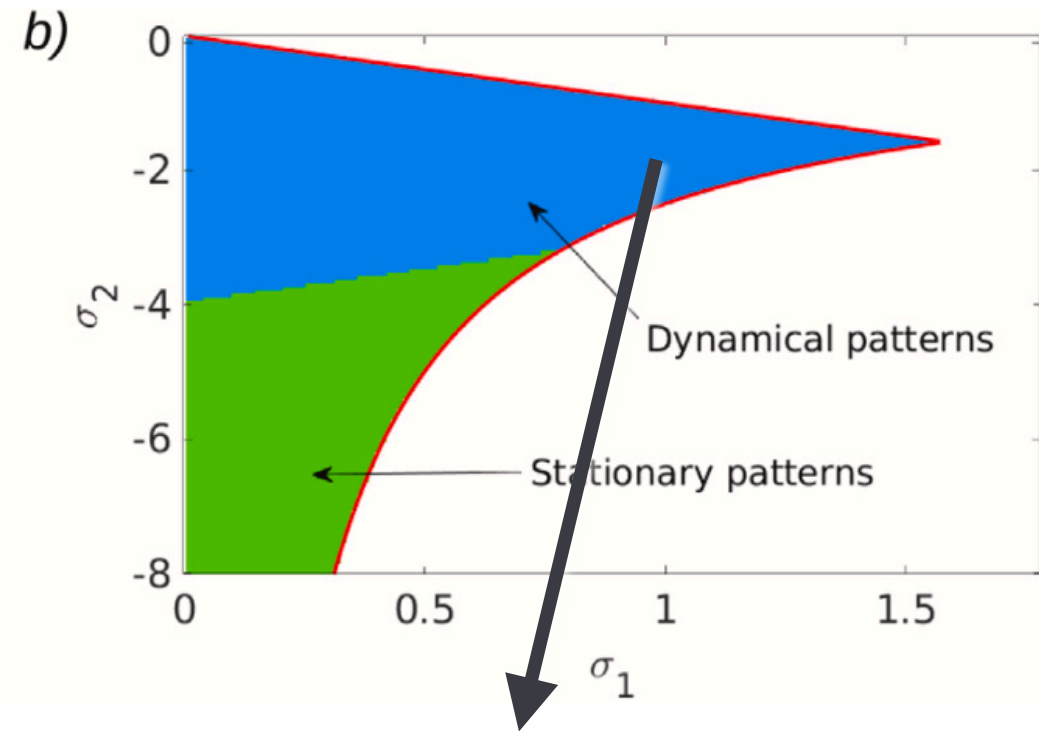
2-Torus (cell complex)

Turing patterns on simplicial complexes with Dirac coupling

$c_2 \neq 0$ Dirac & Laplace



$c_2 = 0$ Dirac



2-Torus (cell complex)

July the 25th, 2024, Alan Turing Institute, London UK

Theory and applications of hypergraphs

HTAW01

22 July 2024 to 26 July 2024

Alan Turing Institute

Isaac Newton Institute
for Mathematical Sciences



Thank you

Any questions?

naxys
Namur Institute for Complex Systems

**UNIVERSITÉ
DE NAMUR**

www.unamur.be

timoteo.carletti@unamur.be

naxys
Namur Center for Complex Systems

Some papers where results can be found

Global Topological Synchronization on Simplicial and Cell Complexes, T. Carletti, L. Giambagli, G. Bianconi, Physical Review Letters, **130**, pp. 187401, (2023)

Turing patterns in systems with high-order interactions, R. Muolo, L. Gallo, V. Latora, M. Frasca, T. Carletti, Chaos Solitons & Fractals. **106**, pp. 112912 (2023)

Finite propagation enhances turing patterns in reaction–diffusion networked systems, T. Carletti , R. Muolo. J Phys: Complexity **2**(4), pp. 045004 (2021)

Diffusion-driven instability of topological signals coupled by the Dirac operator, L. Giambagli et al, Physical Review E , **106** pp. 064314 , (2022)

Dynamical systems on hypergraphs, T. Carletti, D. Fanelli, S. Nicoletti, J Phys: Complexity **1**(3):035006 (2020)

Patterns of non-normality in networked systems., R. Muolo, M. Asllani, D. Fanelli, PK. Maini, T. Carletti, J Theoret Biol **480**:81, (2019)

Some papers where results can be found.

Theory of Turing Patterns on Time Varying Networks, J. Petit, B. Lauwens, D. Fanelli, T. Carletti, Physical Review Letters, **119**, pp. 148301-1–5, (2017)

Tune the topology to create or destroy patterns, M. Asllani, T. Carletti, D. Fanelli, European Physical Journal B. **89**, pp. 260 (2016)

Pattern formation in a two-component reaction-diffusion system with delayed processes on a network, J. Petit, M. Asllani, D. Fanelli, B. Lauwens, T. Carletti, Physica A, **462**, pp.230, (2016)

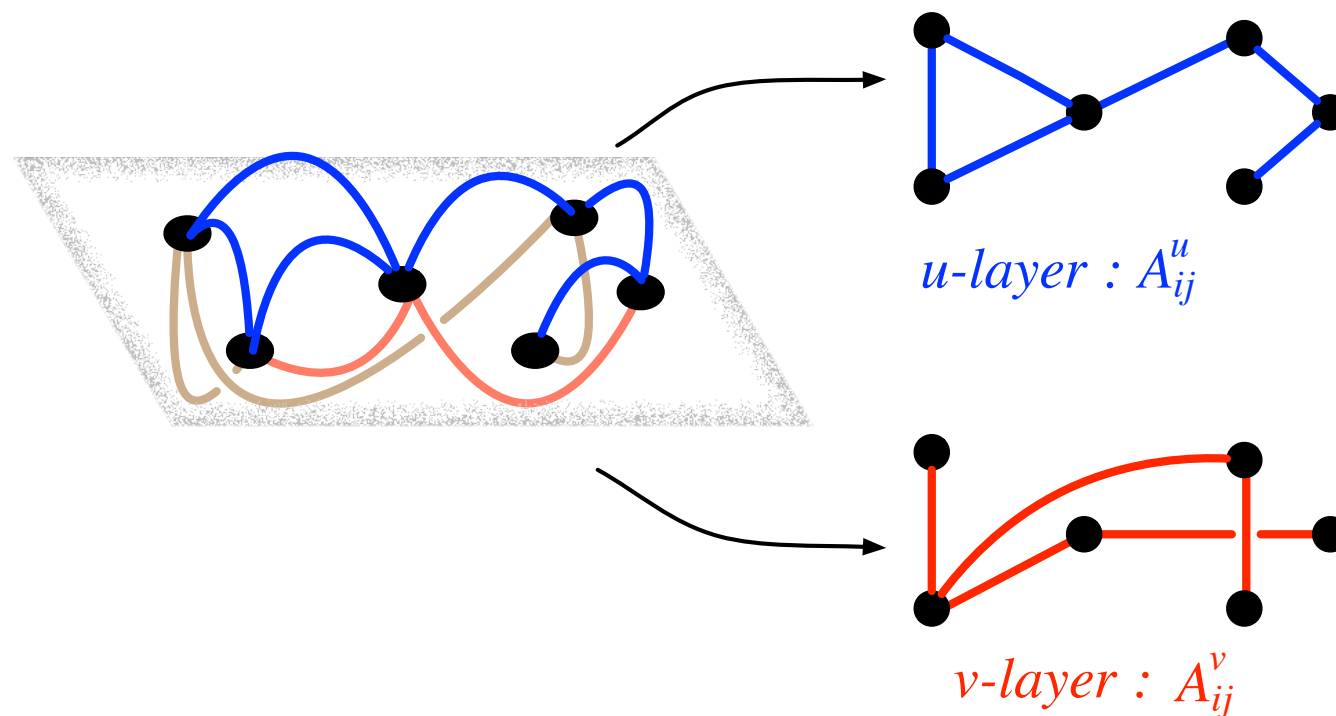
Delay induced Turing-like waves for one species reaction–diffusion model on a network, J. Petit, T. Carletti, M. Asllani, D. Fanelli, Europhysics Letters. **111**, 5, pp. 58002, (2015)

Turing instabilities on Cartesian product networks, M. Asllani, D.M. Busiello, T. Carletti, D. Fanelli, G. Planchon, Scientific Reports. **5**, pp. 12927, (2015)

Turing patterns in multiplex networks, M. Asllani, D.M. Busiello, T. Carletti, D. Fanelli, G. Planchon, Physical Review E ,**90**, 4, pp. 042814, (2014)

Can we control the topology to create (destroy) patterns?

Let us consider a multigraph, e.g. two nodes can be connected through different edges



$$\epsilon = 0$$

$$A^u(0) = A^0$$

$$A^v(0) = A^0$$

$$A^u(\epsilon) = A^0 + \epsilon(A^1 - A^0)$$

$$A^v(\epsilon) = A^0 + \epsilon(A^2 - A^0)$$

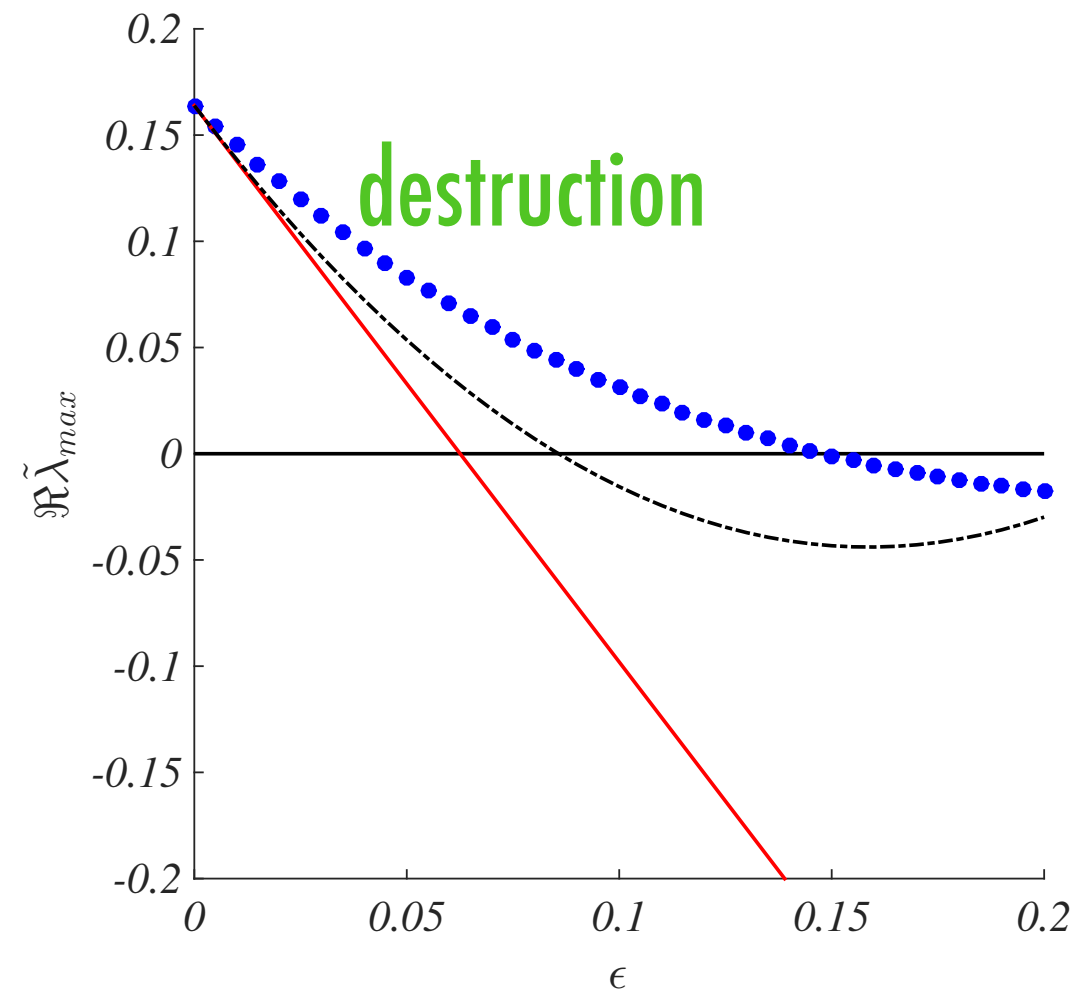
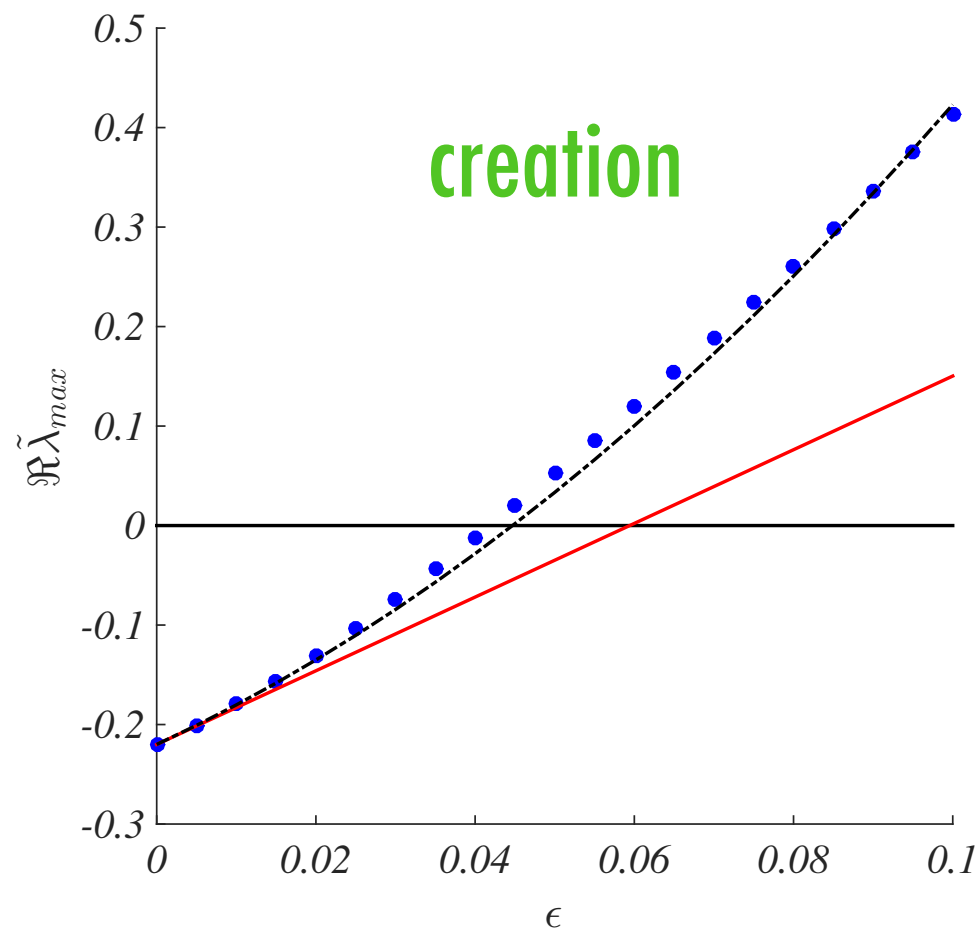
$$\epsilon = 1$$

$$A^u(1) = A^1$$

$$A^v(1) = A^2$$

Can we control the topology to create (destroy) patterns?

theory vs simulations



$\epsilon = 0$

$\epsilon = 1$

$$A^u(0) = A^0$$

$$A^u(\epsilon) = A^0 + \epsilon(A^1 - A^0)$$

$$A^u(1) = A^1$$

$$A^v(0) = A^0$$

$$A^v(\epsilon) = A^0 + \epsilon(A^2 - A^0)$$

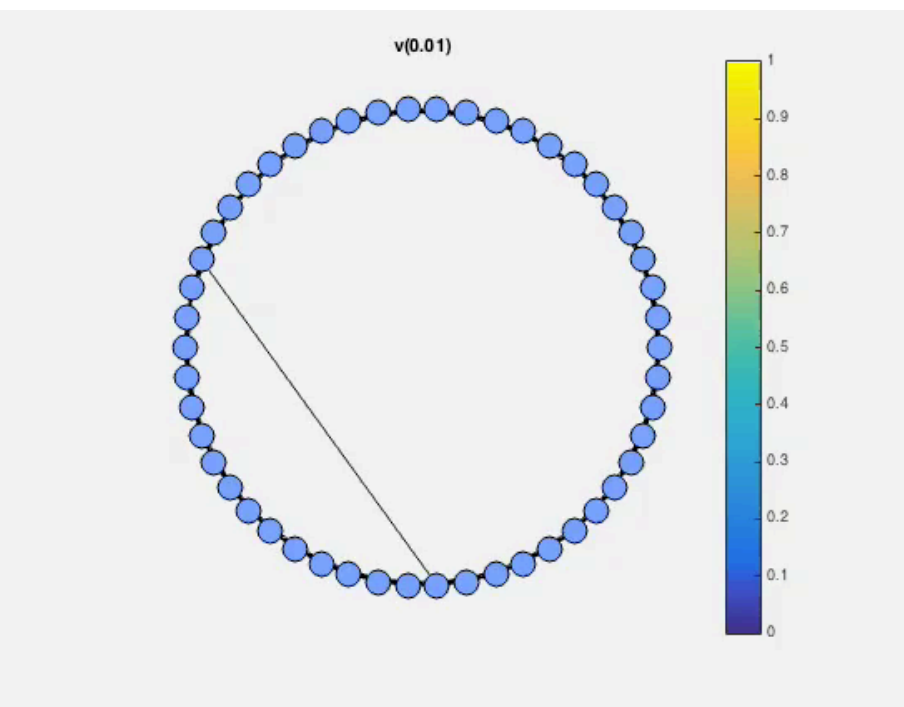
$$A^v(1) = A^2$$

Can we control the topology to create (destroy) patterns?

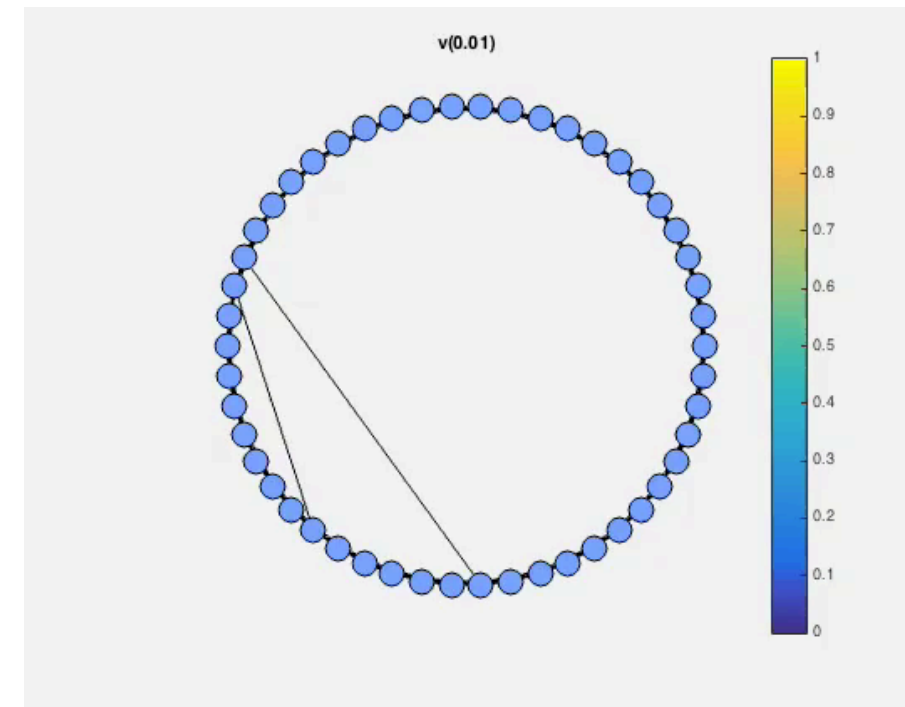
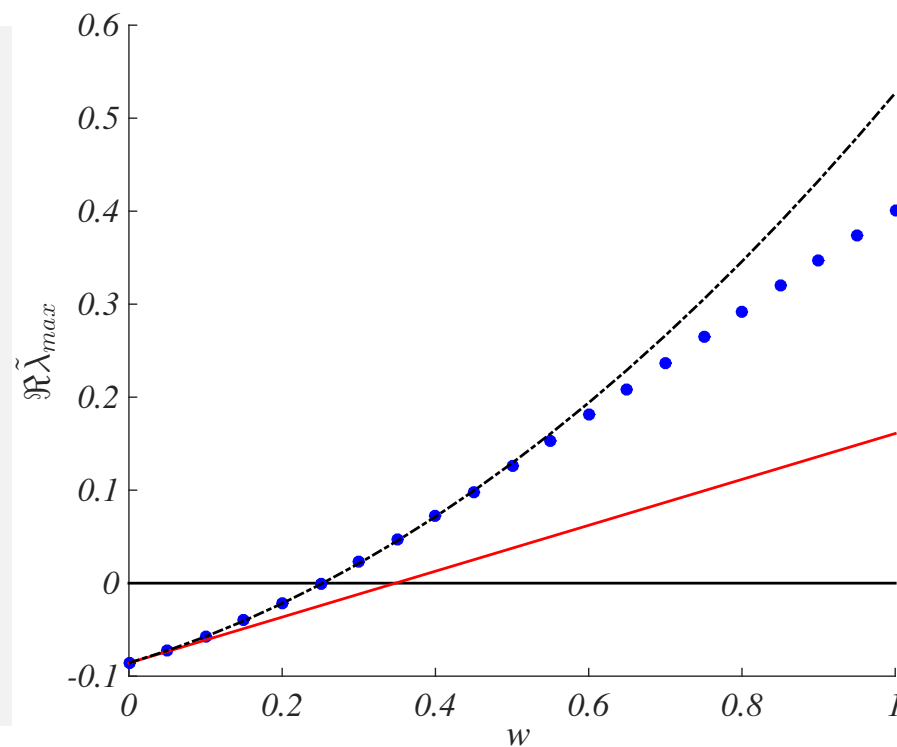
Create patterns by adding a single (optimally chosen) link

$$A^u(w) = A^0$$

$$A^v(w) = A^0 + wT^{(ij)}$$



$w=0$



$w=1$

Delayed models

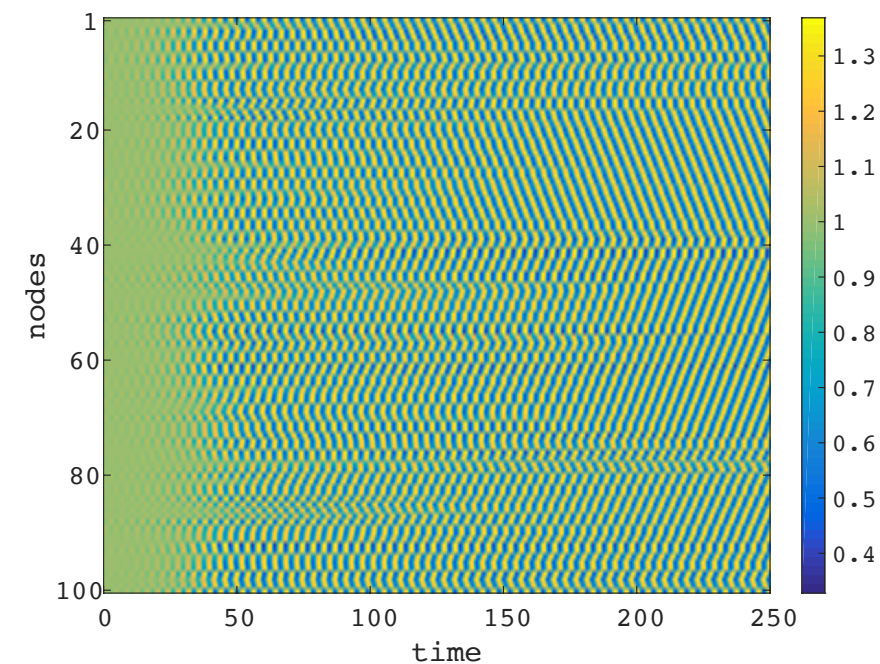
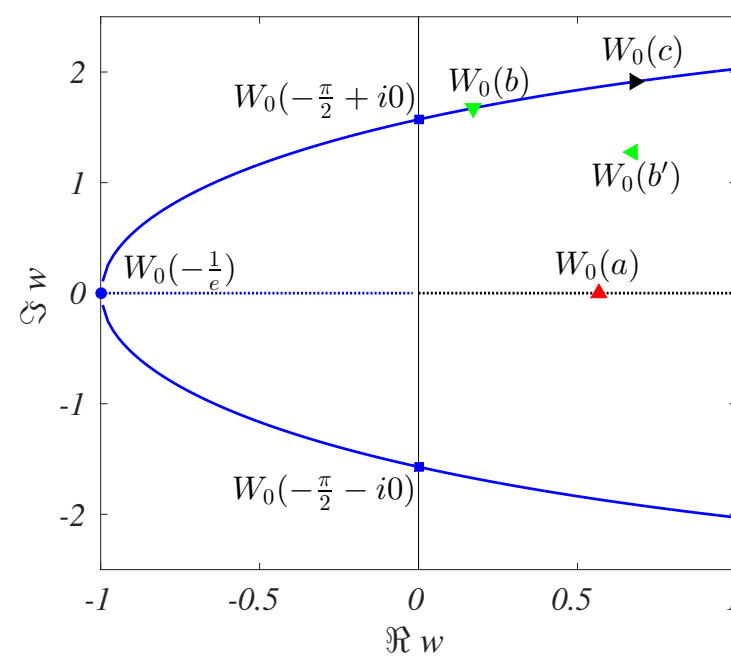
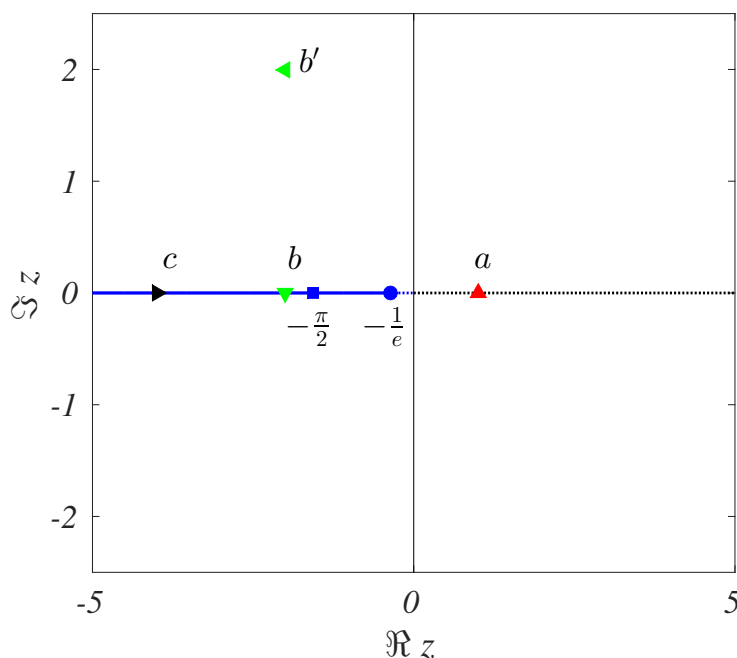
Movement across links takes time, so the diffusion part should contain a delay term.

Also reactions can take time, so the reaction part should contain a delay term.

$$\dot{x}_i(t) = f(x_i(t - \tau_r)) + D \sum_j L_{ij} x_j(t - \tau_d)$$

Observe that one single species is enough to have Turing patterns

The relation dispersion can be analytically computed using the Lambert W-function



Finite propagation on complex networks

M Incidence matrix

L = $-\mathbf{M}^\top \mathbf{M}$ Laplace matrix

Fick's law

$$\chi_e(t) = -D_u [u_j(t) - u_i(t)] \equiv D_u [\mathbf{M}\vec{u}(t)]_e$$

$$\frac{du_i}{dt}(t) = -[\mathbf{M}^\top \vec{\chi}(t)]_i$$

$$\frac{d\vec{u}}{dt}(t) = -\mathbf{M}^\top \vec{\chi} = -D_u \mathbf{M}^\top \mathbf{M} \vec{u} = D_u \mathbf{L} \vec{u}$$

Finite propagation on complex networks

M Incidence matrix

L = $-\mathbf{M}^\top \mathbf{M}$ Laplace matrix

Fick's law

$$\chi_e(t) = -D_u [u_j(t) - u_i(t)] \equiv D_u [\mathbf{M}\vec{u}(t)]_e \quad \frac{du_i}{dt}(t) = -[\mathbf{M}^\top \vec{\chi}(t)]_i$$

$$\frac{d\vec{u}}{dt}(t) = -\mathbf{M}^\top \vec{\chi} = -D_u \mathbf{M}^\top \mathbf{M} \vec{u} = D_u \mathbf{L} \vec{u}$$

Cattaneo's theory

τ_u relaxation / inertial time

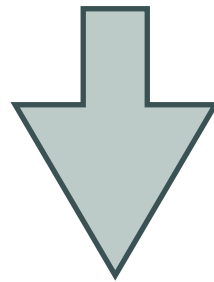
$$\chi_e(t) + \tau_u \frac{d\chi_e}{dt}(t) = D_u [\mathbf{M}\vec{u}(t)]_e \quad \frac{du_i}{dt}(t) = -[\mathbf{M}^\top \vec{\chi}(t)]_i$$

$$\frac{d\vec{u}}{dt}(t) = -\tau_u \frac{d^2 \vec{u}}{dt^2} + D_u \mathbf{L} \vec{u}(t)$$

Relativistic Turing mechanism on complex networks

$$\begin{cases} \dot{u}_i &= f(u_i, v_i) + D_u \sum_j L_{ij} u_j \\ \dot{v}_i &= g(u_i, v_i) + D_v \sum_j L_{ij} v_j \end{cases}$$

Parabolic RD
(Heat equation)



$$\begin{cases} \frac{du_i}{dt} + \tau_u \frac{d^2 u_i}{dt^2} &= f(u_i, v_i) + D_u \sum_{j=1}^n L_{ij} u_j \\ \frac{dv_i}{dt} + \tau_v \frac{d^2 v_i}{dt^2} &= g(u_i, v_i) + D_v \sum_{j=1}^n L_{ij} v_j \end{cases}$$

Hyperbolic RD
(Relativistic Heat equation)

(Cattaneo equation, telegraph equation, damped nonlinear Klein-Gordon equations)

Some results

- Existence of Turing pattern in activator - inhibitor systems with inhibitor diffusing faster than the activator

$$D_v \gg D_u$$

- Existence of Turing pattern in activator - inhibitor systems with inhibitor diffusing slower than the activator

$$D_v \leq D_u$$

- Existence of Turing pattern in inhibitor - inhibitor systems

$$f_u < 0 \text{ and } g_v < 0$$

Some results

- Existence of Turing pattern in activator - inhibitor systems with inhibitor diffusing faster than the activator

$$D_v \gg D_u$$

- Existence of Turing pattern in activator - inhibitor systems with inhibitor diffusing slower than the activator

$$D_v \leq D_u$$

- Existence of Turing pattern in inhibitor - inhibitor systems

$$f_u < 0 \text{ and } g_v < 0$$

Inertia driven Turing instability

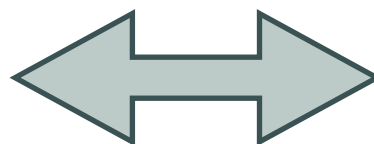
Turing instability in relativistic reaction-diffusion

$$\begin{cases} \frac{d\delta u_i}{dt} + \tau_u \frac{d^2 \delta u_i}{dt^2} = \partial_u f \delta u_i + \partial_v f \delta v_i + D_u \sum_{j=1}^n L_{ij} \delta u_j \\ \frac{d\delta v_i}{dt} + \tau_v \frac{d^2 \delta v_i}{dt^2} = \partial_u g \delta u_i + \partial_v g \delta v_i + D_v \sum_{j=1}^n L_{ij} \delta v_j \end{cases} \quad \begin{aligned} u_i(t) &= \sum_{\alpha} u^{\alpha} e^{\lambda_{\alpha} t} \phi_i^{(\alpha)} \\ \sum_j L_{ij} \phi_j^{(\alpha)} &= \Lambda_{\alpha} \phi_i^{(\alpha)} \quad \forall i, \alpha \end{aligned}$$

$$\begin{cases} \frac{d\hat{u}_{\alpha}}{dt}(t) + \tau_u \frac{d^2 \hat{u}_{\alpha}}{dt^2}(t) = \partial_u f \hat{u}_{\alpha}(t) + \partial_v f \hat{v}_{\alpha}(t) + D_u \Lambda^{(\alpha)} \hat{u}_{\alpha}(t) \\ \frac{d\hat{v}_{\alpha}}{dt}(t) + \tau_v \frac{d^2 \hat{v}_{\alpha}}{dt^2}(t) = \partial_u g \hat{u}_{\alpha}(t) + \partial_v g \hat{v}_{\alpha}(t) + D_v \Lambda^{(\alpha)} \hat{v}_{\alpha}(t) \end{cases}$$

$$\det \begin{pmatrix} \lambda_{\alpha} + \tau_u \lambda_{\alpha}^2 - \partial_u f - \Lambda^{(\alpha)} D_u & -\partial_v f \\ -\partial_u g & \lambda_{\alpha} + \tau_v \lambda_{\alpha}^2 - \partial_v g - \Lambda^{(\alpha)} D_v \end{pmatrix} = p_{\alpha}(\lambda_{\alpha}) = 0$$

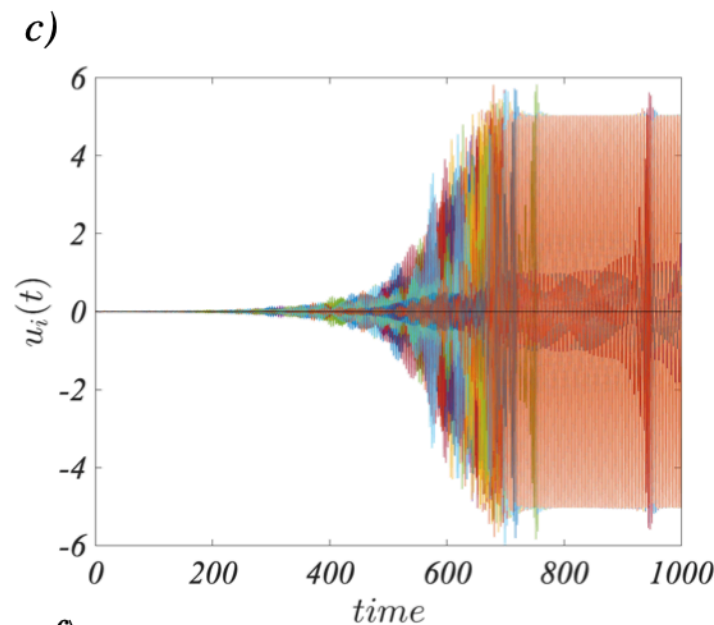
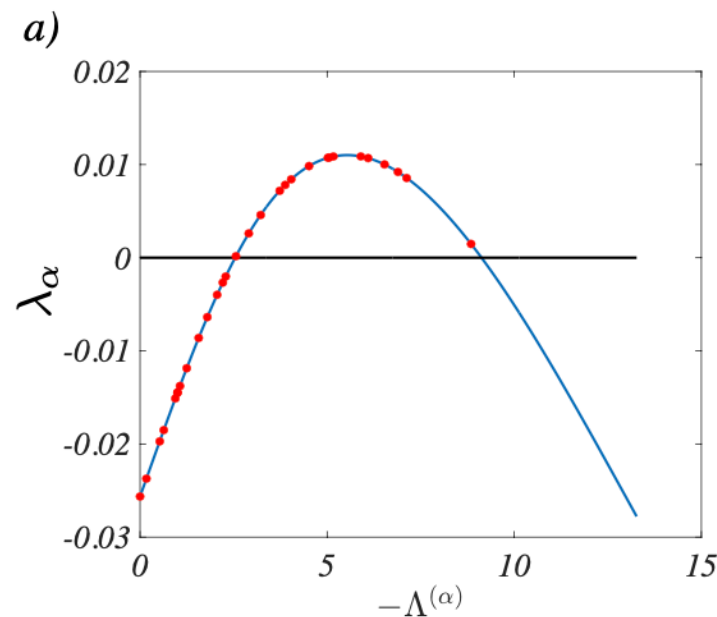
Fourth order polynomial



Routh - Hurwitz criterium

FitzHugh - Nagumo model : inertia driven patterns

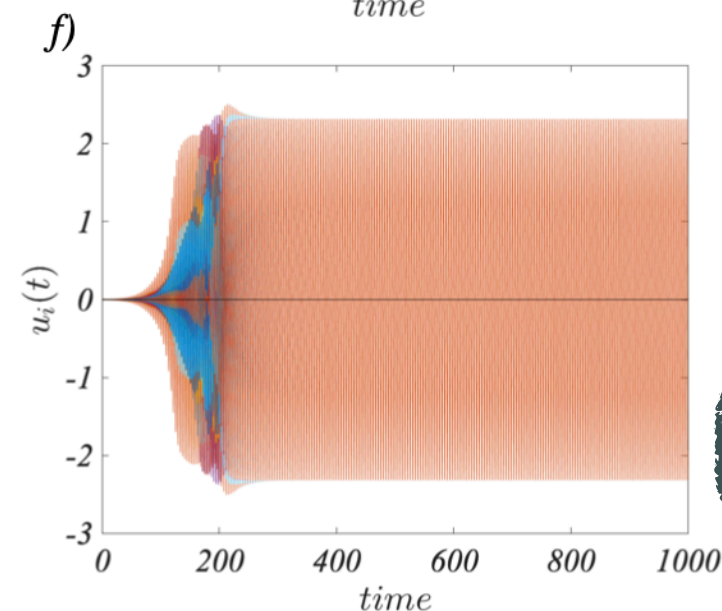
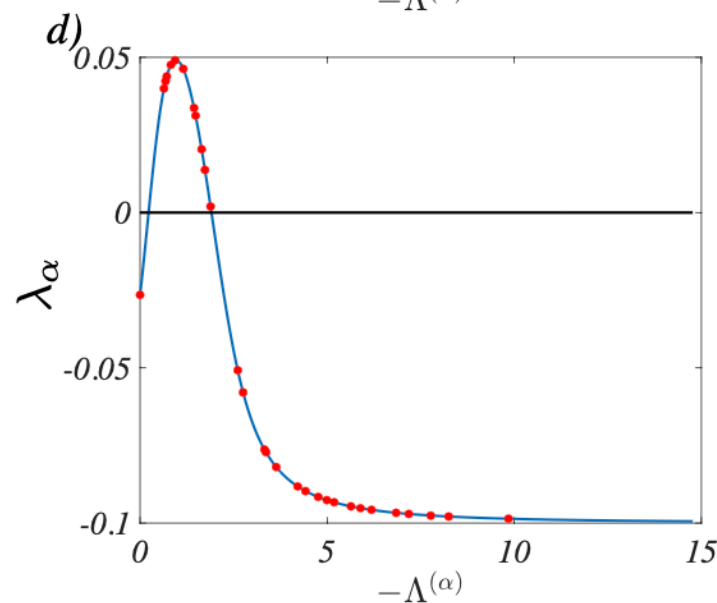
$$\begin{cases} \frac{du_i}{dt} + \tau_u \frac{d^2 u_i}{dt^2} = \mu u_i - u_i^3 - v_i + D_u \sum_{j=1}^n L_{ij} u_j \\ \frac{dv_i}{dt} + \tau_v \frac{d^2 v_i}{dt^2} = \gamma(u_i - \beta v_i) + D_v \sum_{j=1}^n L_{ij} v_j \end{cases}$$



$$\beta = 0.6, \mu = 1.0, \gamma = 4.0$$

$$\tau_u = 5.0, \tau_v = 1.0$$

$$D_u = 2.2 > D_v = 0.2$$



$$\beta = 2.5, \mu = 0.18, \gamma = 4.0$$

$$\tau_u = 1.0, \tau_v = 5.0$$

$$D_u = 2.2 = D_v = 2.2$$